NASA Technical Paper 2796

1988

A Review of Technologies Applicable to Low-Speed Flight of High-Performance Aircraft Investigated in the Langley 14- by 22-Foot Subsonic Tunnel

John W. Paulson, Jr.,
P. Frank Quinto,
Daniel W. Banks,
Guy T. Kemmerly,
and Gregory M. Gatlin

Langley Research Center
Hampton, Virginia

National Aeronautics and Space Administration

Scientific and Technical Information Division

Contents

Summary

An extensive research program has been underway at the NASA Langley Research Center to define and develop the technologies required for low-speed flight of high-performance aircraft. This 10-year program has placed emphasis on both short takeoff and landing (STOL) and short takeoff and vertical landing (STOVL) operations rather than on regular "up and away" flight. A series of NASA in-house as well as joint projects have studied various technologies including high lift, vectored thrust, thrust-induced lift, reversed thrust, an alternate method of providing trim and control, and ground effects. These technologies have been investigated on a number of configurations ranging from industry designs for advanced fighter aircraft to generic wing-canard research models. Test conditions have ranged from hover (or static) through transition to wing-borne flight at angles of attack from $-5°$ to $40°$ at representative thrust coefficients.

Results have indicated that thrust-induced circulation is generally not present in fighter-type configurations because of the small wingspan affected by the exhaust nozzles. However, methods of distributing the exhaust over a large portion of the wingspan have been demonstrated to generate significant levels of induced lift. In general, a powered high-lift system produces pitching moments that will exceed the trim capability of aerodynamic controls, and several concepts have been developed to provide alternate sources of trim. Multifunction nozzles provide thrust spoiling and reversing to allow both the correct net drag levels required for approach and landing while allowing engine thrust to be set at military power and the effective stopping forces during the ground roll.

Introduction

During the past decade there has been a renewal of interest in significantly improving the takeoff and landing performance of fighter aircraft. The threat of runway denial through bomb damage in the European Theater has brought out the possibility of a grounded fighter force because of insufficient runway length for takeoff and landing (refs. 1 to 3). Today's aircraft, such as the F-15 and F-16, can take off in very short distances (less than 1000 ft) when lightly loaded because of extremely high thrust-to-weight ratios (fig. 1), but they are limited to a runway length of about 2500 ft when landing because of relatively low approach lift coefficients (yielding fast approach speeds) and no means of generating really effective stopping forces other than wheel braking (fig. 1). Takeoff runway lengths increase dramatically when external stores are added because the increased drag and weight of the stores result in reduced overall thrust-to-weight ratios. Landing runway lengths also increase with landing gross weight, but stores and fuel can be expended, and often are, to limit landing weight. Since today's aircraft are primarily limited to wheel braking or drag chutes once the aircraft has landed, any degradation in braking effectiveness (such as water, snow, or ice on the runway surface) increases landing lengths to thousands of feet. Even the most conservative estimates of damage-free runway lengths available following an airfield attack indicate that much improved landing performance is required.

The solution to the runway denial problem is, of course, aircraft that are not limited to long lengths of runway for either takeoff or landing. The aircraft will require increased high-lift capability over present fighters to reduce both takeoff and landing speeds, thrust reversing to increase stopping forces on the ground (fig. 2), improved control systems for low airspeed flight, and improved landing-gear systems to allow high-sink-rate landings as well as rough-terrain operations. Adding to the complexity, these features must not compromise the regular "up and away" performance of the aircraft to the point that air superiority cannot be maintained.

For the past 10 years a research program has been underway in the Subsonic Aerodynamics Branch at the NASA Langley Research Center to define and develop technologies that may be applicable to low-speed flight of high-performance aircraft. The emphasis of this research has been directed toward short takeoff and landing (STOL) and short takeoff and vertical landing (STOVL) operations rather than on regular "up and away" flight characteristics. The data base generated would, however, apply to almost any flight condition up to speeds at which compressibility would become a factor. This program has combined NASA in-house research with joint NASA/Department of Defense/Industry research to explore high lift, an alternate means of providing longitudinal trim and control, thrust vectoring and reversing nozzles, and ground effects on advanced fighter/attack configurations.

These technologies have been investigated on several different configurations in the Langley 14- by 22-Foot Subsonic Tunnel. The test parameters have covered a broad range of angles of attack and sideslip, and power effects have been examined from the power-off case up to a thrust coefficient of 3.0, which is representative of military power settings at airspeeds representative of STOL operations. Tests have been conducted at free-stream dynamic pressures from 0 to 70 lbf/ft^2 for both free-air effects and

in-ground-effects conditions. The effect of thrust reversing has also been investigated. The research program has generated a number of reports published under several different formats (refs. 4 to 30). The purpose of this report is to summarize, under one cover, the most significant results to make these more readily available to participants in advanced fighter activities.

Symbols

A	aspect ratio
a	acceleration, ft/sec^2
b	wingspan, ft
C_A	axial-force coefficient, $F_A/q_\infty S$
$C_{A,T}$	static-thrust axial-force coefficient, $[(F_{A,S}/p_a)p_\infty]/q_\infty S$
$C_{A,\mathrm{TR}}$	thrust-removed axial-force coefficient, $C_A - C_{A,T}$
C_D	drag coefficient, $C_A \cos\alpha + C_N \sin\alpha$
$C_{D,\mathrm{TR}}$	thrust-removed drag coefficient, $C_{A,\mathrm{TR}} \cos\alpha + C_{N,\mathrm{TR}} \sin\alpha$
$\Delta C_{D,\mathrm{TR}}$	thrust-induced drag coefficient, $C_{D,\mathrm{TR}} - C_D\vert_{C_T=0}$
C_L	lift coefficient, $C_N \cos\alpha - C_A \sin\alpha$
$C_{L,\mathrm{TR}}$	thrust-removed lift coefficient, $C_{N,\mathrm{TR}} \cos\alpha - C_{A,\mathrm{TR}} \sin\alpha$
$\Delta C_{L,\mathrm{TR}}$	thrust-induced lift coefficient, $C_{L,\mathrm{TR}} - C_L\vert_{C_T=0}$
C_m	pitching-moment coefficient, $M_Y/q_\infty S\bar{c}$
$C_{m,T}$	static-thrust pitching-moment coefficient, $[(M_{Y,S}/p_a)p_\infty]/q_\infty S\bar{c}$
$C_{m,\mathrm{TR}}$	thrust-removed pitching-moment coefficient, $C_m - C_{m,T}$
$\Delta C_{m,\mathrm{TR}}$	thrust-induced pitching-moment coefficient, $C_{m,\mathrm{TR}} - C_m\vert_{C_T=0}$
C_N	normal-force coefficient, $F_N/q_\infty S$
$C_{N,T}$	static-thrust normal-force coefficient, $[(F_{N,S}/p_a)p_\infty]/q_\infty S$
$C_{N,\mathrm{TR}}$	thrust-removed normal-force coefficient, $C_N - C_{N,T}$
C_T	thrust coefficient, $F/q_\infty S$
C_μ	ideal thrust coefficient, $\dot{m}V_j/q_\infty S$
$\bar{c}$	wing mean aerodynamic chord, ft
F	measured static-nozzle resultant-thrust force, $\left(F_N^2 + F_A^2\right)^{1/2}$, lbf
F_A	corrected axial force, $F_{A,B} - F_{A,\mathrm{PT}} - F_{A,\mathrm{FT}}$, lbf
F_N	corrected normal force, $F_{N,B} - F_{N,\mathrm{PT}} - F_{N,\mathrm{FT}}$, lbf
g	gravitational constant ($1g \approx 32.174$ ft/sec^2)
h	height above ground plane, ft
i	incidence angle, deg
L/D	lift-drag ratio
M_Y	corrected pitching moment, $M_{Y,B} - M_{Y,\mathrm{PT}} - M_{Y,\mathrm{FT}}$, ft-lb
$\dot{m}$	measured nozzle mass-flow rate, slugs/sec
NPR	nozzle pressure ratio, p_t/p_∞
p_a	ambient barometric pressure, lbf/ft^2
p_t	nozzle total pressure, lbf/ft^2
p_∞	free-stream static pressure, lbf/ft^2
q_∞	free-stream dynamic pressure, lbf/ft^2
S	wing surface area, ft^2
V_j	ideal jet velocity, ft/sec
W/S	wing loading, lbf/ft^2
α	angle of attack, deg
γ	flight-path angle, deg
Δ	difference between thrust-removed and power-off data
δ	deflection angle, deg
θ_j	jet-deflection angle, $\tan^{-1}\left(\frac{C_{N,T}}{C_{A,T}}\right)$, deg
Λ	wing or spanwise-blowing sweep angle, deg

Subscripts:

B	balance measurement
c	canard

cas	cascade
FT	flowing tare
f	flap
N	nozzle
PRI	primary nozzle
PT	pressure tare
S	static

Abbreviations:

ANC-B	advanced nozzle concepts-B configuration
ATTAC	Advanced Technologies for Tactical Aircraft
a/b	afterburner
BLC	boundary-layer control
CD	convergent-divergent
CDAF	Configuration Development of Advanced Fighters
F.S.	fuselage station, in.
SERN	single-expansion ramp nozzle
SWB	spanwise blowing
VEO	vectored-engine-over
W.L.	waterline, in.
2D	two-dimensional

Configurations and Technologies Investigated

A large variety of fighter/attack configurations have been studied in the Langley 14- by 22-Foot Subsonic Tunnel. The following section gives a brief description of the wind-tunnel facility, model configurations tested, and the technologies studied. A summary, along with references for details such as model geometry, hardware, or test conditions, is presented in table I.

Wind-Tunnel Facility

The Langley 14- by 22-Foot Subsonic Tunnel is a closed-circuit, single-return, atmospheric facility with a maximum free-stream dynamic pressure of 144 lbf/ft^2. Models can be tested up to an angle of attack of about 60° with up to about 25° of sideslip. High-pressure air can be supplied to simulate jet-engine exhaust for powered models. The model support system has vertical travel capability to allow testing both in and out of ground effect.

Model Descriptions

Generic Wing-Canard Fighter Configuration

A NASA in-house research model shown in figure 3 was used to explore thrust vectoring and thrust-induced high lift on a wing-canard configuration designed for transonic maneuvering. The wing and canard designed in reference 9 were added to an existing fuselage that had been built for a vertical takeoff and landing (VTOL) configuration (refs. 6 and 7). The model also had full-span leading- and trailing-edge flaps on both the wing and canard, and the canard incidence was variable. The fuselage had plumbing for high-pressure air to power a pair of nozzles located near the wing trailing edge and a nose jet. The nose jet was initially used for hover testing but was also used to provide trim for STOL testing. High-pressure air was brought onboard the model through an air sting in which the balance was bridged by coiling the air line into a spring inside the air sting. This arrangement has the effect of placing an external linear spring on the balance that can be calibrated and removed from the balance output (ref. 31). The model was later modified to allow twin-engine nacelles and spanwise blowing on the trailing-edge flap system to be tested as shown in figure 4.

Vectored-Engine-Over-Wing (VEO-Wing) Configuration

The VEO-wing model shown in figure 5 was a joint research effort involving NASA, the Air Force Wright Aeronautical Laboratories (AFWAL), and General Dynamics Corporation; it was used to investigate thrust-induced high lift on fighter-type configurations. The model was equipped with twin, rectangular, primary exhaust nozzles, which exhausted high-pressure air over the upper surface of the wing trailing-edge flap, and secondary spanwise-blowing nozzles (located at $0.25\bar{c}$), which directed air over the upper surface of the wing. High-pressure air was delivered to the model through an air sting as discussed above. The trailing-edge flap of the partial-span wing could be deflected up to 30°.

Mach 2 Supercruiser Configuration

The model shown in figure 6 was a joint effort involving NASA, the Boeing Company, and AFWAL and was used to investigate vectored and reversed-thrust effects, induced high lift, and the use of a nose jet for longitudinal trim. The model was equipped with air-powered underwing engine simulators with interchangeable nozzles to allow a variation in both the nozzle vector angle and the exit aspect ratio. The high-pressure air was brought onboard the model

through a nonmetric vertical-tail support system to an internal plenum. The balance was bridged with a series of bellows in the air line to reduce balance/air line interactions. A nose jet designed to provide longitudinal trim was incorporated into the configuration and was supplied with high-pressure air from the main-nozzle plenum chamber and controlled by a separate throttling valve located in the nose of the model. Thrust reversing was available on the low-aspect-ratio exhaust nozzle, and the configuration was tested in ground effect when thrust reversers were installed.

F-15 Thrust-Reverser Configuration

A joint research program involving NASA, AFWAL, and the McDonnell Aircraft Corporation (MCAIR) utilized the model shown in figure 7 to investigate thrust spoiling, reversing, and vectoring, both in and out of ground effect, for STOL approach and landing studies. Several thrust-reversing nozzle concepts were tested in the investigation. Some of the concepts replaced the entire F-15 exhaust nozzle with a new nozzle, whereas other configurations utilized reversers in conjunction with the basic nozzle. High-pressure air was delivered through a vertical post fitted with a coiled air line similar in concept to the air sting described earlier.

Generic High-Sweep Fighter Configuration

A NASA in-house research model shown in figure 8 was used to investigate leading- and trailing-edge flap systems on high-sweep, low-aspect-ratio wings. The model was equipped with segmented, full-span trailing-edge flaps and continuous-camber, drooped leading-edge flaps.

Advanced Technologies for Tactical Aircraft (ATTAC) Configuration

A joint research model (NASA, AFWAL, and the Grumman Aerospace Corporation) shown in figure 9 and based on the configuration of reference 30 was used to investigate thrust vectoring, ground effects, and the use of a blown high-lift canard to provide longitudinal trim. The model was equipped with powered vectoring and reversing exhaust nozzles. High-pressure air was supplied to the model through the nonmetric vertical-tail support system. The canard was fitted with a blowing slot at the knee of the full-span trailing-edge flap, and a Krueger flap was installed to prevent leading-edge separation. The canard blowing slot was supplied high-pressure air from the model plenum through control valves and flow meters located in the model nose. Wing trailing-edge flaps could be deflected to 40°, and the canard flap could be deflected to 30° along with variable canard incidence.

Advanced Nozzle Concepts for STOL and Survivability Configuration

A joint research model (NASA, AFWAL, and the Grumman Aerospace Corporation) shown in figure 10 and based on the configuration of reference 30 was used to investigate vectored thrust and basic nozzle performance parameters for low-speed flight. The model was equipped with two engine simulators with four interchangeable nozzle geometries. High-pressure air was delivered through the air sting (in the generic wing-canard configuration) discussed earlier with an extension to pass through a nonmetric vertical-tail support system.

Advanced Nozzle Concepts-B (ANC-B) Configuration

Another joint research model (NASA, AFWAL, and MCAIR) shown in figure 11 was used to investigate two vectoring/reversing nozzle concepts, mechanical high-lift trailing-edge flaps, leading-edge vortex flaps, and longitudinal trim. The model could be tested with either a two-dimensional convergent-divergent nozzle or a single-expansion ramp nozzle (SERN), both of which could vector and reverse the exhaust. High-pressure air was delivered through a nonmetric blade support system under the model fuselage, and the balance was crossed with a bellows in the air line. The wing was fitted with a full-span, slotted trailing-edge flap and could be tested with either vortex or Krueger leading-edge flaps. The model could also be tested as either a wing-canard or wing-alone configuration.

Propulsive Wing-Canard Configuration

The joint research model (NASA, AFWAL, the Naval Air Development Center (NADC), and Rockwell International Corporation (Columbus, Ohio)) shown in figure 12 was used to study induced lift on low-aspect-ratio wings. The model was equipped with blown flaps on both the wing and canard. A blowing slot was located at the knee of the flaps, and the extent of span covered by the blowing could be varied from quarter-span to full span on the wing and from half-span to full span on the canard. High-pressure air was delivered through the air sting and distributed from the model plenum through four control valves to the wing and canard.

Discussion of Technologies

As stated previously, the four main technology areas investigated were as follows:

1. High lift

2. Alternate means of providing longitudinal trim and control

3. Thrust vectoring and reversing

4. Ground effects

These areas are discussed individually with comments on the possibility of synthesizing some of them into a common fighter/attack configuration as a summary section. The effect of ground presence will be incorporated into the discussion of each technology area where applicable and will also be discussed in a separate section. A discussion of thrust reversers, for example, would not be complete without including ground effects since the majority of reverse-thrust usage occurs during landing and roll out.

Because of the importance and difficulty of landing fighter/attack aircraft in short distances, a great deal of the analysis presented in this paper will be centered around approach and landing operations. It is important to emphasize here that the next generation of fighter aircraft will likely be required to operate at much higher engine power settings, probably near military thrust, during landing than are used on current aircraft.

Jet engines require several seconds to reach high power settings from low power settings because of the inertia of the rotating machinery. Therefore, in order to have effective thrust reversing available on touchdown, the engines will have to be at or near military power on approach to avoid this "spool up" time. With this high power available, engine thrust (mass flow) can be used for high lift and moments to trim the aircraft during approach, as well as effective reverse thrust upon landing. For the general class of fighter/attack aircraft of interest, a STOL approach speed of about 100 to 120 knots is likely and will give rise to thrust coefficients of about 0.75 to 1.00 at aircraft angles of attack between 10° and 15°. Therefore, although these technologies have been investigated over a wide range of parameters (e.g., angle of attack and thrust coefficients) and the data are applicable to any flight at low to medium speeds, most of the analysis and comments contained herein will be centered around approach and landing conditions.

High Lift

The requirement for high lift on advanced aircraft is straightforward. Higher lift means lower takeoff and landing velocities, a condition which translates directly into shorter runway lengths as well as other operational benefits such as lower accident rates and greater landing-gear and tire life. Historically, high lift has been provided by various types of mechanical leading- and trailing-edge flap systems to provide a match between takeoff, landing, and cruise performance requirements. However, compromises in cruise or maneuver performance requirements will generally define an aircraft. Because of weight and complexity and the relatively limited aerodynamic benefit of these often highly compromised mechanical flap systems, runway requirements can become very long for high-performance aircraft.

When operational requirements dictate runway lengths of less than about 2000 ft (i.e., short takeoff and landing), the need for very high lift systems becomes great. This is particularly true for very high performance aircraft such as fighters because their highly swept, low-aspect-ratio wings and generally limited flap systems are not particularly well-suited to producing high lift. One of the major research efforts has thus been to develop a means of producing high lift on highly swept fighter/attack configurations through the use of vectored-thrust lift, thrust-induced lift, and mechanical-flap lift.

The fighter/attack community of the 1970's had the idea that to develop a STOL aircraft it was necessary only to vector the nozzle thrust in the lift direction. Because of the direct-thrust component and the generous amount of thrust-induced lift that would be present (as seen on early STOL transport configurations (refs. 32 to 34)), there would be plenty of high lift available for fighters to operate from runway lengths as short as 400 to 500 ft (ref. 5). Initial research consequently was centered around evaluating the existence of significant levels of induced lift on typical fighter-type wing planforms with 45° to 55° leading-edge sweep and an aspect ratio of about 3.

Thrust-Vectoring Concepts

The models tested were the generic wing-canard and the vectored-engine-over-wing (VEO-wing) configurations shown in figures 3 and 5, respectively. An early version of the VEO wing was tested in several facilities at Langley and it evolved into the configuration shown in figure 5. The low-speed results are not included herein but may be found in reference 31. These configurations employed nozzles with exhaust throat aspect ratios of approximately 4.0. The generic wing-canard nozzle exit was located at the wing trailing edge, and the VEO-wing nozzle exit was located at the trailing-edge-flap hinge line. The latter concept was designed to have the nozzle exhaust flow pass over the upper surface of the flap and exit the flap trailing edge as a thick jet sheet to induce large amounts of circulation lift or so-called supercirculation. The other concept provided a vectored

thick jet sheet at the wing trailing edge to generate this same supercirculation.

Typical longitudinal characteristics (fig. 13) indicate that both configurations produced high lift. With $C_T \approx 1$ and $\alpha \approx 12°$, both have $C_L \approx 2$, which is a very high C_L available for takeoff and landing. When the basic configuration lift, flap lift, and the direct-thrust component in lift are removed from the total aerodynamics as discussed in references 11, 21, 23, and 35, the resulting forces are thrust induced, as illustrated in figure 14. For the generic wing-canard and VEO-wing configurations, the levels of thrust-induced lift (fig. 15) are relatively small (about 5 to 10 percent of total configuration lift) when compared with the direct-thrust component. In fact, because of the shape of the induced-lift curve (i.e., a very rapid increase in $\Delta C_{L,\mathrm{TR}}$ at low C_T followed by essentially straight curves at higher C_T as seen in fig. 16), it can be determined that most, if not all, of the induced-lift increment is due to the nozzle exhaust flow providing boundary-layer control to help reattach separated flow near the nozzle on the trailing-edge flap (ref. 35). That is to say that thrust-induced supercirculation is not really present on these two configurations.

As it would turn out, this proved to be the case for every fighter/attack configuration tested with vectored nozzles of relatively low aspect ratio (i.e., $A < 4.0$ or 5.0). The levels of induced-circulation lift are very low, on the order of 0.1 or 0.2, and the supercirculation seen on STOL transport configurations was not present on fighter/attack configurations. (See refs. 6, 9, 11, 15, 18, 19, and 29.)

There are a few other questions that must be addressed when analyzing longitudinal aerodynamic characteristics:

1. Can the configuration be trimmed?
2. Does the configuration have an L/D appropriate for the area of flight being analyzed? (That is, a configuration on landing approach should not have thrust greater than drag or a negative L/D.)
3. Is the stability level reasonable?

For example, the generic wing-canard configuration had a pitching-moment coefficient less than -0.5 for $C_T = 1.0$ at $\alpha < 16°$ (fig. 13(a)), which would require more nose-up pitching moment to provide trim than the canard was capable of producing (fig. 17). This then was not a viable configuration. Also, when $C_T = 1.0$, $C_D < 0$ (or there is excess thrust); although excess thrust is needed for takeoff, landing could not be accomplished with this level of net thrust. Therefore, this configuration, although capable of generating high lift, cannot be trimmed or landed at the thrust levels required to generate the high lift.

Similar trends for the VEO wing are apparent in the lift and drag data of figure 13(b). The moment data show, however, that this configuration can be trimmed. The level of instability required to allow trim at $\alpha \approx 10°$ to $12°$ is at least 50 percent, and this would constitute a very high level of instability for any configuration.

The problems for these two configurations occur because the high lift was produced by vectoring the main exhaust nozzles that were located well behind the configuration moment center, with the result that the configurations could not be trimmed. Had induced-circulation lift been the controlling mechanism, the center of the propulsive lift would have moved forward on the wing and closer to the moment center. The result would have been only a small shift in the zero-lift pitching moment. The reason that so little supercirculation was developed on these configurations is that the exhaust from the low-aspect-ratio nozzles actually affected a rather small portion of the wing when compared with the jet flap or externally blown flap, STOL transport concepts. The high-aspect-ratio wings on the transport concepts have the exhaust flow distributed over as great a portion of the wingspan as possible to achieve high levels of supercirculation lift.

Blowing Configurations

One approach to obtaining improved circulation lift for fighter configurations seemed to be to distribute the exhaust flow over a greater extent of the wingspan. Two different concepts were investigated:

1. The exhaust flow could be distributed through a primary slotted nozzle located at the flap hinge line, like blown flap concepts, to affect up to the full wingspan.
2. Spanwise blowing could be used in which the exhaust flow would be directed in a spanwise direction by secondary nozzles so that a larger portion of the wingspan would be affected than was the case when only vectored main nozzles were used.

Chordwise Blowing on Flaps

The propulsive wing-canard configuration (fig. 12) employed a slotted nozzle at the flap hinge line to generate circulation lift (concept 1) by blowing the exhaust over the trailing-edge flap. This had a twofold effect in that the high-energy flow over the flap provided boundary-layer control to maintain attached flow on the flap, thereby improving flap effectiveness, and the exhaust exited the flap trailing edge in the form of a jet sheet (like a jet flap) to generate induced-circulation lift. The configuration was such that the blowing on the flap would be varied

to cover the quarter, half, or full wingspan. As with the low-aspect-ratio nozzles previously discussed, the quarter-span blowing generated low levels of circulation lift because only a small extent of the trailing-edge flap was affected by the exhaust flow. The level of induced-circulation lift increased for half- and full-span blowing and accounted for 33 to 50 percent of the total configuration lift at $C_T = 1$ as shown in figures 18(a) and 18(b).

It should be noted in the data that the levels of thrust-induced lift tend to reach a maximum for both the quarter- and half-span blowing cases (i.e., the data show no increase in $\Delta C_{L,\mathrm{TR}}$ after $C_T \approx 1.5$); whereas the full-span blowing case shows increasing $\Delta C_{L,\mathrm{TR}}$ up to the testing limit of $C_T \approx 2.9$, thus showing the importance of affecting as much of the wingspan as possible when generating powered circulation lift. The thrust-induced pitching moment is presented in figure 18(c). Here again there are significant nose-down pitching moments which indicate that the center of lift is located at about $0.70\bar{c}$, as would be expected for such a short-chord blown flap (ref. 36). However, this pitching moment is less than would be produced by pure thrust vectoring.

A major mechanical difficulty of this concept could be encountered in actually integrating the required ducting and slotted nozzles into the wing-flap systems of an operational fighter configuration. Therefore, alternate methods were investigated of providing exhaust flow over the outer portion of the wing by way of spanwise blowing from secondary exhaust nozzles.

Above-Wing Spanwise Blowing

The VEO-wing model was equipped with a spanwise-blowing nozzle located at the wing quarter-chord on the side of the main engine nacelle (fig. 5). This concept provided an exhaust that flowed over the wing upper surface parallel to the wing leading edge and spread out over the outboard portions of the wing trailing-edge flap system (fig. 19). This upper-surface spanwise flow can affect the aerodynamics of this configuration as follows:

1. The high-energy flow provided boundary-layer control on the wing and flap upper surfaces.

2. The exhaust flow leaving the trailing-edge flap could act as a thick jet sheet to provide some induced-circulation lift.

3. The flow on the wing upper surface effectively increased the wing thickness and camber as indicated in sketch A.

Comparing the data of figure 20 with the data of figures 15 and 18 indicates that this concept is better at generating thrust-induced lift than the main nozzles alone, but it was not as effective as the full-span blown flap. This is not surprising since the spanwise-blowing flow would incur losses not experienced by the blown flap. The jet is mixing, interacting with the free-stream flow, and flowing over the wing surface for some distance before affecting the flap. This would cause the spanwise jet to be less efficient at either maintaining attached flow on the flap or providing the trailing jet sheet required for induced circulation. Although perhaps inefficient, the spanwise blowing certainly affects a much greater portion of the wingspan than the vectored nozzles (see fig. 19) and thus produces significantly greater levels of thrust-induced lift than the main nozzles alone.

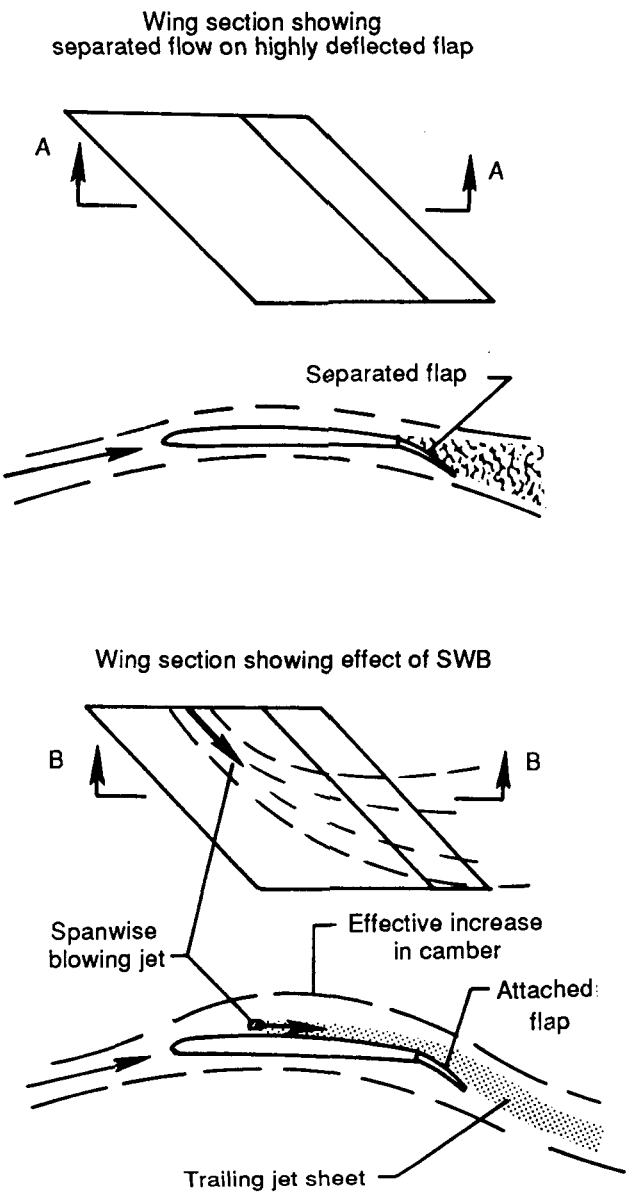

Sketch A

Underwing Spanwise Blowing

The two advanced medium STOL transport aircraft of the 1970's (YC-14 and YC-15) used successful blown flap systems to produce high levels of circulation lift. The upper-surface blown flap method utilized viscous Coanda effects to turn the exhaust flow downward over the curved upper surface of the wing-flap system, whereas the externally blown flap uses impingement of the exhaust flow upon the deflected flap to produce the downward flow as shown in sketch B.

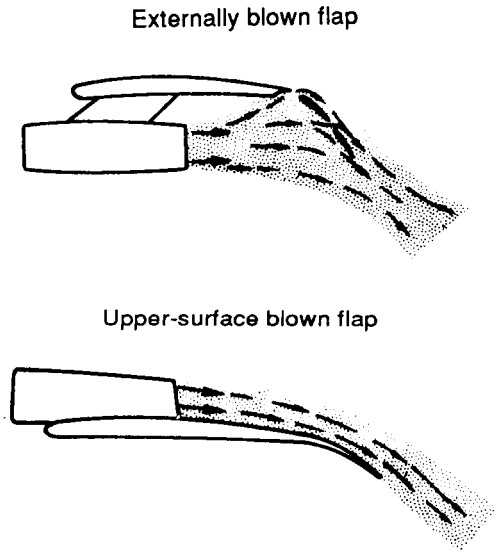

Sketch B

Although the externally blown flap concept worked well for transport aircraft such as the YC-15, the wing pylon-mounted engines were not acceptable for very high performance aircraft such as fighters because of excessive profile and wave drag. The underwing spanwise-blowing concept shown in figures 4 and 21 was developed to take advantage of the lower surfaces of the wing and flaps in turning the flow while avoiding the high-drag problems associated with underwing pylon-mounted engines. In this concept the spanwise exhaust flow issues from a secondary nozzle located in the side of the main engine nacelle but on the underside of the wing-flap system. The spanwise flow can be blown parallel to the trailing-edge flap so that it first interacts with the free-stream flow to turn in a downstream direction to then be deflected downward by the flap, or it can be blown directly into the flap to be deflected downward.

In either case the flow will spread because of the blockage of the flap itself and this will increase the effective span of the jet. By affecting a greater portion of the flap span, the jet should tend to increase levels of induced-circulation lift above that of deflected nozzle concepts. Since circulation lift increases with increased jet-sheet deflection, this concept was expected to provide higher levels of $\Delta C_{L,\mathrm{TR}}$ as the trailing-edge flap deflection was increased (i.e., forcing the jet sheet downward) as compared with upper-surface blowing concepts where, at high deflections, the flow cannot remain attached to the upper surface of the flap.

The induced aerodynamic data of figure 22 show increasingly high levels of circulation lift as flap deflection increases. The peak value of circulation lift is at $\delta_f = 45°/45°$ (inboard-flap/outboard-flap deflections) and $C_\mu \approx 1.0$, and is about 22 percent of the total configuration lift (ref. 23). The drop-off in $\Delta C_{L,\mathrm{TR}}$ for $C_\mu > 1.2$ is indicative of the spanwise jet penetrating so far outboard that it not only misses a portion of the inboard flap but also blows out beyond the end of the flap and is not deflected downward. (See fig. 23.) In order to prevent this occurrence, the spanwise jet must be angled slightly aft from the position parallel to the flap hinge line so that the jet actually impinges on the flap lower surface. The data (fig. 24) show that a jet deflection of 15° or 30° into the flap (i.e., $\Lambda = 45°$ or 60°) produces higher levels of $\Delta C_{L,\mathrm{TR}}$ than when $\Lambda = 30°$ (parallel to the hinge line), thus indicating that the jet is generally impinging on and spreading over the flap.

Mechanical Flaps

As an alternative to complex powered-lift systems, attention was also given to mechanical-flap systems including both leading- and trailing-edge devices. An extensive investigation of leading-edge vortex flaps and leading-edge Krueger flaps in combination with full-span, slotted trailing-edge flaps was conducted using the configuration shown in figure 11. The data of figure 25 show that the full-span trailing-edge flap was a very effective high-lift device on the wing-canard configuration. As is true with powered high-lift systems, this flap produced large nose-down pitching moments that taxed the trim capability of the canard. Trim was to be provided by the vectoring nozzle and will be discussed in a subsequent section of this paper. Further increases in lift were provided at high angles of attack ($\alpha > 12°$) along with increases in L/D as the leading-edge Krueger flap maintained attached leading-edge flow.

Leading-edge vortex flaps on the wing-alone configuration, although not increasing the configuration lift, did nevertheless increase L/D at $C_L > 0.5$ as the leading-edge vortex acted on the forward-facing flap surface (fig. 26). This was accompanied by an early

unstable break in the pitching-moment curve because the sharp leading-edge flap established a well-defined vortex flow at a lower angle of attack than the clean wing leading edge. When the vortex flaps were deflected up 45°, then the vortex on the upper surface created not only higher lift but also higher drag as would be used for approach and landing.

High-Lift Summary

Although the high-lift systems investigated were successful to various degrees in producing high lift, they suffered from two drawbacks:

1. Difficulty in trimming the nose-down pitching moments generated by the high lift with conventional aerodynamic controls.
2. Excessive thrust for approach and landing because of the high power settings required to generate the high lift.

Even with these two problems, the basic simplicity of the spanwise-blowing concepts and their relatively high levels of induced-circulation lift seem to make them a reasonable concept. The problems of integration into a configuration and developing methods for providing trim and spoiling excess thrust seem to be within reason.

Alternate Methods for Longitudinal Trim

The requirement for longitudinal trim is obvious, but it is sometimes overlooked during research programs. An aircraft out of trim simply will not fly; and if the required trimming moments saturate or exceed the available aerodynamic control power, then some supplemental means must be provided to obtain trim and control as illustrated in figure 27. Several options are available to provide the necessary forces for balancing the aerodynamic moments. These options may involve any of the following: (1) reconfiguring the geometry so that the force causing the large pitching moments (i.e., a highly loaded flap) is not so far from the moment center (or center of gravity), (2) providing extra control surfaces (either power augmented or three surface configurations), or (3) providing direct force devices such as vectoring nozzles or nose jets. Reconfiguring the geometry is not always a viable option because other mission constraints such as cruise efficiency, maximum Mach number, or maneuvering limits might well dictate where the wing must be located. Therefore, most of the research on this technology area has focused on the use of powered control surfaces (to provide higher forces than conventional aerodynamic surfaces) and direct force devices such as control jets.

Nose Jet

The generic wing-canard configuration of figure 3, although capable of producing reasonable levels of high lift, could not be trimmed by the existing canard (which was sized on the basis of maneuvering control forces and cruise stability) and had excess thrust for landing. An analysis of this situation (ref. 8) led to the conclusion that a small nose jet could be sized to provide sufficient direct lift for trimming the pitching moment and would allow the canard to provide the necessary control forces for both takeoff and landing. For example, figure 28 illustrates that a nose jet located far forward on the body could be sized to provide an increment in zero-lift pitching moment for trim only. Because of the long moment available, the jet would have to provide a force of only $C_L = 0.2$ to provide trim for both takeoff and landing. This concept analysis led to a study that defined a nose jet to provide trim for the configuration shown in figure 6. The model was a high-speed penetrator aircraft (ref. 13) that was desired to have some STOL capability. It was equipped with vectoring main nozzles to provide direct-thrust high lift which easily exceeded the trim capability of the canard. The small nose jet was placed farther forward on the configuration than a normal lift engine would be in order to take advantage of a long moment arm to produce the nose-up pitching moments needed for trim. The jet was sized to have about 12 to 15 percent of total lift and was angled aft to prevent reverse thrust at angles of attack below 12°.

The configuration aerodynamics are shown in figure 29. Trim could not be achieved by the canard with the main nozzles vectored 43° and $C_T = 0.75$, even though the configuration was designed to operate with a 15-percent unstable static margin. By using the nose jet with $C_T = 0.11$ (or 13 percent of total thrust), the configuration can be trimmed with a sufficient margin of canard control power left to provide longitudinal control. It should be noted that the drag at this condition is slightly low (i.e., excess thrust) for proper approach. The additional drag of landing gear, speed brakes, etc., should increase the drag to a level more appropriate for approach at these thrust levels. In this case, trim was obtained by placing a small direct lift force forward on the configuration to produce nose-up pitching moment.

Main Nozzle Vectoring

An alternative to a nose jet might be to use main nozzle vectoring to provide a small downward force near the aft end of a configuration. By taking advantage of a long moment arm to the center of gravity, this down force could generate sufficient pitching

moment to obtain trim without unduly reducing lift. This does eliminate the large lift increments available from the main engine exhaust, but a good high-lift system on the wing can generate the needed lift. The configuration of figure 11 shows an attack concept with full-span slotted flaps for high-lift and vectoring/reversing nozzles. In this concept the high-lift flaps produce large nose-down pitching moments (as do most flap systems). Because of the very long moment arm to the vectoring nozzles, a small negative lift force is required to trim the configuration. This force is smaller than the lift produced by the flaps, thus resulting in a net increase in lift that can be trimmed (fig. 30).

Blown High-Lift Canards

Another alternative to obtaining the trimming forces is to increase the effectiveness of canard surfaces by using long moment arms and blown flaps to give positive lift increments for generating more pitching moment. The concept shown in figure 9 is a wing-canard dual-role fighter/attack configuration using a trailing-edge flap system and vectoring main nozzle to provide the high lift and drag required for approach. The canard was equipped with a full-span blown flap and leading-edge Krueger flap to increase its high-lift capability. The high-lift performance is presented in figure 31. Note that although the blown canard provided a significant nose-up pitching moment, the total lift remained unchanged because the increased canard downwash unloaded the main wing as the lift increased on the canard surface. The discussion in reference 9 indicates that this arrangement can result in nearly constant total C_L over a range of canard loadings. Again, the configuration drag is near zero without the additional drag from landing gear, speed brake, etc. Because of the effectiveness of blown flaps, this concept requires a thrust level of only 2 to 3 percent of total thrust to provide the required trimming moments as opposed to 10 to 20 percent for direct force devices. This approach is probably the most elegant method of providing trim in that it blends well with a configuration and uses a very efficient form of induced high lift rather than brute force.

Trim Summary

In general, it appears that any configuration likely to represent an advanced fighter will require some form of augmented thrust or powered lift to achieve the necessary levels of high lift required for STOL operations. Because of the large pitching moment associated with many high-lift concepts and the low airspeed needed on STOL approaches, some new method will be needed to supplement conventional aerodynamic surfaces to provide longitudinal trim while leaving control surfaces free for controlling the aircraft. The three concepts just discussed all appear to be capable of providing trim for an advanced fighter configuration. Each configuration will suffer to some extent a penalty for increased weight and volume, two items of extreme importance in high-performance aircraft. Therefore, a detailed design integration including mission requirements will be needed to allow selection of an appropriate trimming concept.

Thrust Reversing and Vectoring

One of the keys to effective STOL operations will be the ability of a configuration to provide military power thrust reversing from very shortly after landing to near-zero velocity to minimize the ground roll, particularly during poor weather conditions where wheel-braking effectiveness is reduced. In order to have military power available within about 1 sec of touchdown, the aircraft engines must be at or near that power setting while the aircraft is on final approach. If the approach were flown at normal (i.e., low) power settings, then the time lag required for the engines to spool up to military power after the throttle command would be excessive and the effectiveness of the reverse thrust applied to touchdown would be lost. The problem then becomes a question of what to do with all the excess thrust present on approach, since this class of aircraft will accelerate and/or climb rapidly at military power.

Some amount of thrust can be used to generate lift or control forces as discussed previously, but some of the excess thrust will likely have to be spoiled in some fashion to give the proper "thrust minus drag" or net drag values for the desired approach slope. Thus, with high power settings during the approach, the only time lag from touchdown to full reverse thrust is the time for mechanical devices to vector the exhaust (about 1 sec) rather than the time for the engine to spool from near flight idle to military power (about 4 to 5 sec). Thrust reversers are generally limited to use above some velocity level where hot gas ingestion into the engine inlet or foreign object damage (FOD) may become a problem. This is typically at a velocity where significant energy is left in the aircraft and stopping the aircraft can still be quite a problem under poor braking conditions. A solution is needed to eliminate or reduce hot gas ingestion and FOD to allow thrust-reverser operation to a velocity as low as possible.

There are basically two types of thrust spoiling/reversing/vectoring nozzle types currently under

study. The first type has the main nozzle closed on approach and all the exhaust flow passing through secondary nozzles located on the top and bottom of the engine. As shown in figure 32, this nozzle concept has a series of variable-position or rotating vanes that can vector the exhaust flow over a wide range of angles to provide a desired net thrust after spoiling the majority of the thrust by symmetrical thrust cancellation from the upper and lower nozzles. The second type of vectoring nozzle has symmetrical fixed-geometry secondary nozzles and a main nozzle that is partially closed on approach (referred to as "a multifunction nozzle"). As shown in figure 33, this nozzle achieves a desired net thrust by varying the amount of exhaust flow that passes through the variable main nozzle. This forces the remaining exhaust flow out the reverse nozzles, thereby accomplishing the dual purposes of symmetrically spoiling forward thrust and also providing a reverse-thrust component to reduce the effective amount of forward thrust. Both nozzle types then vector all exhaust flow forward (45° to 55°) with the main nozzle closed for full thrust reversing shortly after touchdown.

Thrust Reversing

Both of these thrust-reversing nozzle concepts have been studied. The detailed results of the rotating-vane reverser concept are classified and found in reference 26; these results will not be discussed herein. This discussion will be focused on the multifunction nozzle concept. This nozzle concept was tested in two variations on the configuration shown in figure 11. The first nozzle was a two-dimensional convergent-divergent (2D-CD) concept with fixed reverser port angles and a vectoring main nozzle (detailed in fig. 34). The second concept was a single-expansion ramp nozzle (SERN) concept also having fixed reverser port angles and a vectoring main nozzle (detailed in fig. 35). The SERN was also equipped with "splay doors" that were intended to vector the exhaust flow away (i.e., outboard) from the fuselage to reduce exhaust impingement on the ground plane. This will minimize aerodynamic interference of the exhaust plume with the configuration, minimize hot gas ingestion into the engine inlets, and reduce the risk of foreign object damage (FOD) to aircraft engines. The longitudinal aerodynamics of the configuration (see fig. 36) indicate that either nozzle (2D-CD or SERN) can provide a net thrust minus drag appropriate for approach. The vectoring capability of either nozzle allows for a wide range of trimmed conditions while maintaining approach L/D.

Splay Door Reversing

One area of concern in thrust-reversing operations is the interaction of the hot exhaust plume with the ground, the airframe, and the engine inlets. Adverse interactions can require the thrust reverser to be shut off at relatively high ground speeds, thereby reducing the time available for effective thrust reversing. The "splay door" reverser is intended to vector the exhaust away from the configuration to minimize the adverse interactions and allow thrust-reverser operations to lower forward speeds. The photographs of figure 37 indicate that the reverser flow field does not penetrate as far forward when the "splay doors" are used as compared with the flow field generated without splay doors.

For analysis purposes, comparisons of the point where the flow field reaches the area of the engine inlet show that the splay door configuration could be operated down to a dynamic pressure of about 15 lbf/ft^2 as opposed to 30 lbf/ft^2 for a configuration without splay doors for an NPR of 2.5 or about military power. This analysis assumed that the reverser would need to be shut down at the point where the engine exhaust reached the inlet to prevent foreign object damage or hot gas reingestion into the inlet. For this nozzle there is a loss in reverser effectiveness (i.e., lower drag) when the reverse flow is directed away from the fuselage centerline. (See top right of fig. 38.) Although generating slightly lower stopping forces, this nozzle concept allows for a lower operating speed before the reverser must be shut off. The lower energy state at reverser shutoff for the aircraft allows much shorter runway lengths when poor weather conditions exist.

As shown in figure 38 the calculated ground rolls for a configuration with or without the splay door nozzle are about equal when good wheel braking is available. If wheel braking is reduced, the lower operating speeds for the splay door configuration show a marked reduction in landing runway required.

Thrust-Reversing Summary

It can be said that several nozzle concepts appear to provide the net thrust needed for approach while allowing military power thrust settings needed for effective reverse thrust once the aircraft is on the ground. It also appears that the reverse flow should be directed away from the aircraft to allow lower velocity operations before the reverser must be shut down. The nozzle concepts investigated also can provide main nozzle vectoring to maintain trim during approach. The main drawbacks to this type of nozzle are likely to be weight and complexity.

Ground Effects

Although it has been discussed previously in this report, the subject of ground effects as a separate technology is a critically important one and requires careful attention. When an aircraft approaches the ground, the flow field around the body is constrained as illustrated in figure 39. The downwash from lifting surfaces or vectored exhaust flows is not able to flow through the solid boundary of the ground but must instead either stagnate or flow outward, parallel to the boundary. The net effect of this redirected flow is essentially to induce an upwash on the aircraft with an attendant increase in the effective aspect ratio of the wing. As a result, lift is increased, drag is reduced, and a nose-down increment in pitching moment is generally induced.

This combination of effects is illustrated in figure 40 for an unpowered fighter configuration and in figure 41 for the propulsive wing-canard research configuration. The overall trend of increasing lift is quite evident on both configurations but is larger on the propulsive wing-canard configuration at high thrust levels. Even with the small changes in drag, the increase in lift is sufficient to produce substantial increases in L/D that reduce the aircraft sink rate and flatten the flight path as the ground is approached. All configurations tested with powered exhausts exhibited the trend of increased lift in ground effect; only the magnitude differed. Drag and pitching moment tended to vary somewhat as they are apparently more sensitive to configuration differences.

Significant ground effects are possible when reverse thrust is employed because the reversed exhaust flows interact with the free stream, the ground plane, and the airframe. For the wing-canard configurations tested, the results shown in figures 42 and 43 are typical. The trends in these figures are different from the conventional trends in that lift is reduced and large nose-up increments in pitching moment occur. As the reverser flow field moves forward, it can envelop the wing, thus reducing the angle of attack and/or dynamic pressure and reducing the wing lift. Meanwhile, the canard, because it is far forward, does not yet feel the reverser flow field and maintains lift. The net effect is a loss in total lift accompanied by a nose-up pitching moment. This combination of effects could lead to problems on actual aircraft since the loss of lift can be expected to result in hard landings and the nose-up change in pitching moment can lift the nose if sufficient control power is not available.

As mentioned in the thrust-reversing section of this paper, dealing with vectoring the reverse flow away from the fuselage and ground can help to reduce these effects since the effect of the exhaust plume is delayed to lower speeds as illustrated in figure 44. The effect on the configuration of figure 11 is shown in figure 45 where the difference in approach configurations is the splay door and the resulting reverse-thrust vector angle. For the case without the splay door, the data indicate the typical loss in lift and nose-up pitching moment as the reverse flow reduces wing lift while the canard is still lifting. This effect is not apparent in the data for the configuration with splay doors deployed. Instead, the lift increased and the pitching moment decreased as the ground plane was approached. These results along with the floor tufts of figure 37 led to the conclusion that the splay doors eliminated a potential adverse ground effect for this configuration by keeping the flow field directed away from the aircraft body and wing.

Static ground effects tend to have a common trend as the ground plane is approached, that is, lift is increased. However, if vectored or reversed thrust is present, large lift losses can be encountered as the exhaust plane interacts with the airframe.

Recent experimental evidence (ref. 37) has shown that rate of descent is an important parameter in simulating ground effects, especially for thrust-reversing configurations. Therefore, care should be taken in interpreting all static ground effect results.

Synthesis of Technologies

An effort was made to develop an advanced STOL fighter aerodynamic configuration based on incremental aerodynamic data that could be applied to a baseline configuration. Reference 30 (reporting on Configuration Development of Advanced Fighters (CDAF)) presented an advanced dual-role fighter/attack aircraft concept developed during the late 1970's. This CDAF configuration, which was designed as a conventional takeoff and landing aircraft, gave rise to wind-tunnel models like those in figures 9 and 10 which closely represented the original geometry. As it would happen, the NASA generic wing-canard configuration (fig. 4) is also fairly similar to this fighter configuration. It was felt that incremental data from these three wind-tunnel models (used to investigate various STOL technologies) could be applied to the original configuration data to build up an aerodynamic configuration with minimum errors from configuration effects.

Because of the similarity between the CDAF and the ATTAC configurations, the increments from the high-lift blown canard (fig. 46) were included directly in configuration aerodynamics. The baseline aerodynamics are presented in figure 47. These aerodynamics, which are for zero thrust of the main nozzle, no flap deflection, and BLC blowing on the canard flap, include the effect of the canard downwash on the rest

of the configuration. The configuration aerodynamics must meet the following criteria to be viable:

1. The angle of attack should not exceed 15° to eliminate the need for excessively long landing gear to prevent tail strikes on takeoff and landing.
2. The lift coefficient should be greater than 1.2 in order to give an approach velocity less than 110 knots, if given a landing wing loading around 50 lbf/ft^2.
3. The pitching moment must be zero (i.e., trimmed) at the approach angle of attack without excessive pitch instabilities.
4. The lift and net drag (i.e., thrust drag) must allow for an approach glide slope around 4° with the thrust set to military power.

The baseline aerodynamics (fig. 48) indicate that $C_L = 1.2$ occurs at about $\alpha = 20°$. The powerful blown canard produces significant nose-up pitching moment and the unpowered drag is clearly too high for a normal glide slope.

Incremental data were applied to this baseline in order to produce the final aerodynamics shown in figure 48. The increment in flap lift came from the data for a generic wing-canard configuration with a full-span trailing-edge flap deflected 26°. The data in reference 23 had indicated that deflecting the flap greater than 26° did not really increase lift but did increase nose-down pitching moment and drag. The induced-lift increment also came from this configuration with the flap deflected 26° and the spanwise blowing nozzles exhausting military thrust. The flap and SWB generate significant levels of lift and nose-down pitching moment but have rather little effect on drag because the flow over the flap remains attached. When the direct-thrust component from the SWB nozzles is included, there is no change in pitching moment because the nozzle thrust vector is almost through the moment center of the configuration. Thrust changes both the lift and drag to the extent that the configuration now has excess thrust. Landing-gear speed brakes and the like were not incorporated into the wind-tunnel model; but by including their drag, as estimated from reference 38, they produced L/D consistent with normal approach glide slopes.

Finally, the configuration still has excessive nose-up pitching moment that can be used for control. It would appear that a configuration like CDAF could be turned into an aerodynamically viable STOL vehicle. The SWB nozzle could be constructed similarly to the rotating-vane concepts (ref. 26); then the nozzle could provide not only induced lift and direct thrust on approach but also effective reverse thrust during landing rollout. Also, since the reverse thrust would not impinge upon the ground, the problems of ground plane interference affecting aerodynamics and inlet ingestion, which can severely limit thrust-reverser usefulness, can most likely be reduced or even eliminated. The final configuration might then look something like that in figure 49.

As a final check on the aerodynamic viability of this configuration, calculations were made to predict the ground roll that might be achieved. (See fig. 50.) A no-flare landing scenario was assumed with 50 percent of military power available for thrust reversing from 1 sec after touchdown to a velocity of 10 knots. Braking forces were supplied using an antiskid system that varied friction coefficients from 0.025 at 140 knots to 0.54 at 0 knot. Using the approach aerodynamics just discussed ($C_L > 1.2$) to set approach airspeed yields very low, predicted ground rolls. Indications are that 1200 ft might even be possible on icy runway surfaces. This short ground roll is brought about by allowing the thrust reversers to operate down to 10 knots. Of course, touchdown dispersion and reduction in aircraft performance will lengthen the total runway required for landing, but it would seem that 1500 to 1800 ft should be a reasonable field length to expect from such a configuration.

Conclusions

For the past 10 years an extensive research program has been underway in the Subsonic Aerodynamics Branch at the NASA Langley Research Center to define and develop technologies to make possible low-speed flight of high-performance aircraft. The emphasis of this research has been directed toward short takeoff and landing (STOL) and short takeoff and vertical landing (STOVL) operations rather than on regular "up and away" flight characteristics, although the data base generated would apply to almost any subsonic flight condition where compressibility is not a factor. This program has combined NASA in-house research with joint NASA/Department of Defense/Industry research to explore several important areas on advanced fighter/attack configurations: high lift, an alternate means of providing longitudinal trim and control, thrust vectoring and reversing nozzles, and ground effects. A number of different technologies have been investigated in the Langley 14- by 22-Foot Subsonic Tunnel on a number of different configurations over an angle-of-attack range from −4° to 50° at angles of sideslip from −15° to 15°. Free-stream dynamic pressures ranged from 0 to 70 lbf/ft^2, thrust coefficients from 0 to 3.0, and ground heights from wheel touchdown to free-air conditions. The most significant findings of this research are summarized as follows:

1. High levels of induced-circulation lift are not present on fighter-type configurations that have vectoring exhaust nozzles of aspect ratio 4 or less because of the limited percentage of the wingspan affected by the exhaust flow.

2. Spanwise blowing on the wing produced significant induced-circulation lift. The underwing spanwise blowing on the trailing-edge flap system was found to induce lift increments amounting to as much as 22 percent of the total configuration lift.

3. All powered high-lift systems investigated have suffered large nose-down pitching moments that exceed the trim capability of normal aerodynamic control surfaces. The high thrust levels needed for high lift will require thrust spoiling to permit a STOL or STOVL approach and landing.

4. Three alternate methods of providing longitudinal trim have been demonstrated on fighter-type configurations: a small nose jet sized only for trim at approach airspeeds rather than during hover, a blown high-lift canard, and simple exhaust thrust vectoring. In various amounts, these concepts all suffer extra weight, volume, and complexity (items which are of extreme importance in high-performance aircraft).

5. The use of partial thrust spoiling from multifunction nozzles can provide correct net drag levels for approach and landing with engine thrust set at military power. This will reduce the time delay after touchdown for application of effective reverse thrust to about 1 sec.

6. Thrust reversing, although essential to short landing operations, can produce unwanted aerodynamic characteristics, particularly if employed during the approach to landing. Vectoring the reverse flow away from the configuration through the use of "splay doors" was shown to be a viable method of reducing or eliminating aerodynamic problems as well as problems of foreign object damage and hot gas ingestion.

7. Static ground effects can be significant and cause lift losses when vectored or reverse thrust is employed. However, recent evidence indicates that rate of descent can have a large impact on the actual dynamic ground effects and that care should be used when interpreting static ground effects results.

NASA Langley Research Center
Hampton, VA 23665-5225
March 8, 1988

References

1. Byrnes, John M.; Richey, G. Keith; and Lowry, Randall B.: Views on V/STOL Tactical Fighter Aircraft: Technology Needs and Relationships to the Runway Denial Problem. *The Impact of Military Applications on Rotorcraft and V/STOL Aircraft Design,* AGARD-CP-313, June 1981, pp. 8-1–8-13.
2. Barlow, Robert C.; Collier, Keith I.; and Richey, G. Keith: Military Aircraft Technology—Needs and Trends for the 80's. AIAA-81-1691, Aug. 1981.
3. Hendrickson, Ronald H.; Krepski, Robert E.; and Hudson, Raymond E., Jr.: Incorporating STOL Capability Into Tactical Fighter Aircraft Concepts. AIAA-84-0573, Jan. 1984.
4. Whitten, P. D.; Kennon, I. G.; and Stumpfl, S. C.: Experimental Investigations of a Nozzle-Wing Propulsive-Lift Concept. AIAA Paper No. 76-625, July 1976.
5. Whitten, P. D.; and Howell, G. A.: *Investigations of the VEO-Wing Concept in an Air-to-Ground Role.* AFFDL-TR-79-3031, U.S. Air Force, Mar. 1979.
6. Yip, Long P.; and Paulson, John W., Jr.: *Effects of Deflected Thrust on the Longitudinal Aerodynamic Characteristics of a Close-Coupled Wing-Canard Configuration.* NASA TP-1090, 1977.
7. Thomas, James L.; Paulson, John W., Jr.; and Yip, Long P.: Deflected Thrust Effects on a Close-Coupled Canard Configuration. *J. Aircr.,* vol. 15, no. 5, May 1978, pp. 287–292.
8. Paulson, John W., Jr.; Thomas, James L.; and Winston, Matthew M.: Transition Aerodynamics for Close-Coupled Wing-Canard Configuration. AIAA Paper 79-0336, Jan. 1979.
9. Paulson, John W., Jr.; and Thomas, James L.: *Summary of Low-Speed Longitudinal Aerodynamics of Two Powered Close-Coupled Wing-Canard Fighter Configurations.* NASA TP-1535, 1979.
10. Paulson, J. W., Jr.: Analysis of Thrust-Induced Effects on the Longitudinal Aerodynamics of STOL Fighter Configurations. AIAA-80-1879, Aug. 1980.
11. Paulson, J. W., Jr.: Analysis of Thrust-Induced Effects on the Longitudinal Aerodynamics of STOL Fighter Configurations. *J. Aircr.,* vol. 18, no. 11, Nov. 1981, pp. 951–955.
12. Hiley, P. E.; Wallace, H. W.; Booher, M. E.; and Reinsberg, J. G.: *Advanced Nozzle Concepts Program. Summary of Results and Nozzle Integration Design Criteria.* AFWAL-TR-81-3165, Vol. I, U.S. Air Force, Jan. 1982. (Available from DTIC as AD B066 835L.)
13. Hutchinson, R. A.; and Sussman, M. B.: *Propulsive Lift STOL Aerodynamics Research Test.* AFWAL-TR-81-3169, U.S. Air Force, Feb. 1982. (Available from DTIC as AD B064 944L.)
14. Paulson, John W.; Whitten, Perry D.; and Stumpfl, Stephen C.: *Wind-Tunnel Investigation of the Powered Low-Speed Longitudinal Aerodynamics of the Vectored-Engine-Over (VEO) Wing Fighter Configuration.* NASA TM-83263, 1982.
15. Banks, Daniel W.; Quinto, P. Frank; and Paulson, John W., Jr.: *Thrust-Induced Effects on Low-Speed Aerodynamics of Fighter Aircraft.* NASA TM-83277, 1982.
16. Paulson, J. W., Jr.; Gatlin, G. M.; Quinto, P. F.; and Banks, D. W.: Trimming High Lift for STOL Fighters. AIAA-83-0168, Jan. 1983.
17. Quinto, P. Frank; and Paulson, John W., Jr.: *Flap Effectiveness on Subsonic Longitudinal Aerodynamic Char-*

acteristics of a Modified Arrow Wing. NASA TM-84582, 1983.

18. Hutchinson, R. A.; Sussman, Mark B.; Mainquist, R.; and Paulson, J. W., Jr.: STOL Wind Tunnel Test Results for a Tactical Supercruiser. AIAA-83-1224, June 1983.
19. Krepski, R. E.; and Hendrickson, R. H.: *Investigation of Advanced Technologies for Tactical Aircraft. Volume IV—Concept Validation--Wind Tunnel Test Program Results, Part II—Wind Tunnel Test Data.* AFWAL-TR-82-3069, Vol. IV, Pt. II, U.S. Air Force, Aug. 1983. (Available from DTIC as AD B079 146L.)
20. Paulson, J. W., Jr.; Gatlin, G. M.; Quinto, P. F.; and Banks, D. W.: Trimming Advanced Fighters for STOL Approaches. *J. Aircr.,* vol. 20, no. 11, Nov. 1983, pp. 957–962.
21. Quinto, P. Frank; and Paulson, John W., Jr.: *Thrust-Induced Effects on Subsonic Longitudinal Aerodynamic Characteristics of a Vectored-Engine-Over-Wing Configuration.* NASA TP-2228, 1983.
22. Banks, D. W.; and Paulson, J. W., Jr.: Approach and Landing Aerodynamic Technologies for Advanced STOL Fighter Configurations. AIAA-84-0334, Jan. 1984.
23. Paulson, John W., Jr.; Quinto, P. Frank; and Banks, Daniel W.: *Investigation of Trailing-Edge-Flap Spanwise-Blowing Concepts on an Advanced Fighter Configuration.* NASA TP-2250, 1984.
24. Stewart, V. R.; and Paulson, J. W., Jr.: The Aerodynamic Characteristics of a Propulsive Wing/Canard Concept in STOL. AIAA-84-2396, Oct.–Nov. 1984.
25. Banks, Daniel W.; and Paulson, John W., Jr.: Approach and Landing Technologies for STOL Fighter Configurations. *J. Aircr.,* vol. 22, no. 4, Apr. 1985, pp. 277–282.
26. Banks, Daniel W.; and Paulson, John W., Jr.: *Aerodynamic Characteristics and Predicted Landing Performance of an F-15 Fighter With Two Thrust-Reverser Configurations.* NASA TP-2466, 1985.
27. Stewart, V. R.: *Aerodynamic Characteristics of a Propulsive Wing/Canard Concept at STOL Speeds.* NASA CR-177982, 1985.
28. Gatlin, Gregory M.; Banks, Daniel W.; and Paulson, John W., Jr.: *Longitudinal Aerodynamic Characteristics of an Advanced Fighter Configuration With Various High-Lift Devices at Low Speed.* NASA TP-2561, 1986.
29. Callahan, Clifton J.; and Doonan, James G.: *Advanced Exhaust Nozzle Concepts for Short Takeoff and Landing (STOL) and Survivability. Volume I—Foundations of Program and Principal Study Results.* AFWAL-TR-85-3045, Vol. I, U.S. Air Force, May 1986.
30. Bavitz, Paul C.; et al.: *Configuration Development of Advanced Fighters.* AFWAL-TR-80-3142, U.S. Air Force, Nov. 1980.

    Volume 1, Executive Summary.
    Volume 2, Concept Derivation.
    Volume 3, Concept Definition and Validation.
    Volume 4, Wind Tunnel Test Program.
31. Leavitt, Laurence D.: *Longitudinal Aerodynamic Characteristics of a Vectored-Engine-Over-Wing Configuration at Subsonic Speeds.* NASA TP-1533, 1979.
32. *STOL Technology.* NASA SP-320, 1972.
33. *V/STOL Aerodynamics.* AGARD-CP-143, Oct. 1974.
34. *Take-off and Landing.* AGARD-CP-160, Jan. 1975.
35. Mavriplis, Fotis; and Gilmore, David: Investigation of Externally Blown Flap Airfoils With Leading Edge Devices and Slotted Flaps. *V/STOL Aerodynamics,* AGARD-CP-143, Oct. 1974, pp. 7-1–7-12.
36. McCormick, Barnes W., Jr.: *Aerodynamics of V/STOL Flight.* Academic Press, Inc., 1967.
37. Kemmerly, Guy T.; Paulson, John W., Jr.; and Compton, Michael: Exploratory Evaluation of a Moving-Model Technique for Measurement of Dynamic Ground Effects. AIAA-87-1924, June–July 1987.
38. Hoerner, Sighard F.: *Fluid-Dynamic Drag.* Publ. by the author (148 Busteed Drive, Midland Park, New Jersey 07432), 1965.

Table I. Summary of Configurations and Technologies Investigated

Configuration	Technologies	Figure	Reference
Generic wing-canard fighter model	Spanwise blowing, induced lift, nose jet for trim, canard effects, mechanical flaps, and vectored thrust	3, 4	6, 9, 22, 23
Vectored-engine-over-wing (VEO-wing) model	Spanwise blowing, induced lift, and vectored thrust	5	14, 21
Mach 2 supercruiser model	Reverse thrust, induced lift, nose jet for trim, and vectored thrust	6	13
F-15 thrust-reverser model	Reverse thrust, ground effects, thrust spoiling, and vectored thrust	7	26
Generic high-sweep fighter model	Mechanical flaps	8	17
Advanced Technologies for Tactical Aircraft (ATTAC) model	High-lift canard for trim, ground effects, vectored thrust, and reverse thrust	9	19
Advanced exhaust nozzle concepts for STOL and survivability model	Nozzle type and vectored thrust	10	29
Advanced nozzle concepts-B (ANC-B) model	Ground effects, trim, nozzle type, mechanical flaps, vortex flaps, vectored thrust, and reverse thrust	11	12, 28
Propulsive wing-canard model	Induced lift, canard effects, and ground effects	12	24, 27

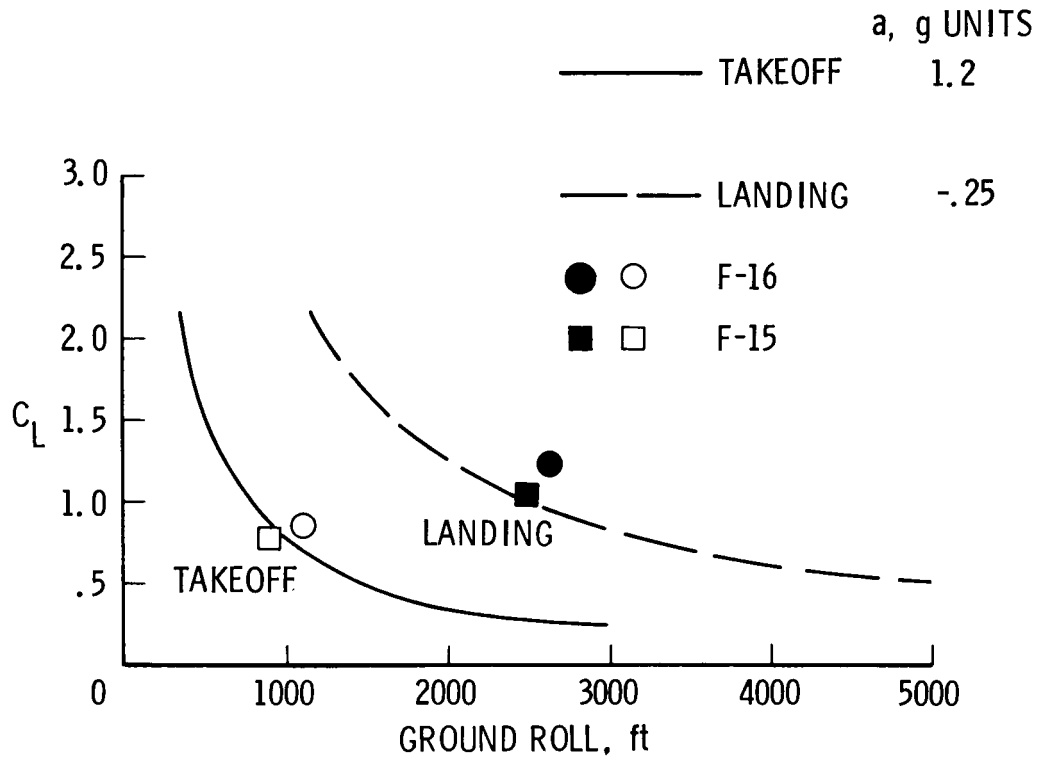

Figure 1. Effect of lift coefficient on calculated ground rolls for lightly loaded takeoff and landing conditions.

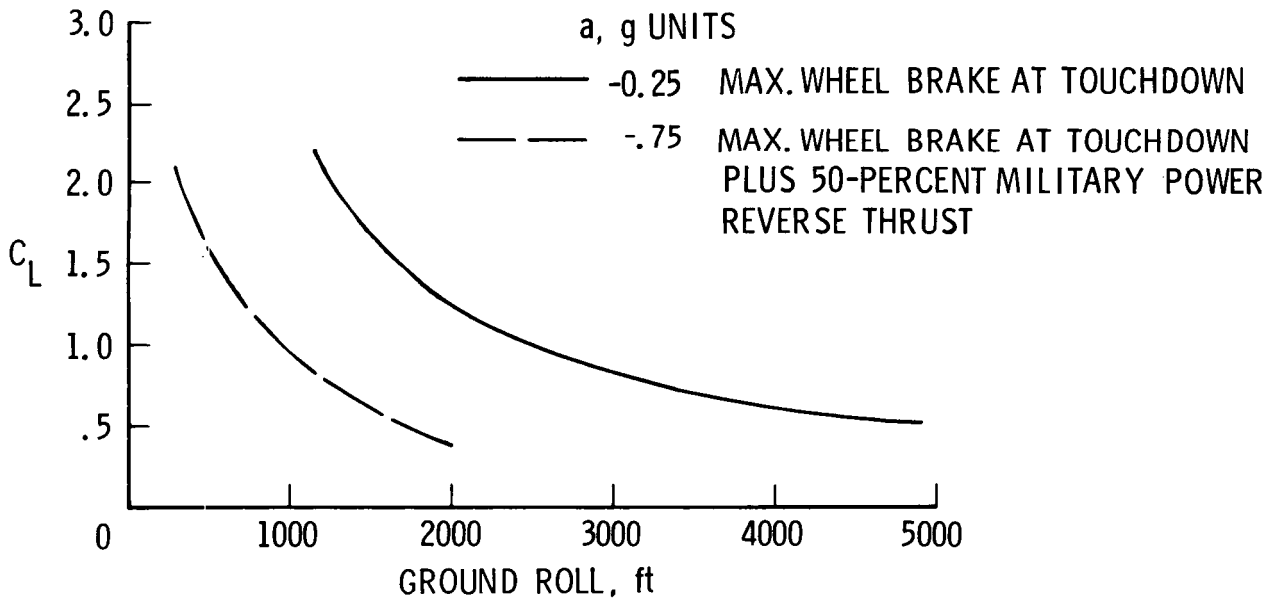

Figure 2. Effect of reverse thrust on calculated landing ground rolls.

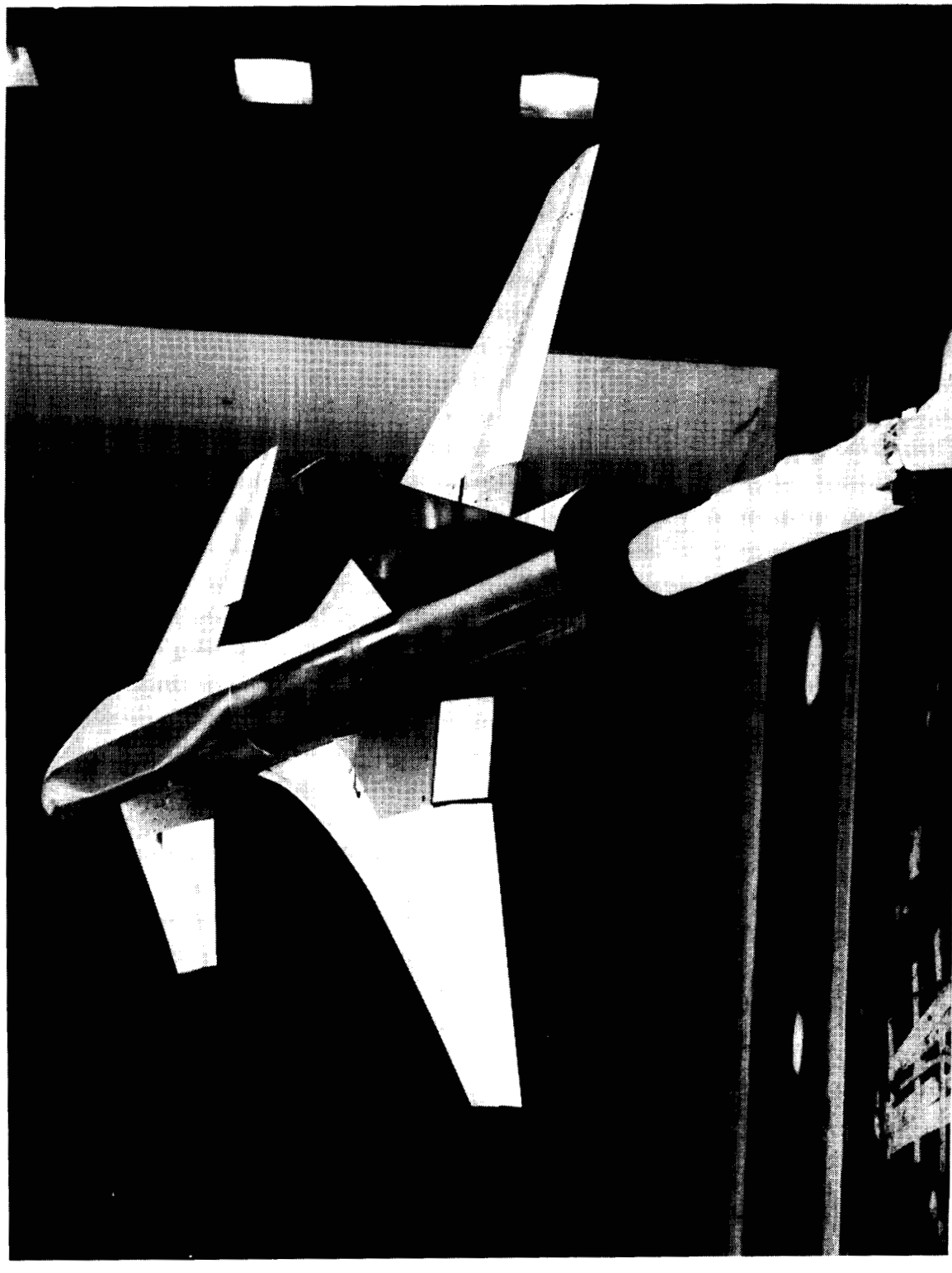

L-77-8141

(a) Installation in the Langley 14- by 22-Foot Subsonic Tunnel.

Figure 3. Generic wing-canard fighter configuration.

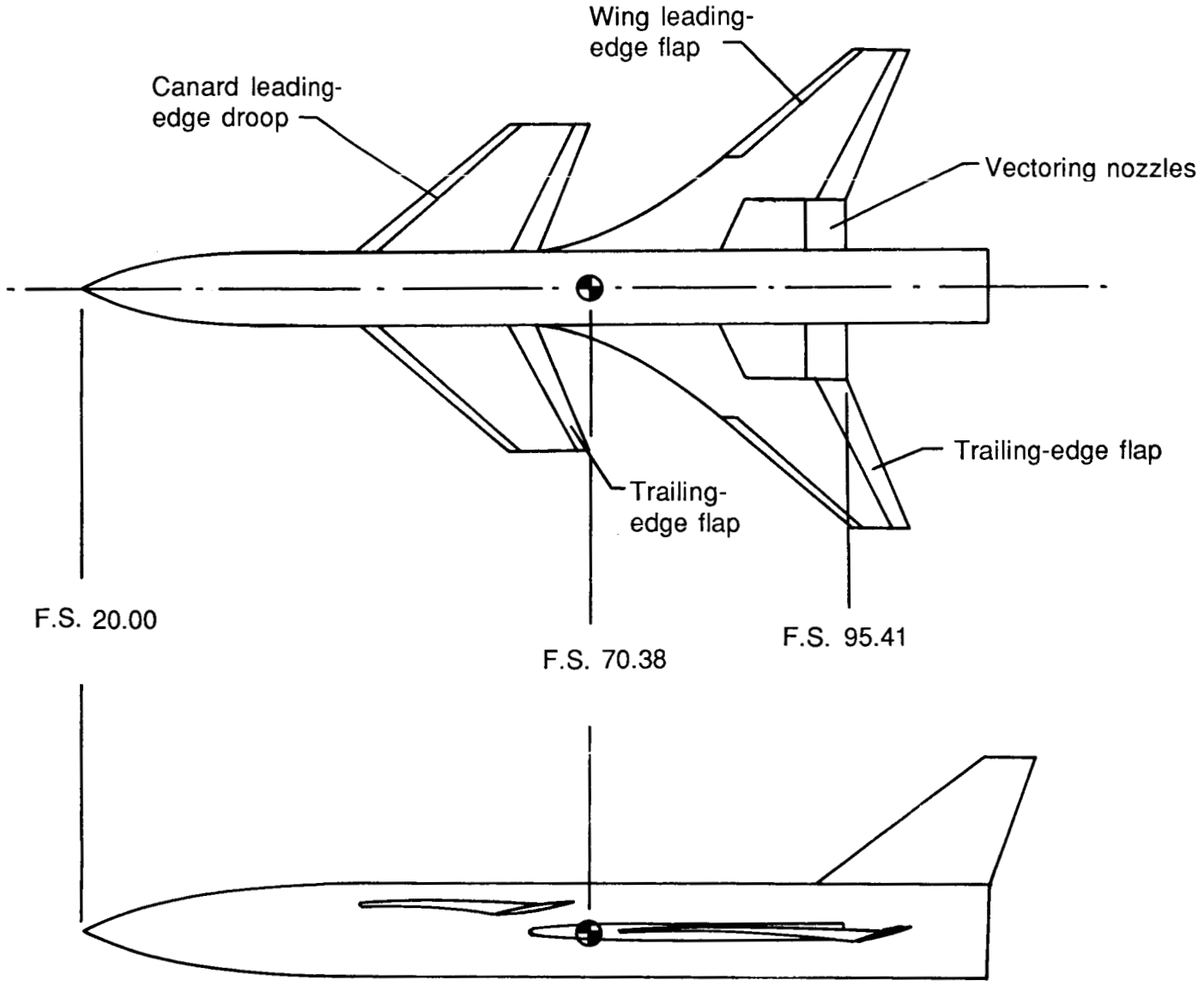

(b) Geometry sketch. Linear dimensions are given in inches.

Figure 3. Concluded.

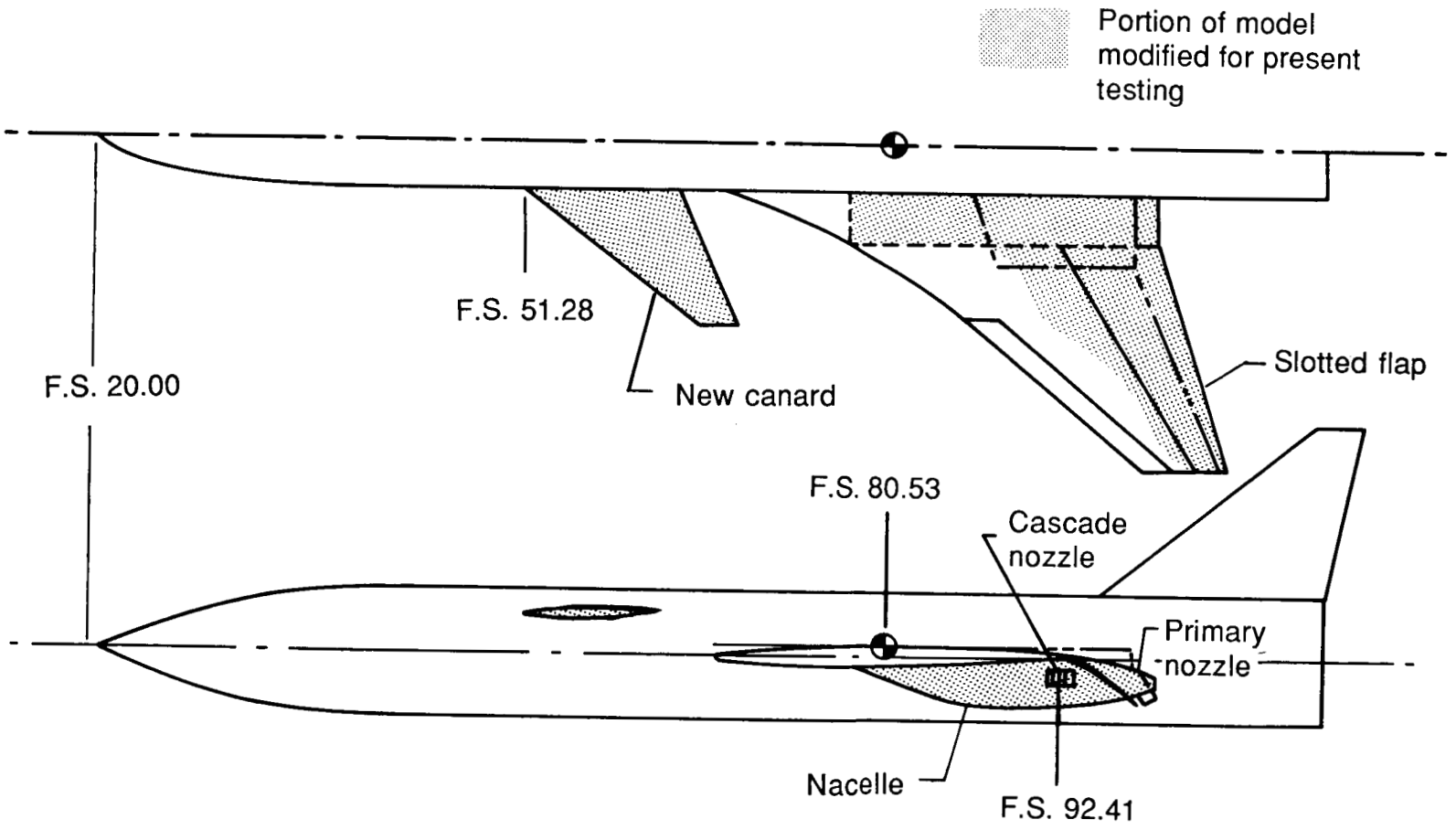

(a) Geometry sketch. Linear dimensions are given in inches.

Figure 4. Modified generic wing-canard fighter configuration.

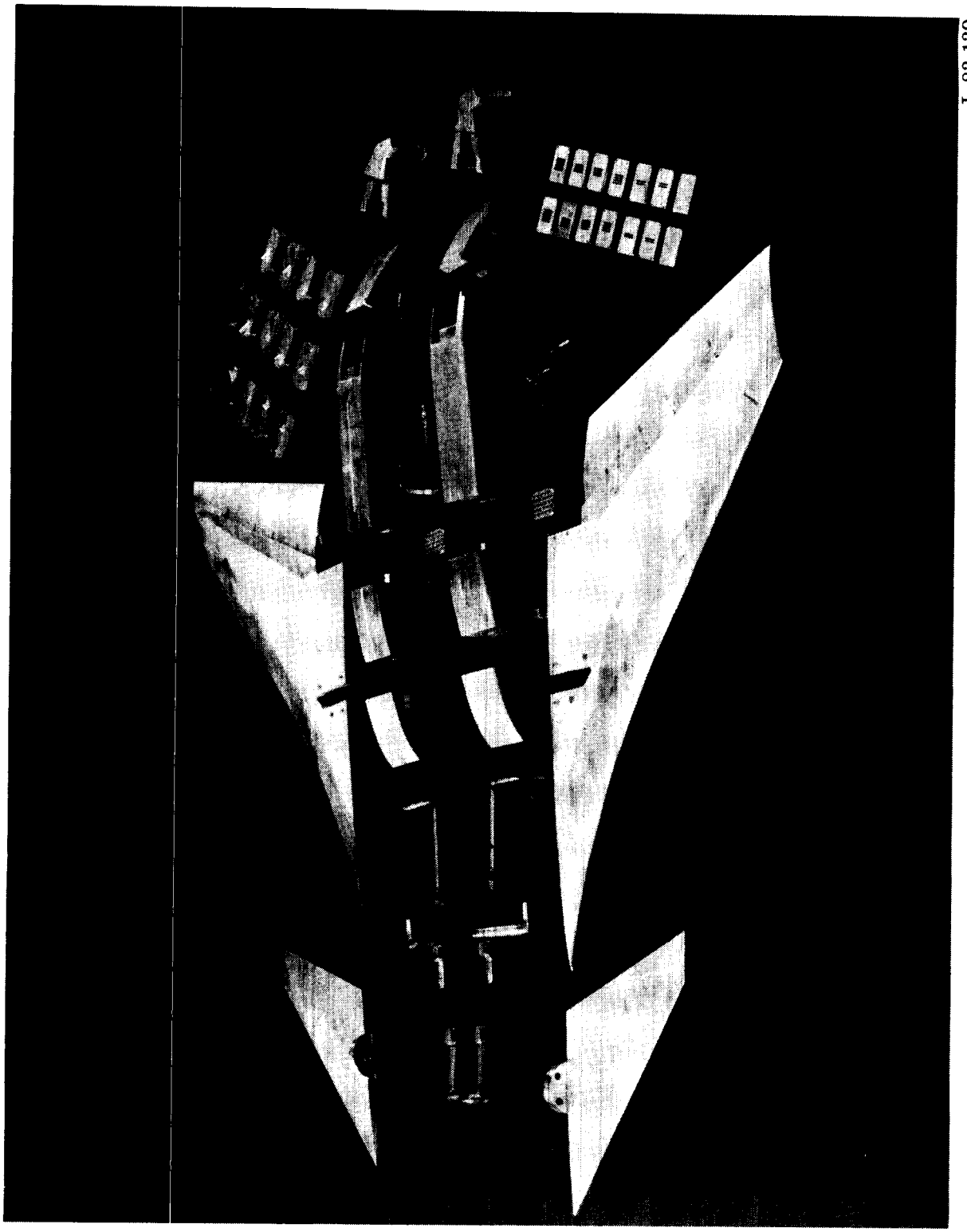

L-83-139

(b) New and modified parts for generic wing-canard fighter model.

Figure 4. Concluded.

L-79-1830

(a) Installation in the Langley 14- by 22-Foot Subsonic Tunnel.

Figure 5. Vectored-engine-over-wing configuration.

L-79-1833

(b) Three-quarter rear view of chordwise main and spanwise blowing nozzles of VEO-wing model.

Figure 5. Continued.

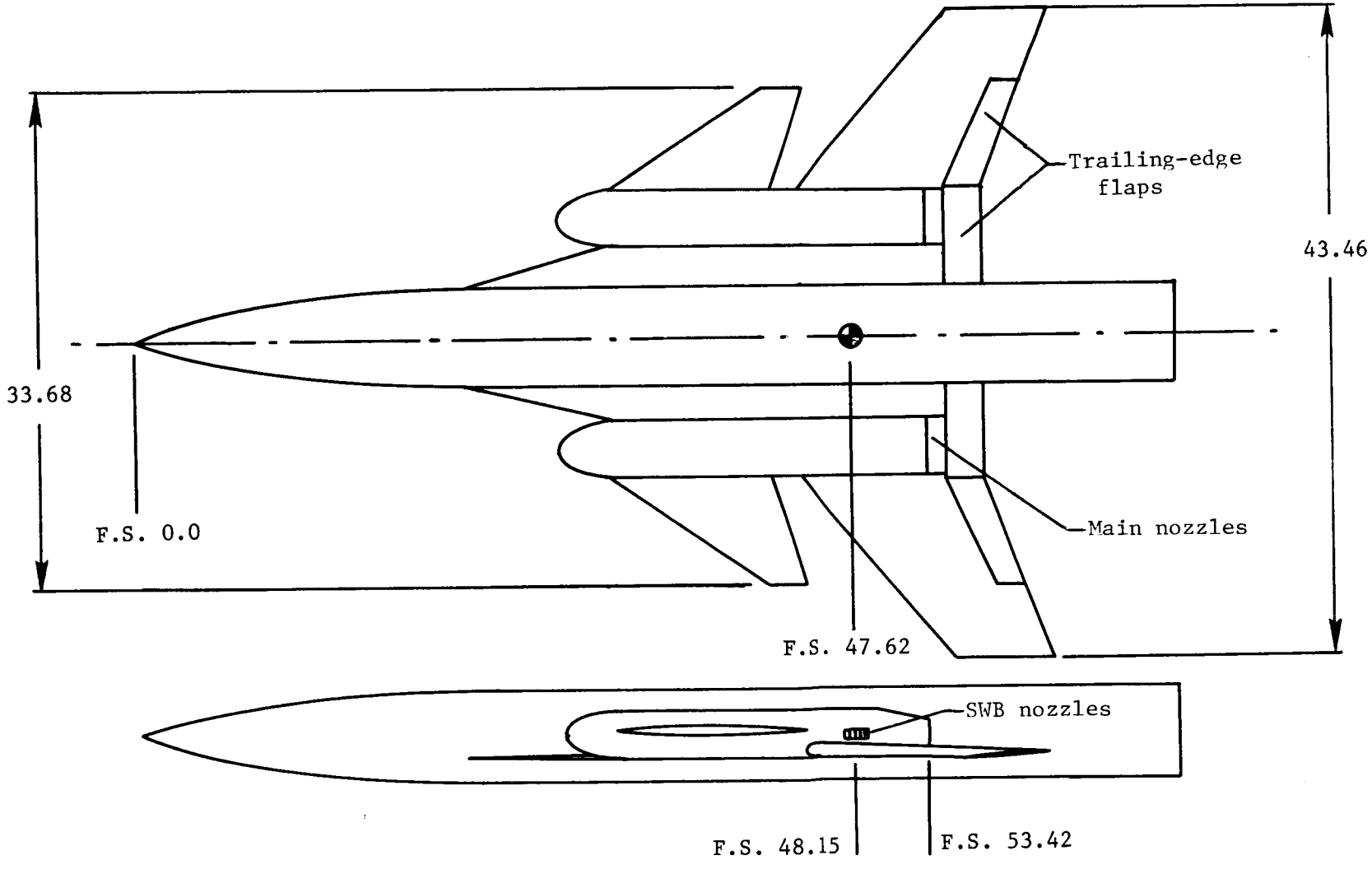

(c) Sketch of vectored-engine-over-wing model. Linear dimensions are given in inches.

Figure 5. Concluded.

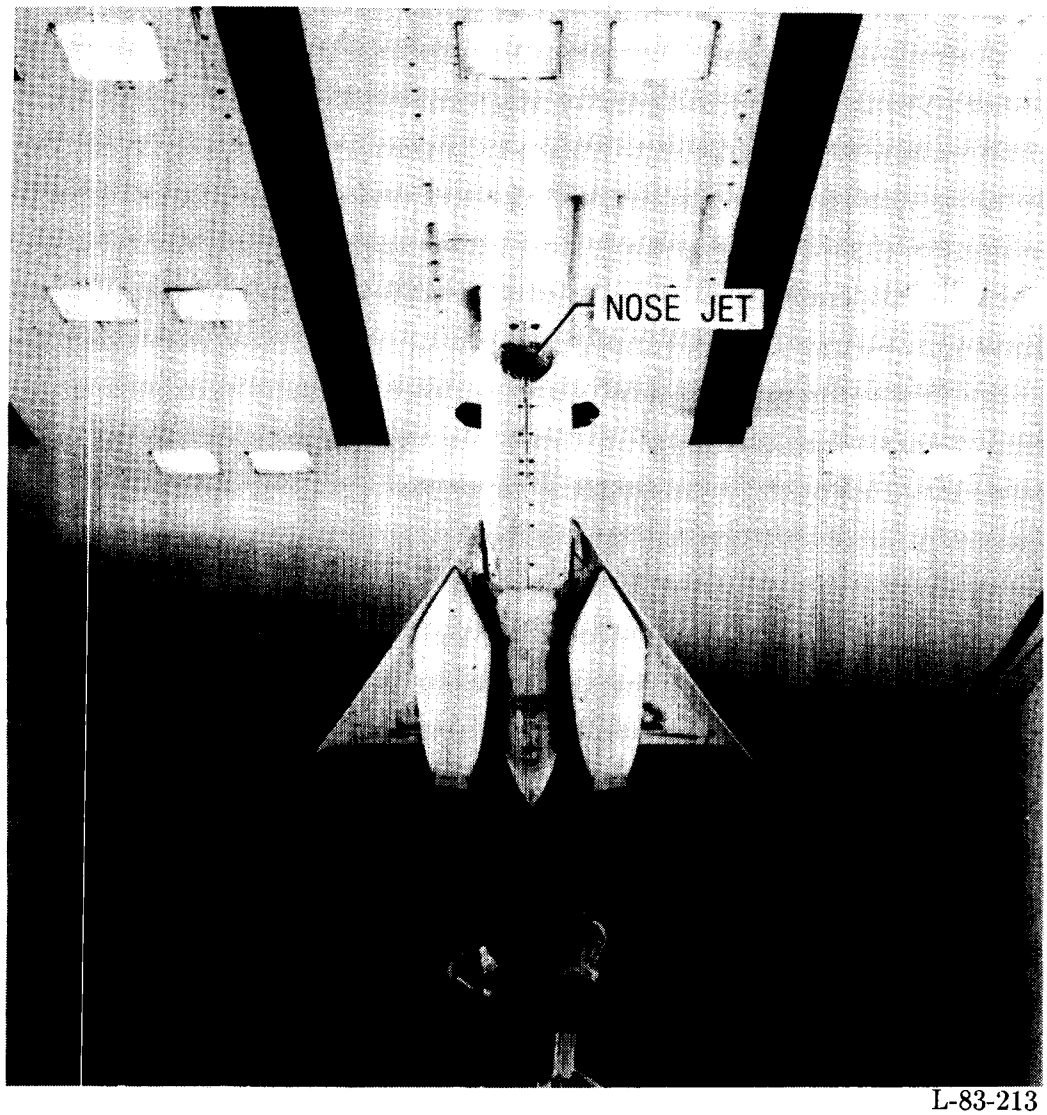

L-83-213

(a) Installation in the Langley 14- by 22-Foot Subsonic Tunnel.

Figure 6. Mach 2 supercruiser configuration.

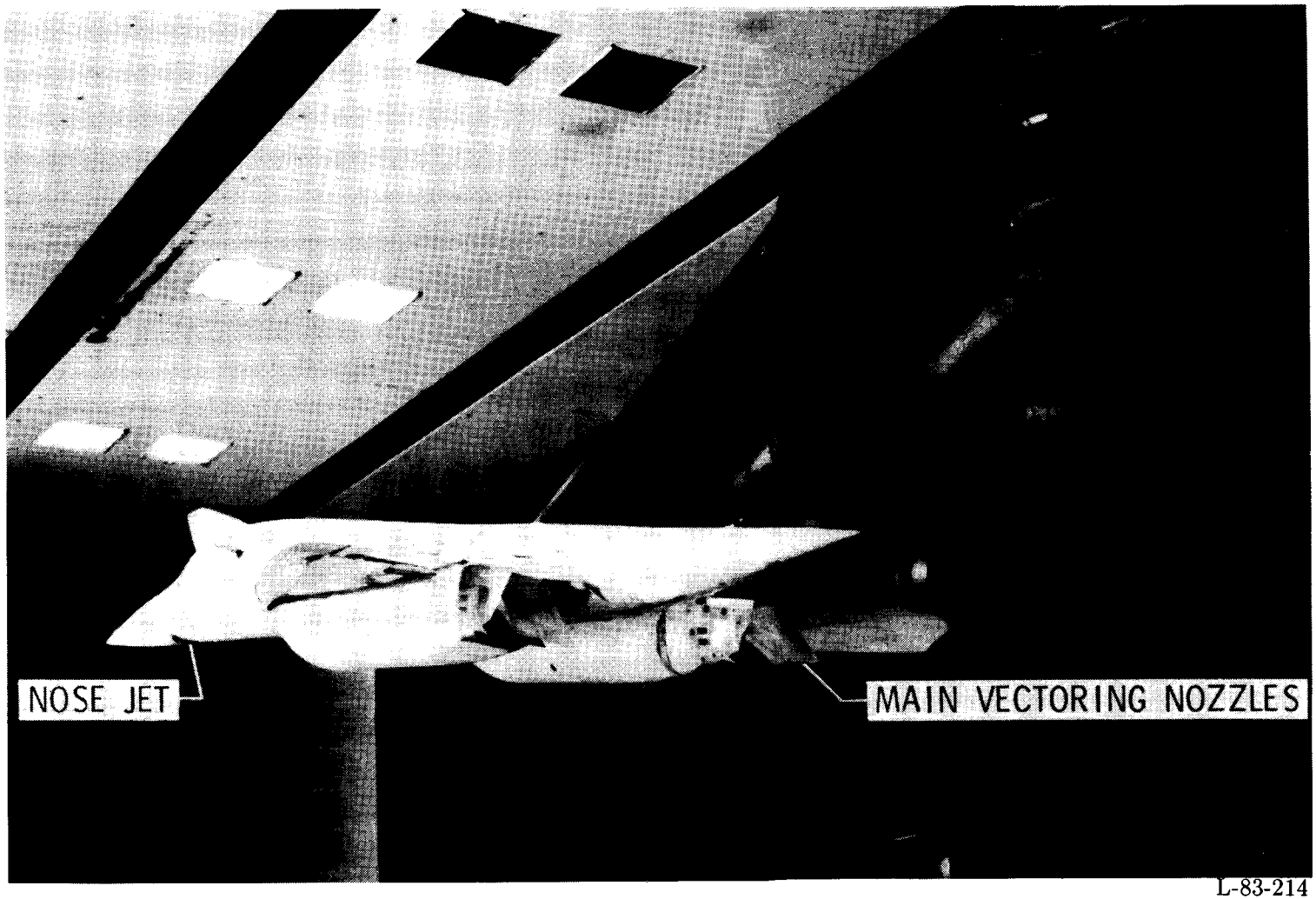

(b) Rear view of installation in the Langley 14- by 22-Foot Subsonic Tunnel showing tail mounting system.

Figure 6. Continued.

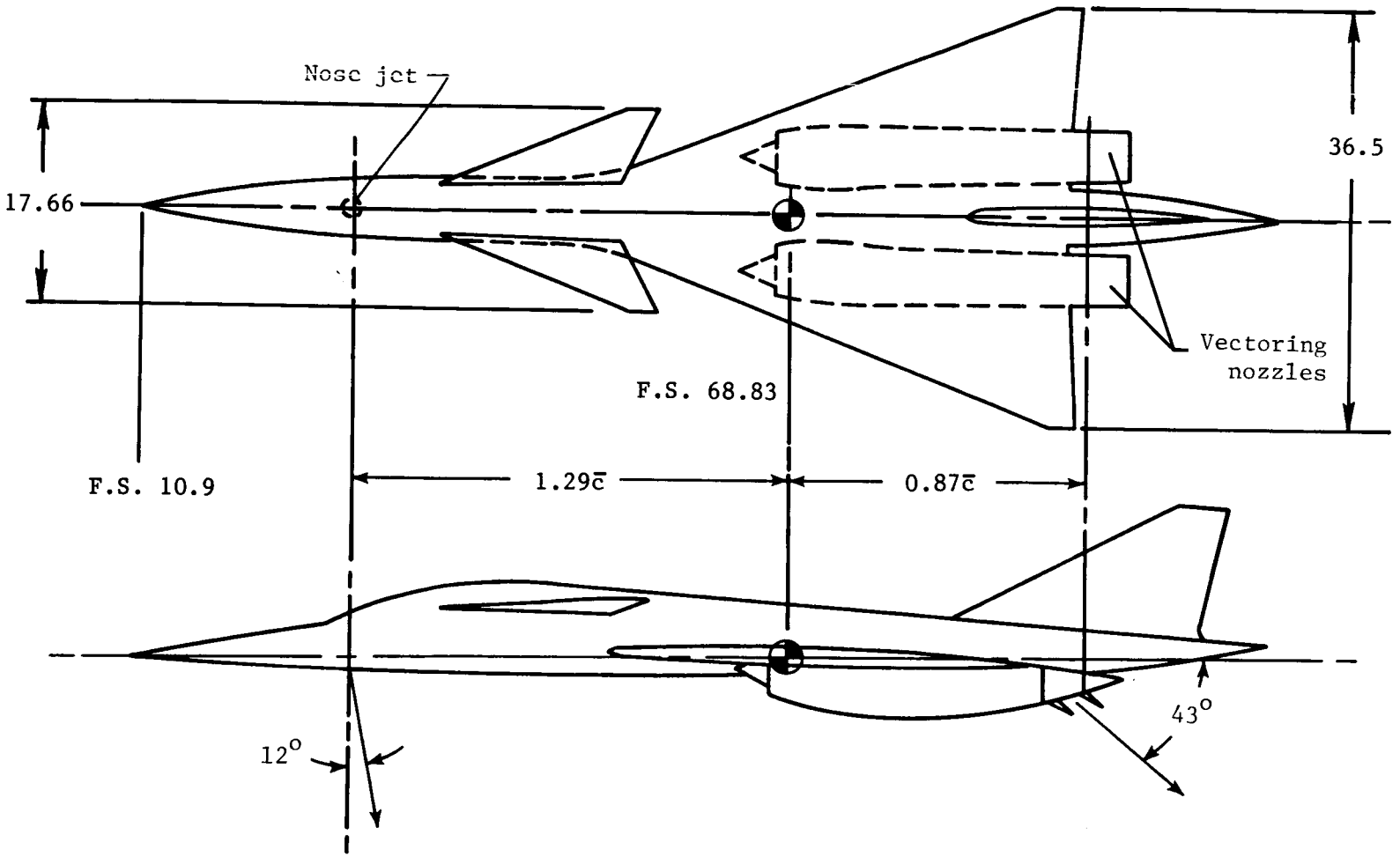

(c) Geometry sketch. Linear dimensions are given in inches.

Figure 6. Concluded.

(a) Installation in the Langley 14- by 22-Foot Subsonic Tunnel.

Figure 7. F-15 thrust-reverser configuration.

L-88-16

(b) Close-up of rotating-vane thrust reverser.

Figure 7. Concluded.

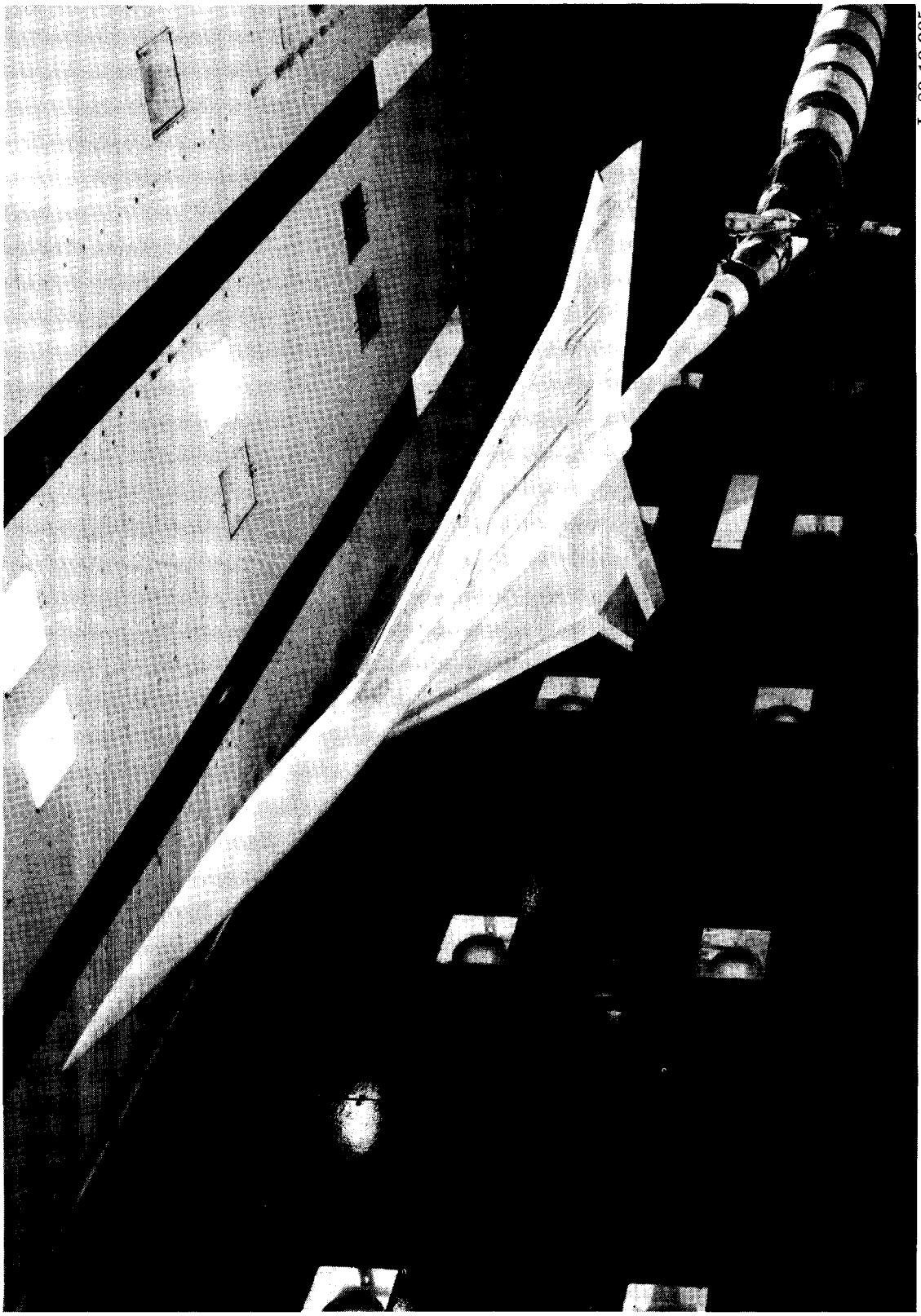

L-80-10,905

(a) Installation in the Langley 14- by 22-Foot Subsonic Tunnel.

Figure 8. Generic high-sweep fighter configuration.

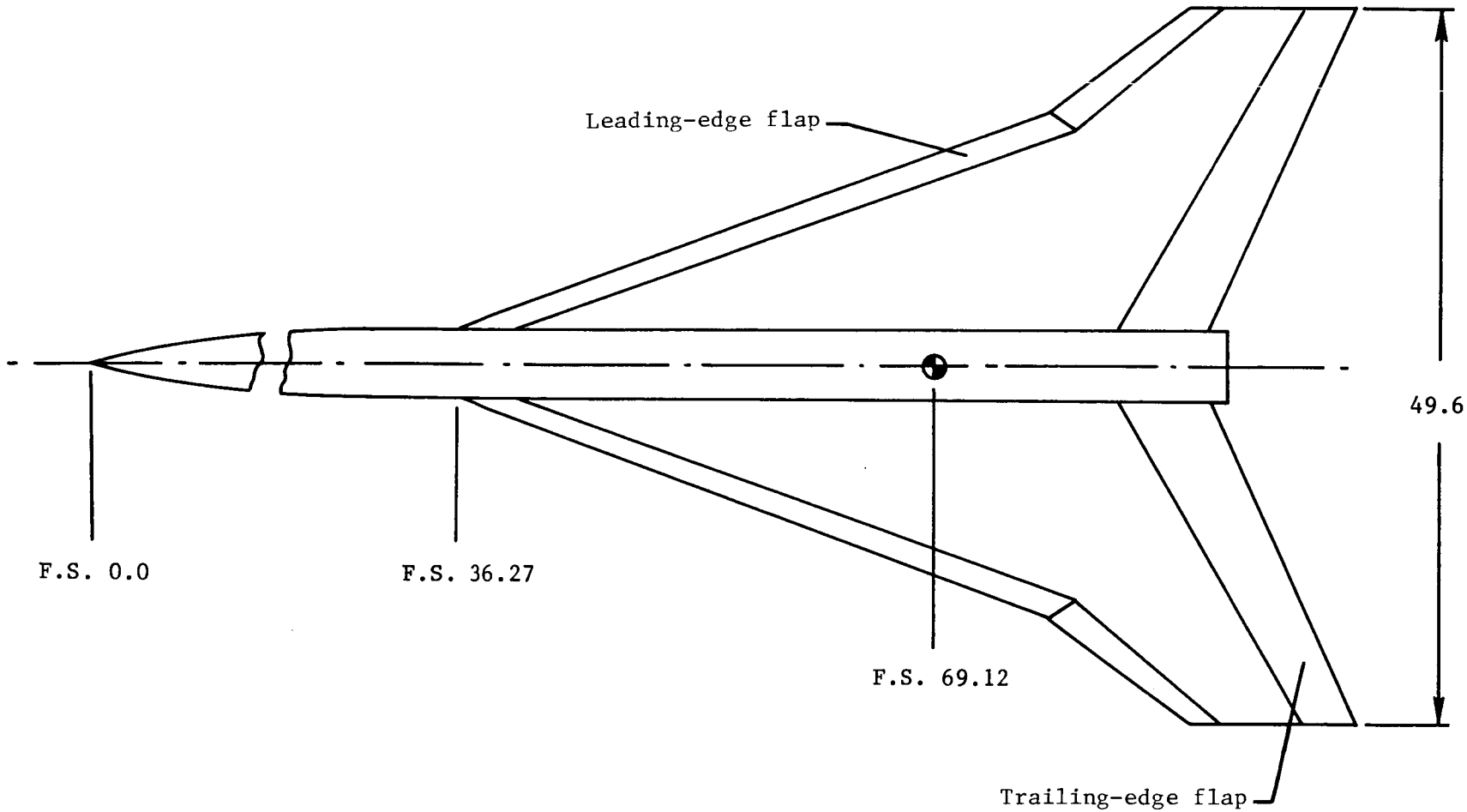

(b) Geometry sketch. Linear dimensions are given in inches.

Figure 8. Concluded.

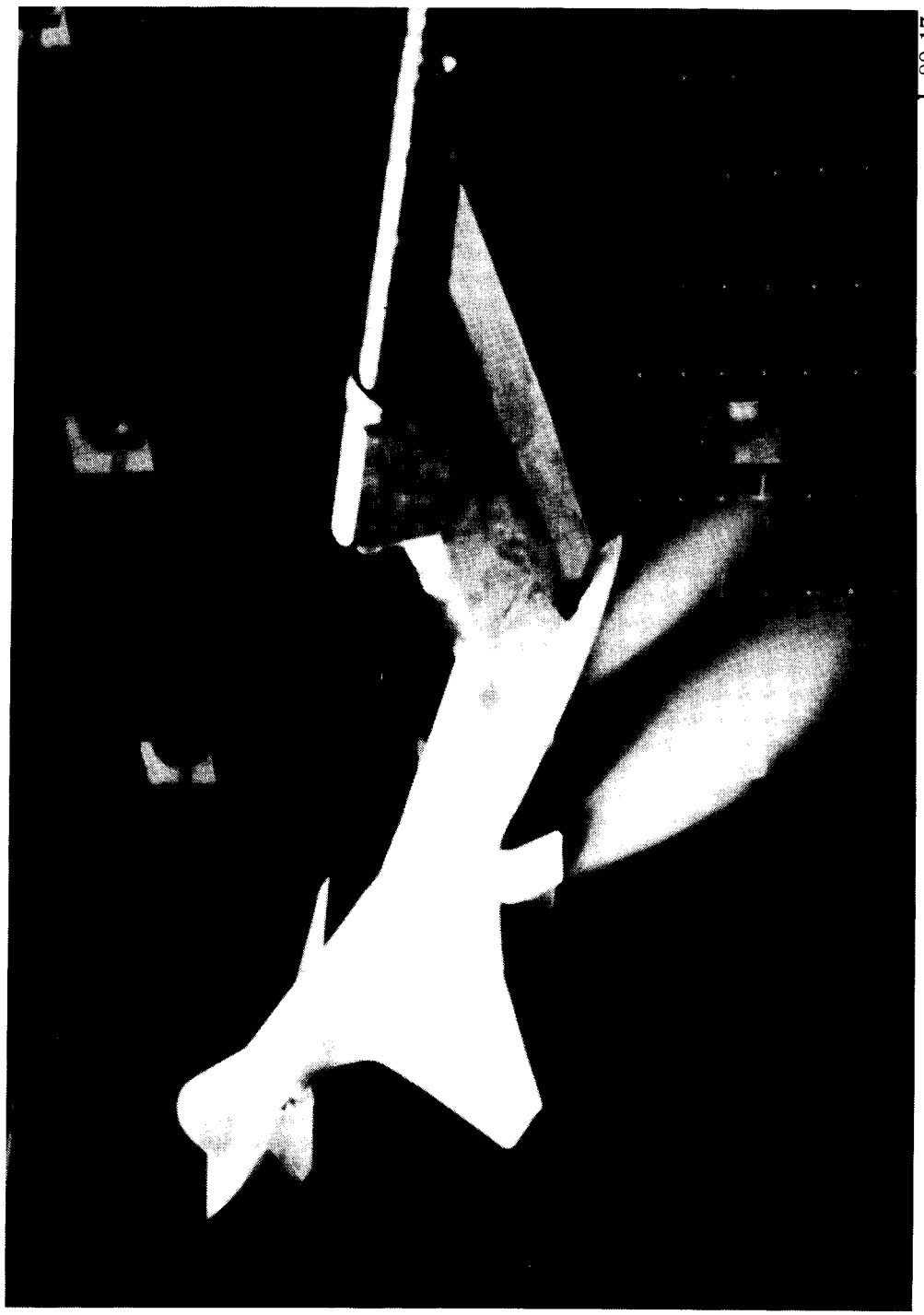

L-88-17

(a) Installation in the Langley 14- by 22-Foot Subsonic Tunnel.

Figure 9. Advanced Technologies for Tactical Aircraft (ATTAC) configuration.

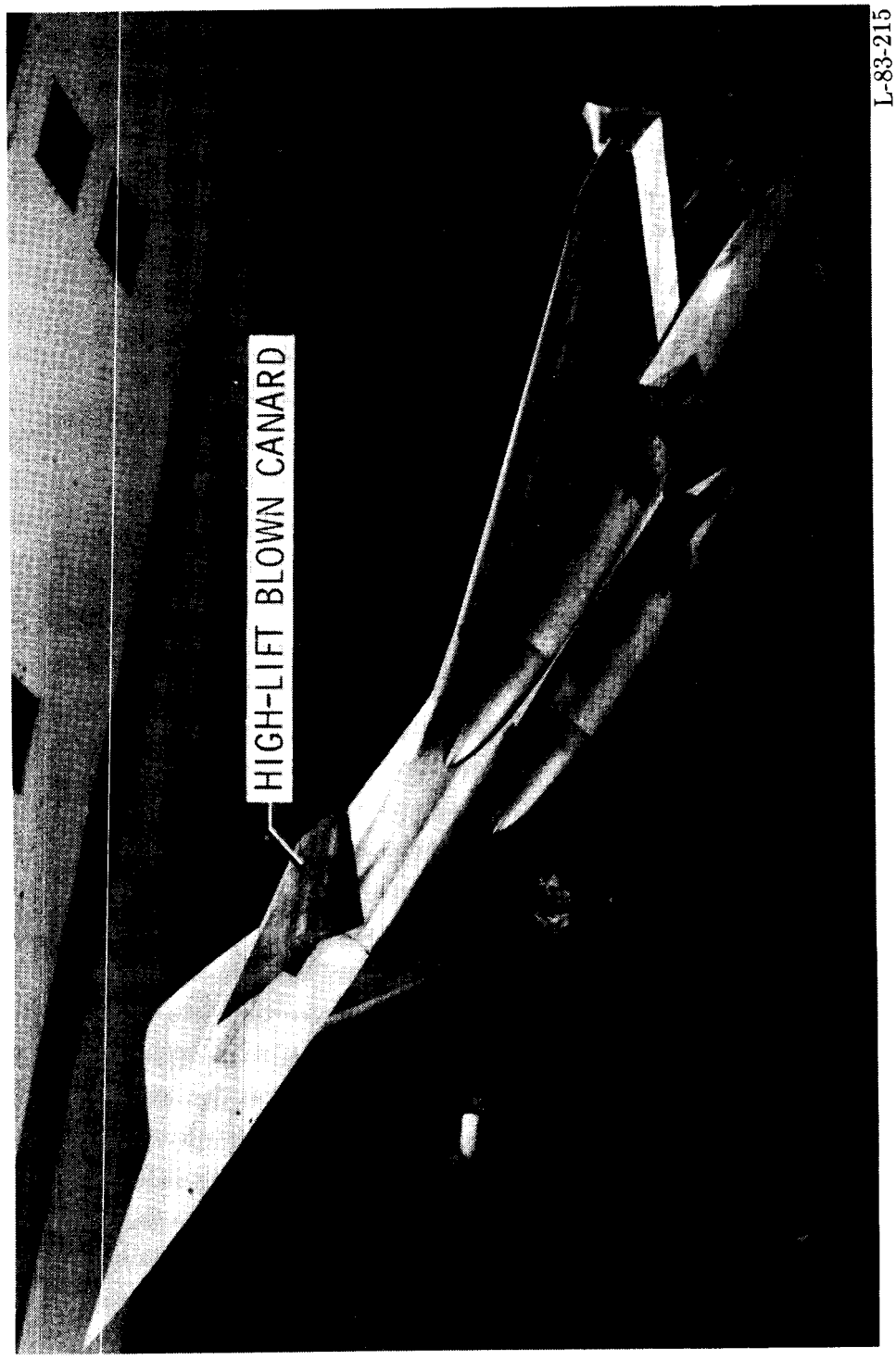

L-83-215

(b) Installation showing high-lift blown canard.

Figure 9. Continued.

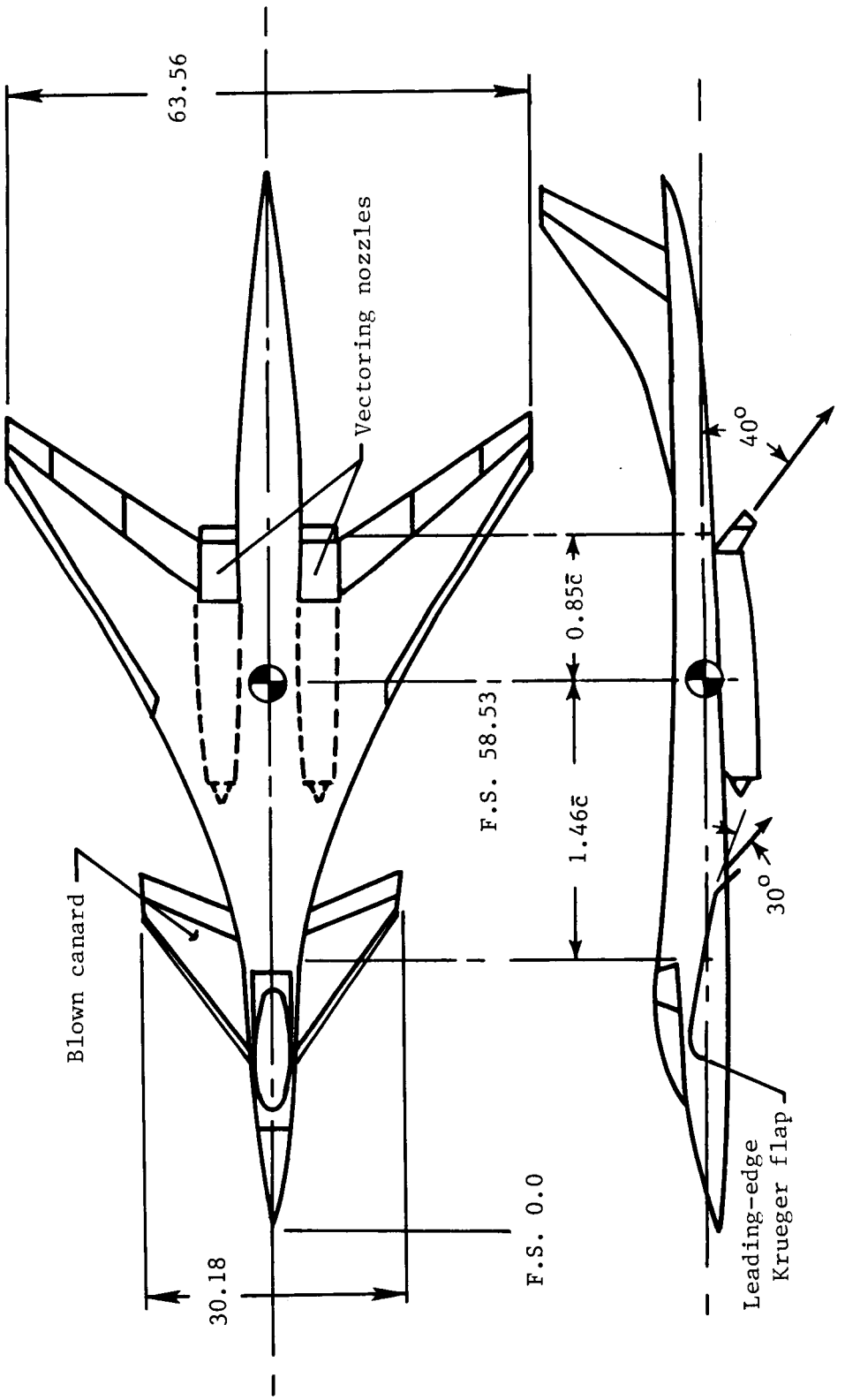

(c) Geometry sketch. Linear dimensions are given in inches.

Figure 9. Concluded.

L-83-5981

Figure 10. Installation of advanced nozzle concepts for STOL and survivability configuration in the Langley 14- by 22-Foot Subsonic Tunnel.

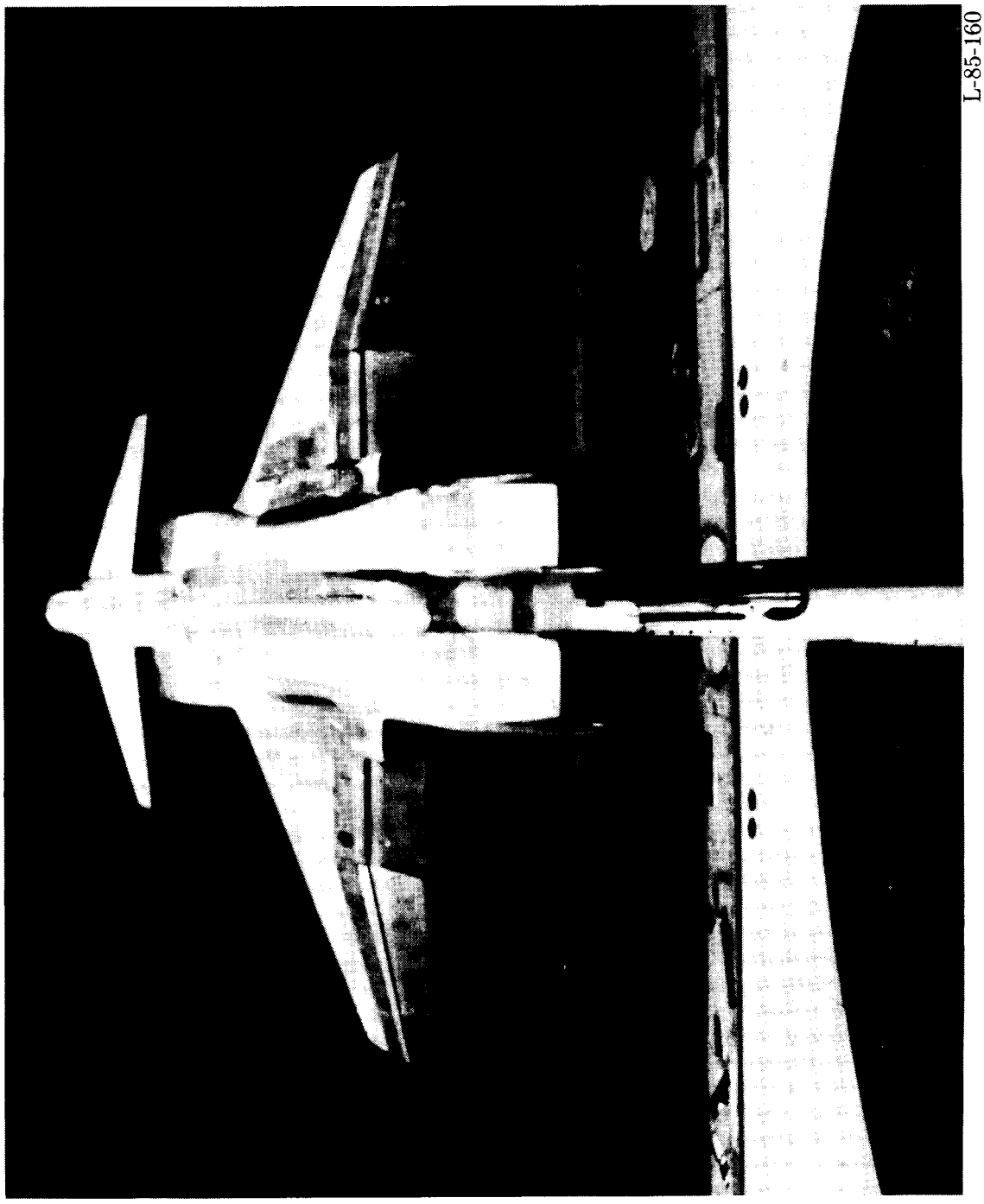

L-85-160

(a) Installation in the Langley 14- by 22-Foot Subsonic Tunnel.

Figure 11. Advanced nozzle concepts-B configuration.

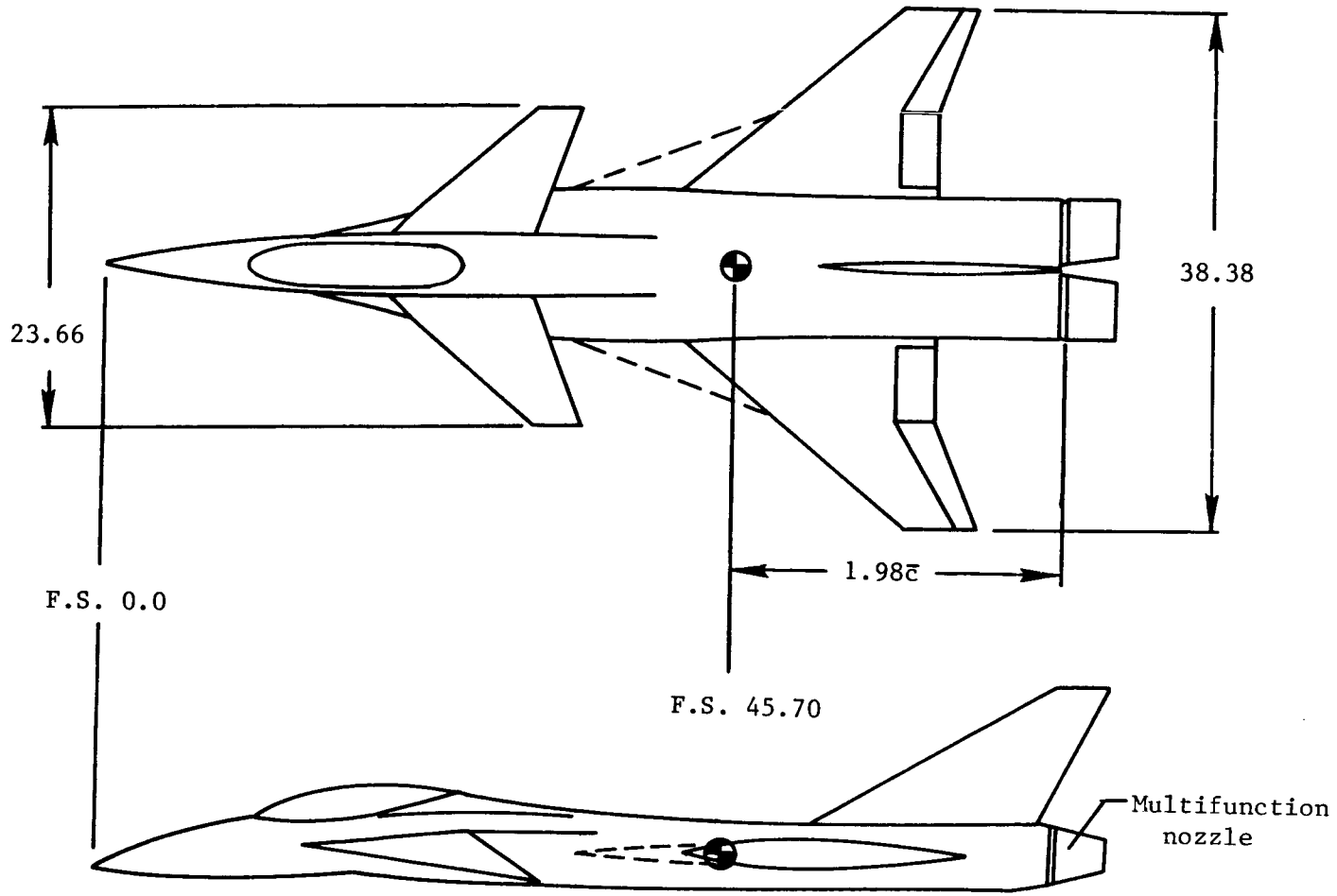

(b) Geometry sketch. Linear dimensions are given in inches.

Figure 11. Continued.

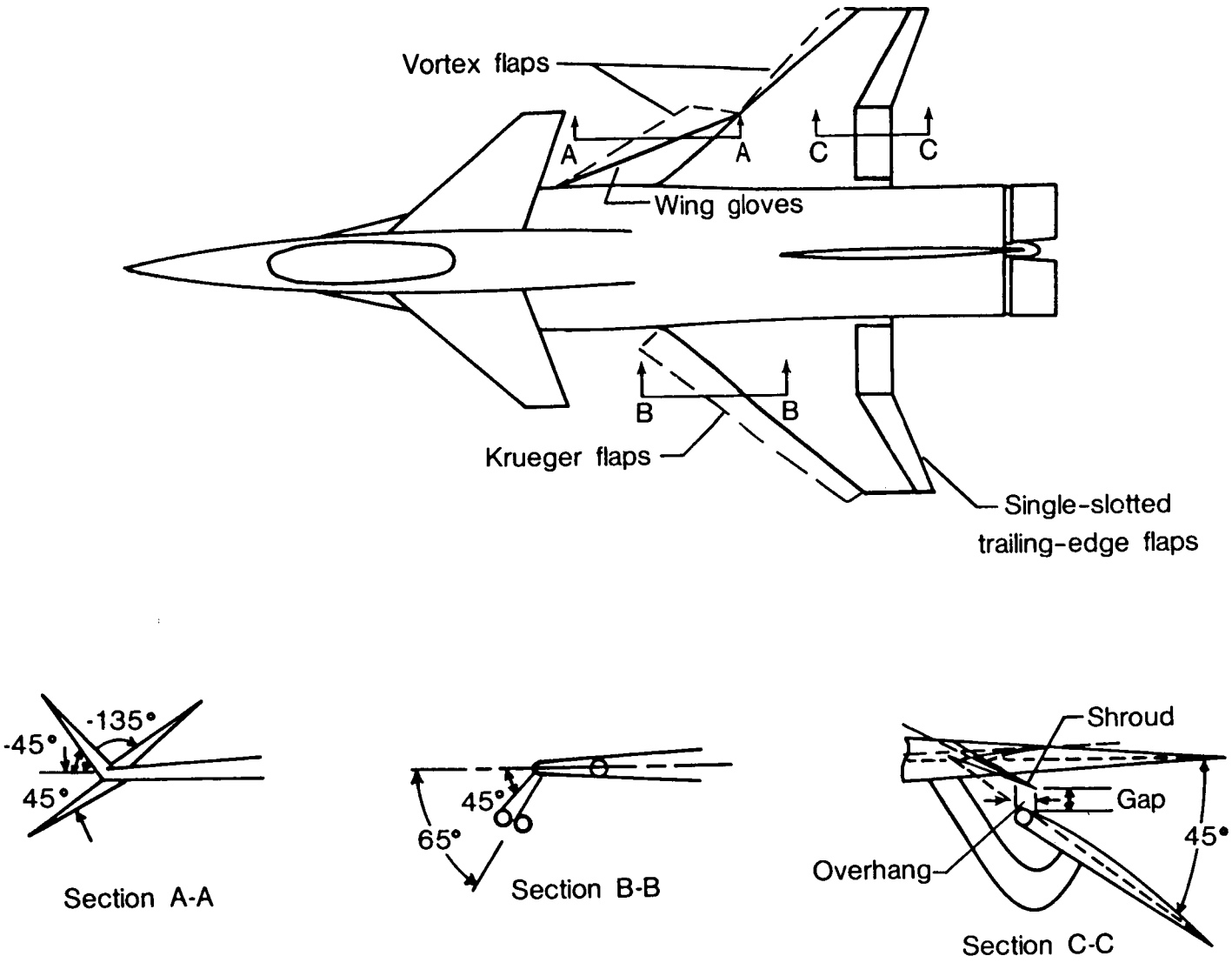

(c) Geometry sketches of various wing-flap combinations tested.

Figure 11. Concluded.

L-84-12,687

(a) Installation in the Langley 14- by 22-Foot Subsonic Tunnel.

Figure 12. Propulsive wing-canard configuration.

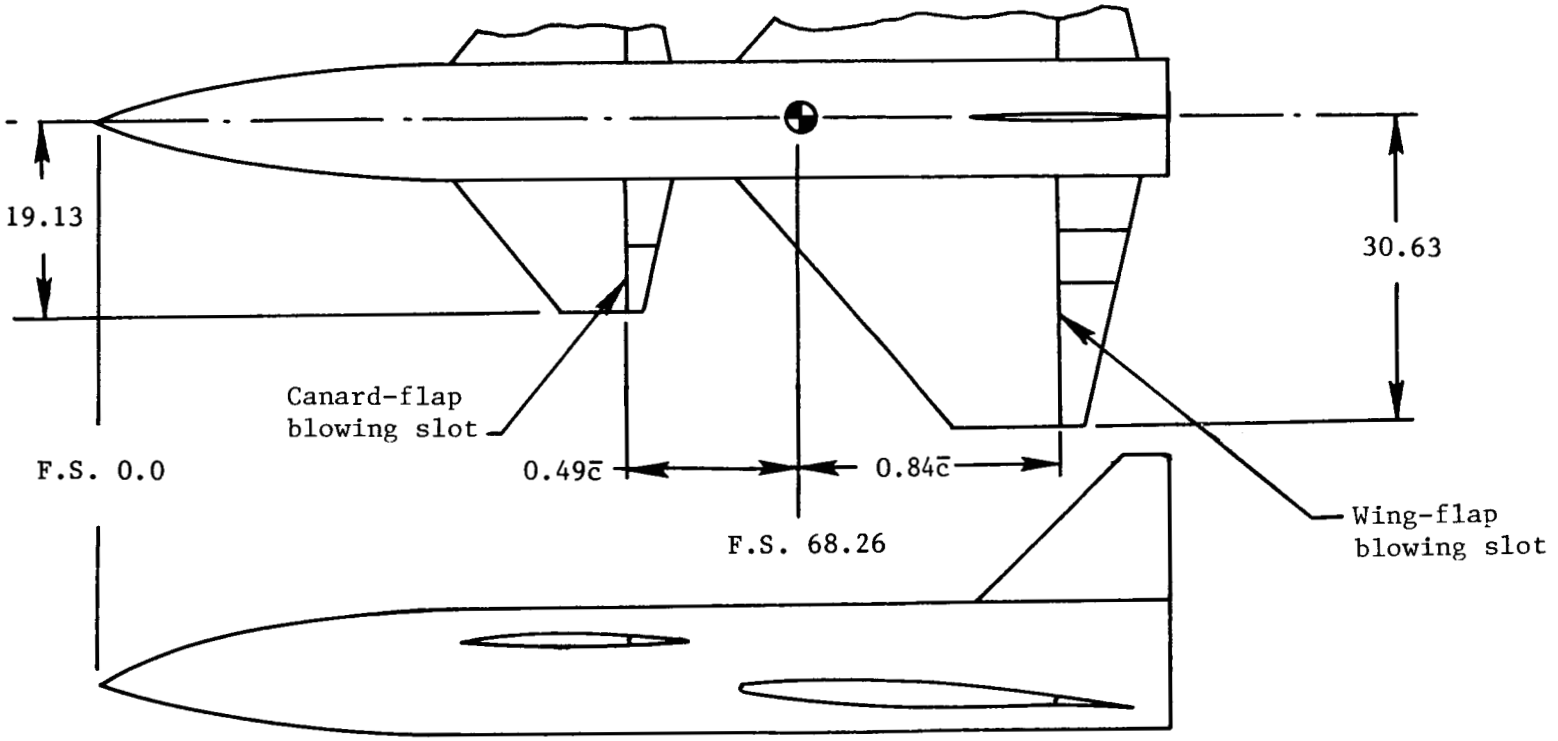

(b) Geometry sketch. Linear dimensions are given in inches.

Figure 12. Concluded.

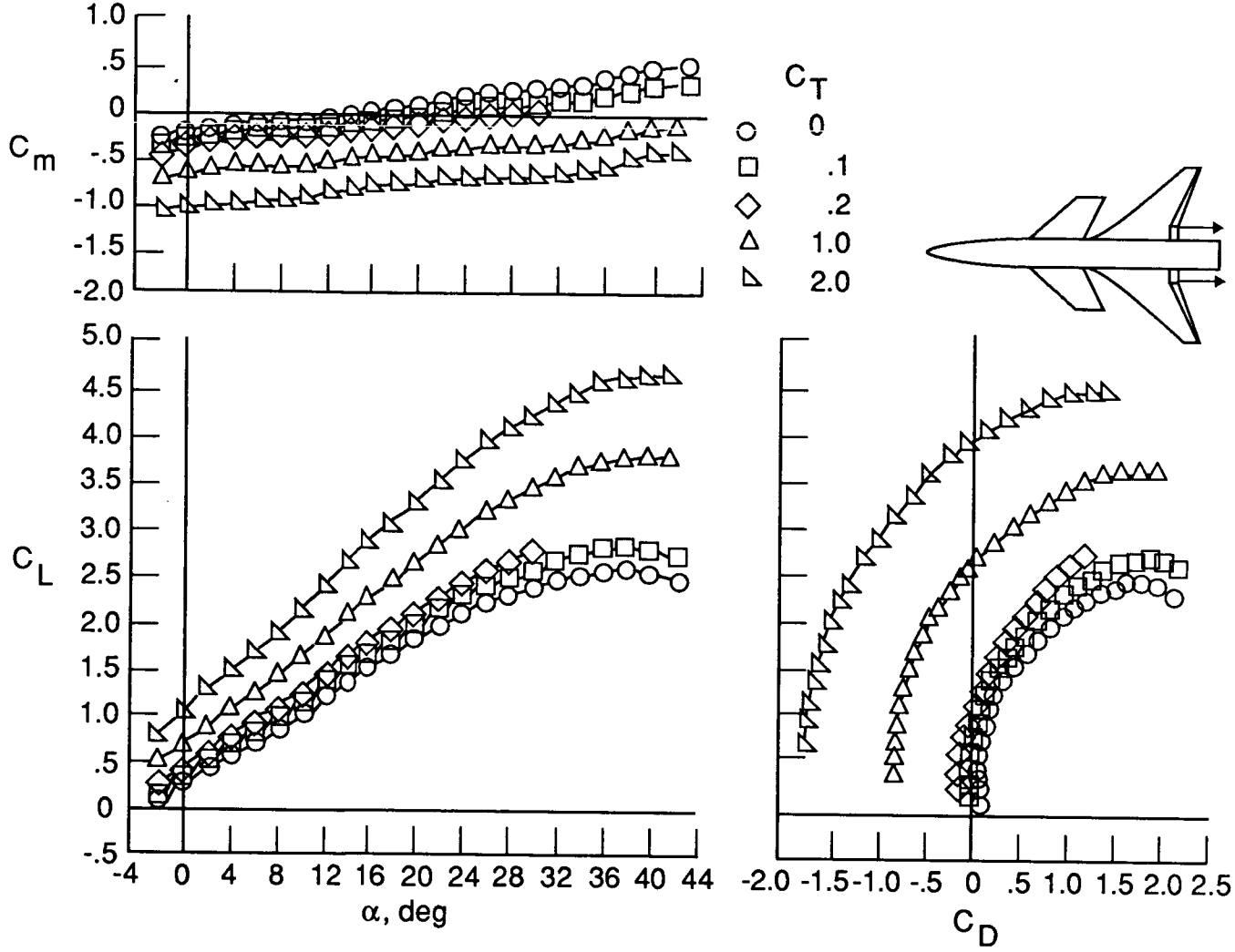

(a) Wing-canard configuration. $\delta_f = 20°$; $\delta_N = 20°$.

Figure 13. Longitudinal aerodynamics of generic wing-canard and VEO-wing fighter configurations.

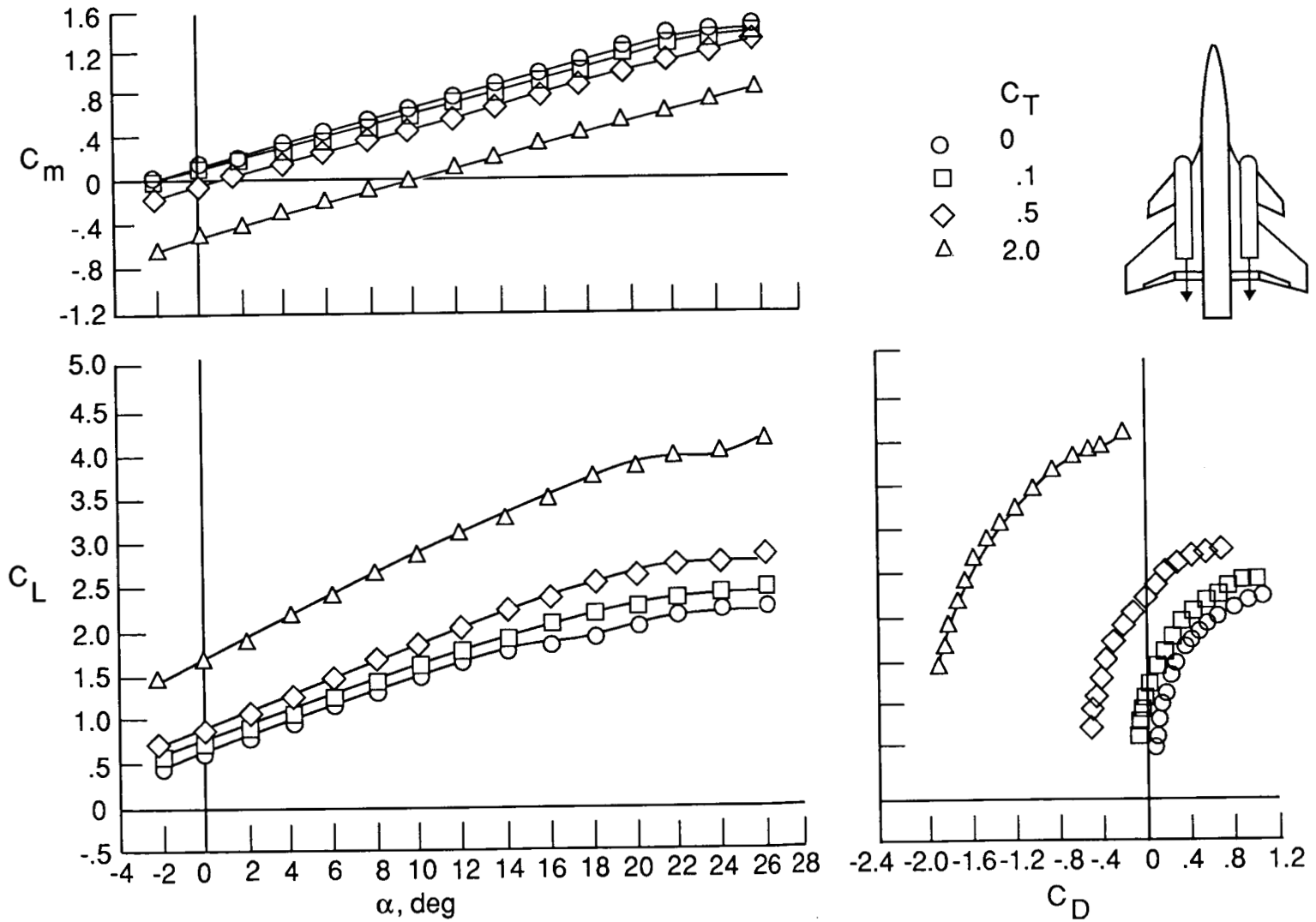

(b) VEO-wing configuration. $\delta_f = 30°$.

Figure 13. Concluded.

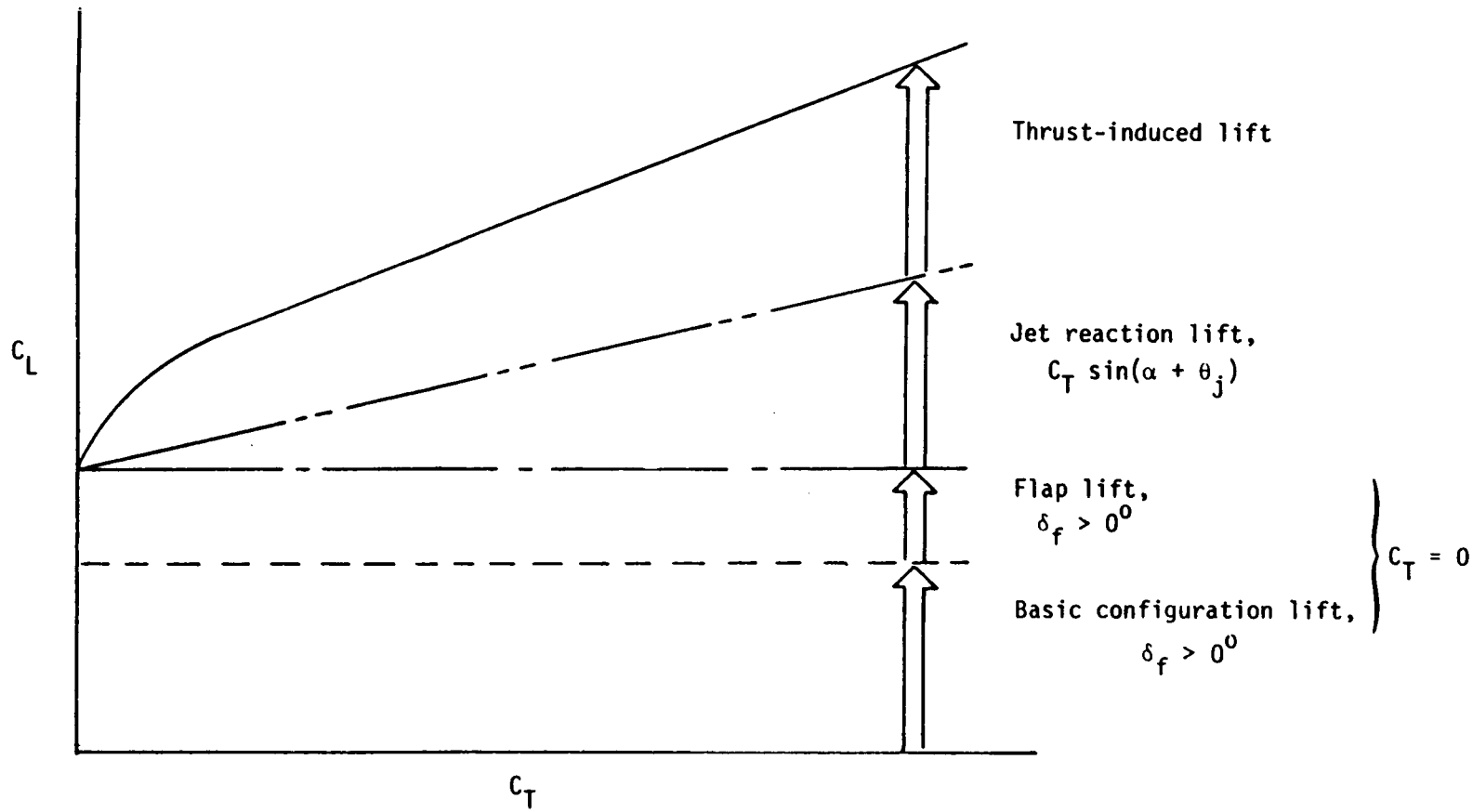

Figure 14. Components of powered lift at a constant angle of attack.

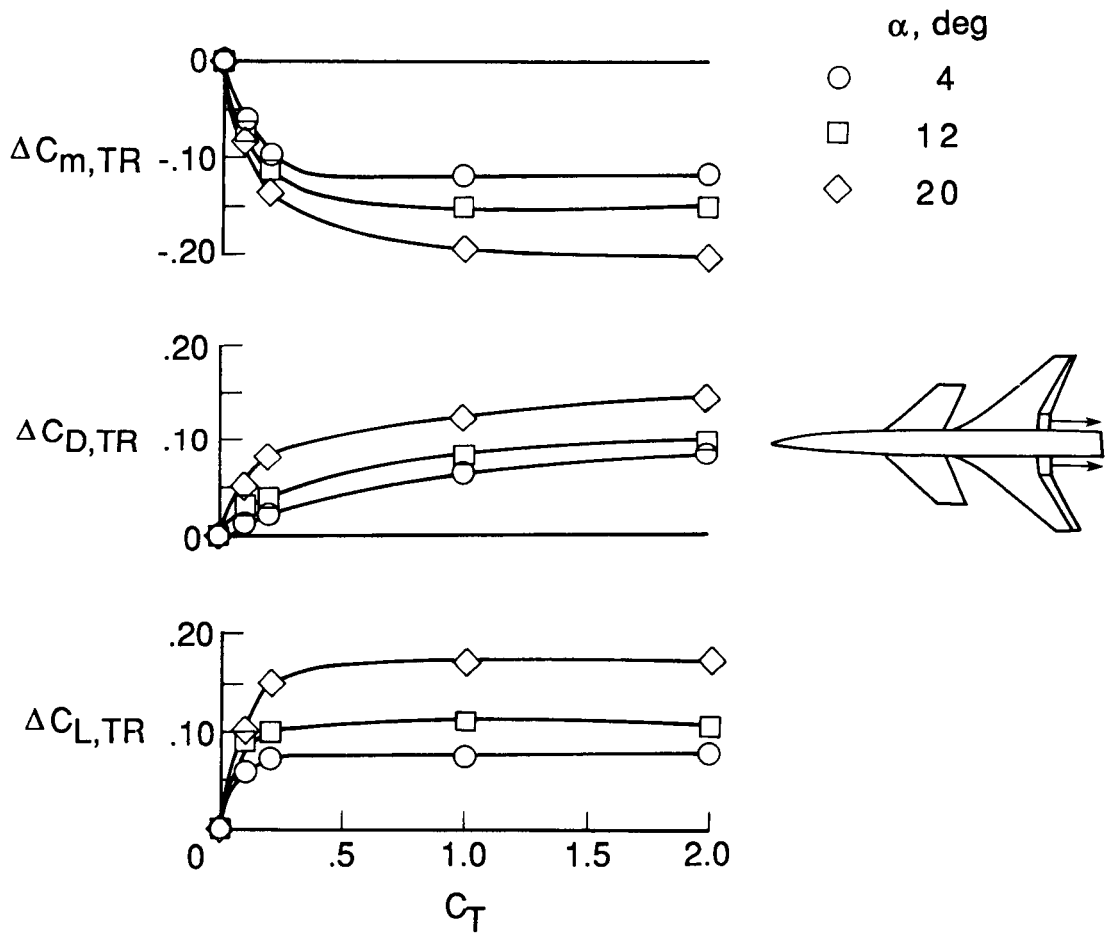

(a) Generic wing-canard fighter configuration. $\delta_f = 20°$; $\delta_N = 20°$.

Figure 15. Thrust-induced aerodynamics for generic wing-canard and VEO-wing fighter configurations.

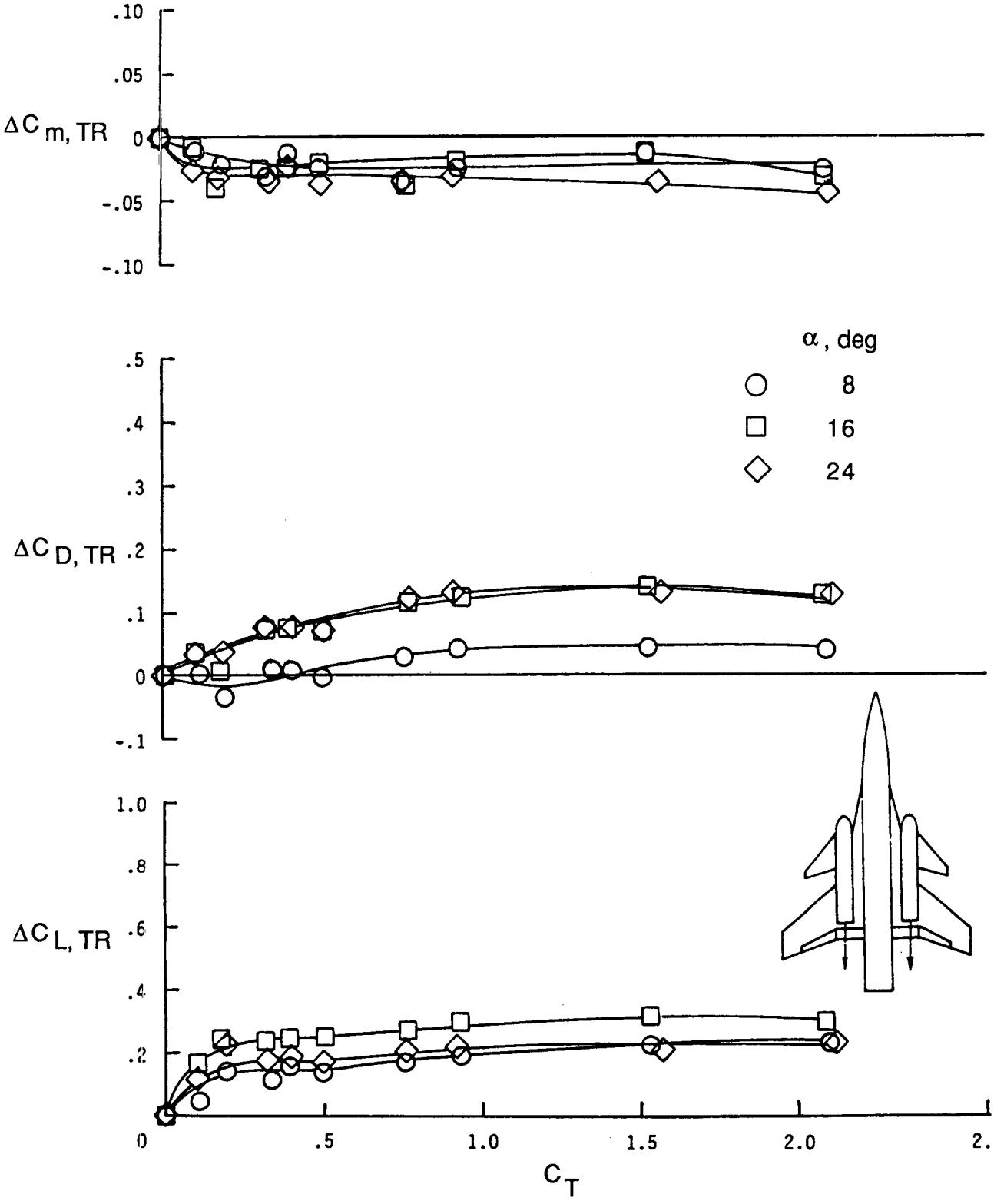

(b) VEO-wing fighter configuration. $\delta_f = 30°$.

Figure 15. Concluded.

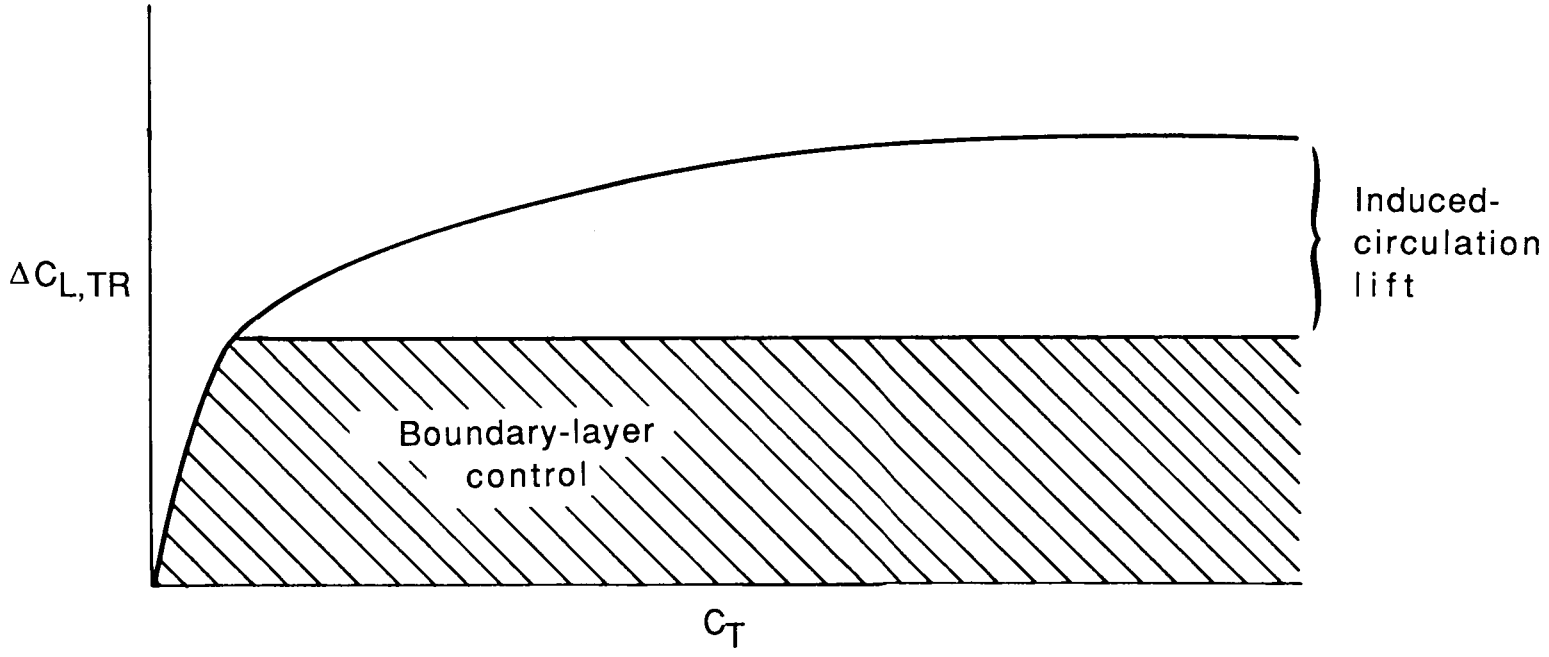

Figure 16. Components of thrust-induced lift.

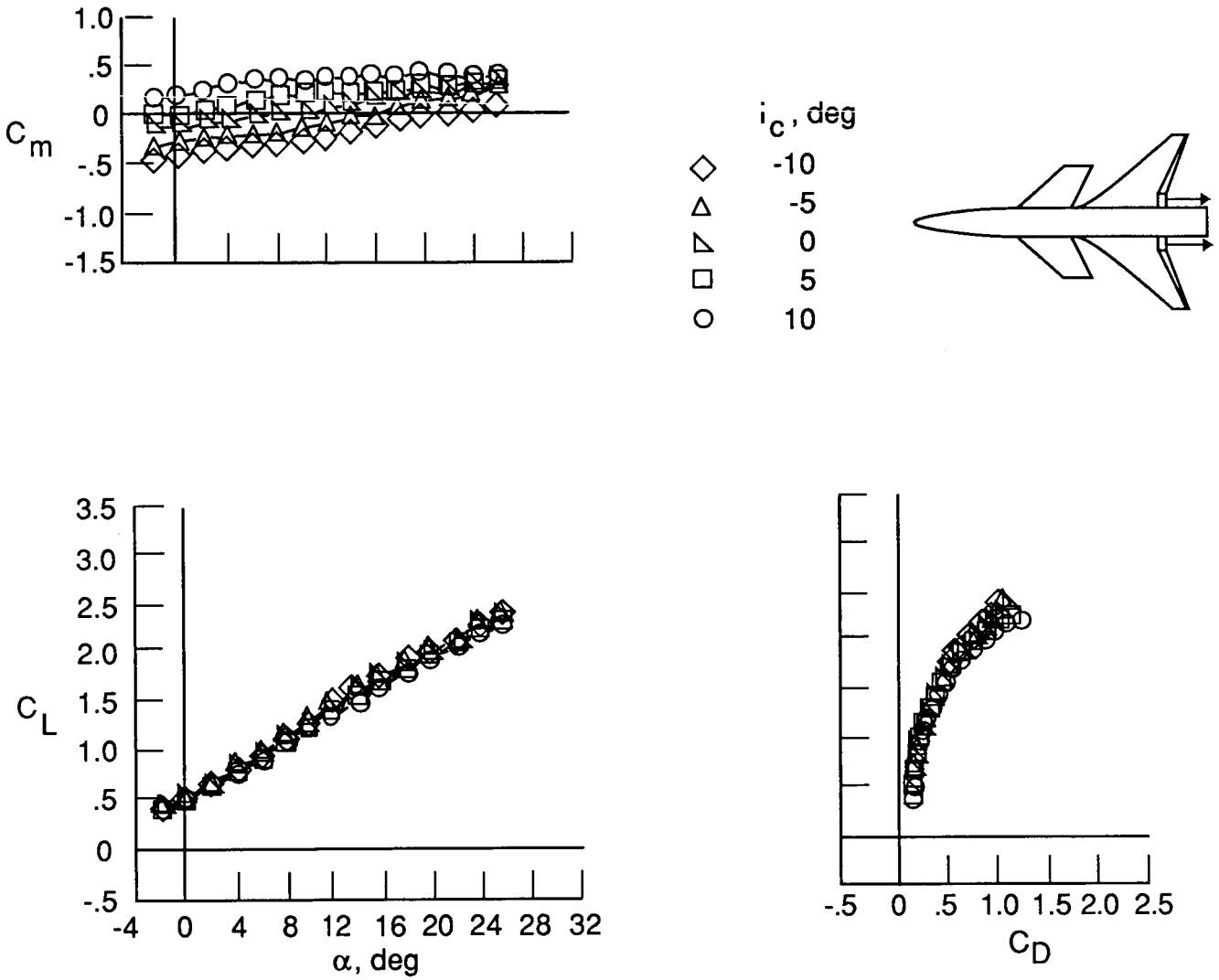

Figure 17. Effect of canard incidence on longitudinal aerodynamics of generic wing-canard fighter configuration. $C_T = 0$; $\delta_f = 20°$; $\delta_{f,c} = 20°$.

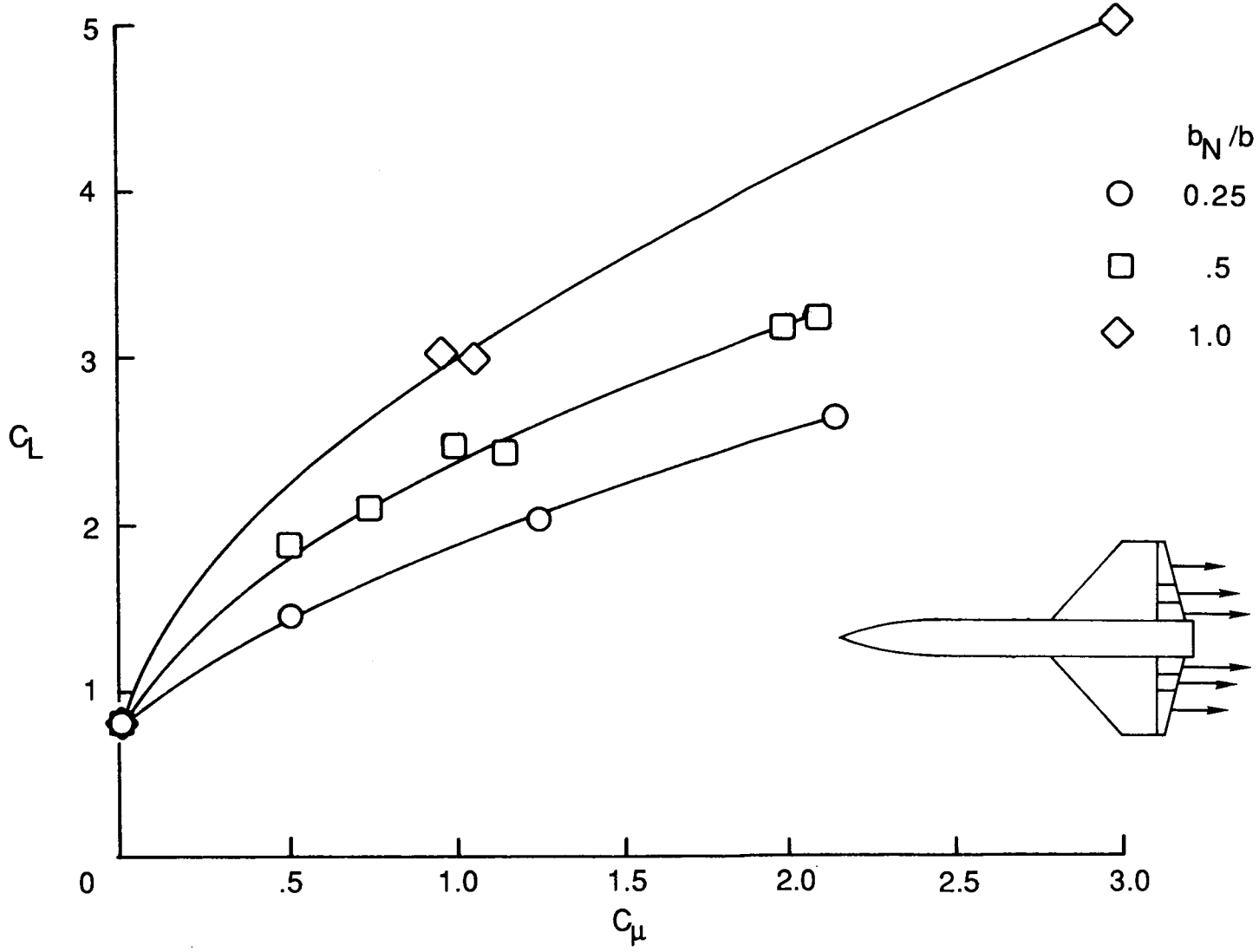

(a) Total lift coefficient versus thrust coefficient.

Figure 18. Effect of b_N/b on lift characteristics of propulsive wing-canard configuration. $\delta_f = 40°$; $\alpha = 8°$; wing alone.

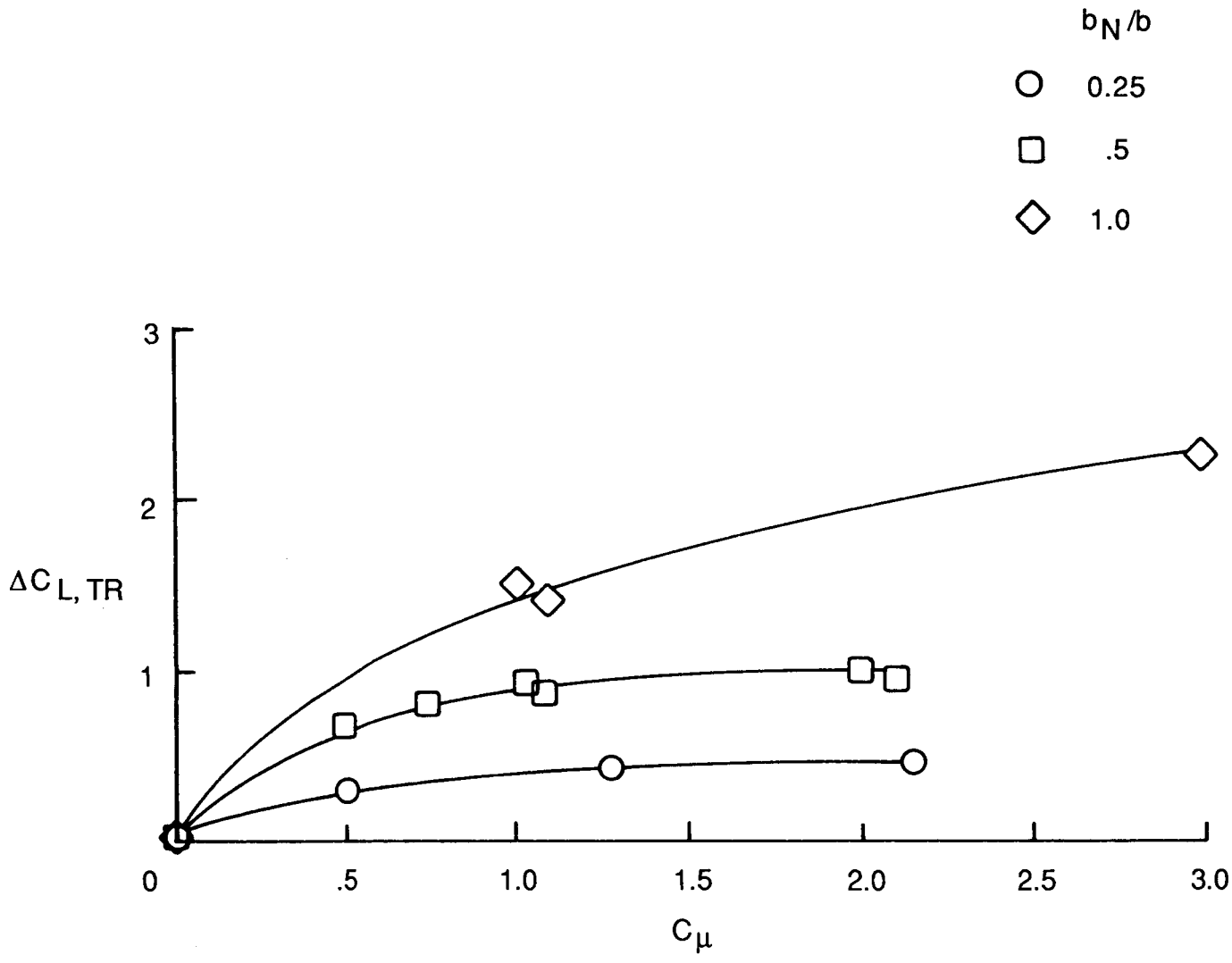

(b) Thrust-induced lift versus thrust coefficient.

Figure 18. Continued.

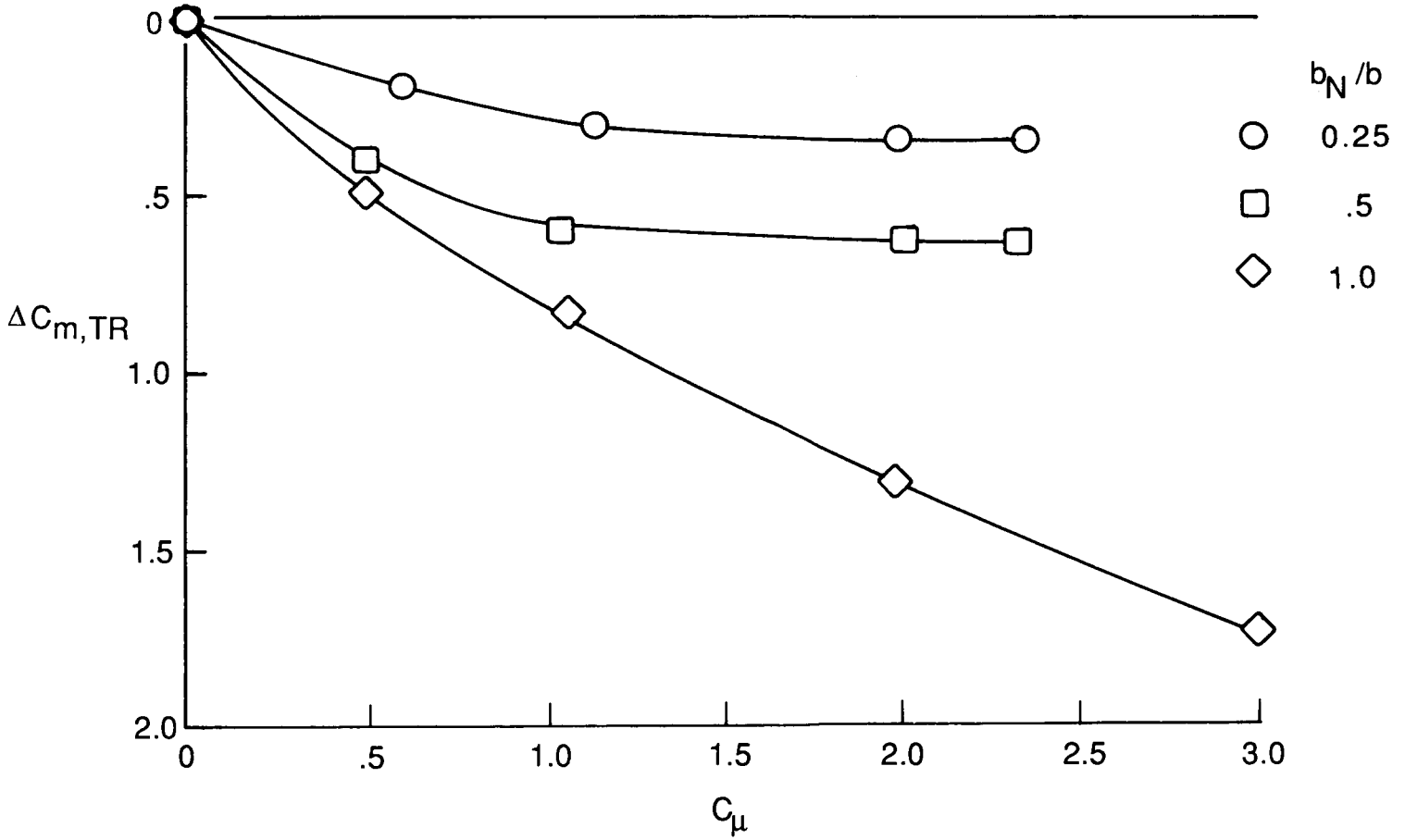

(c) Thrust-induced pitching moment versus thrust coefficient.

Figure 18. Concluded.

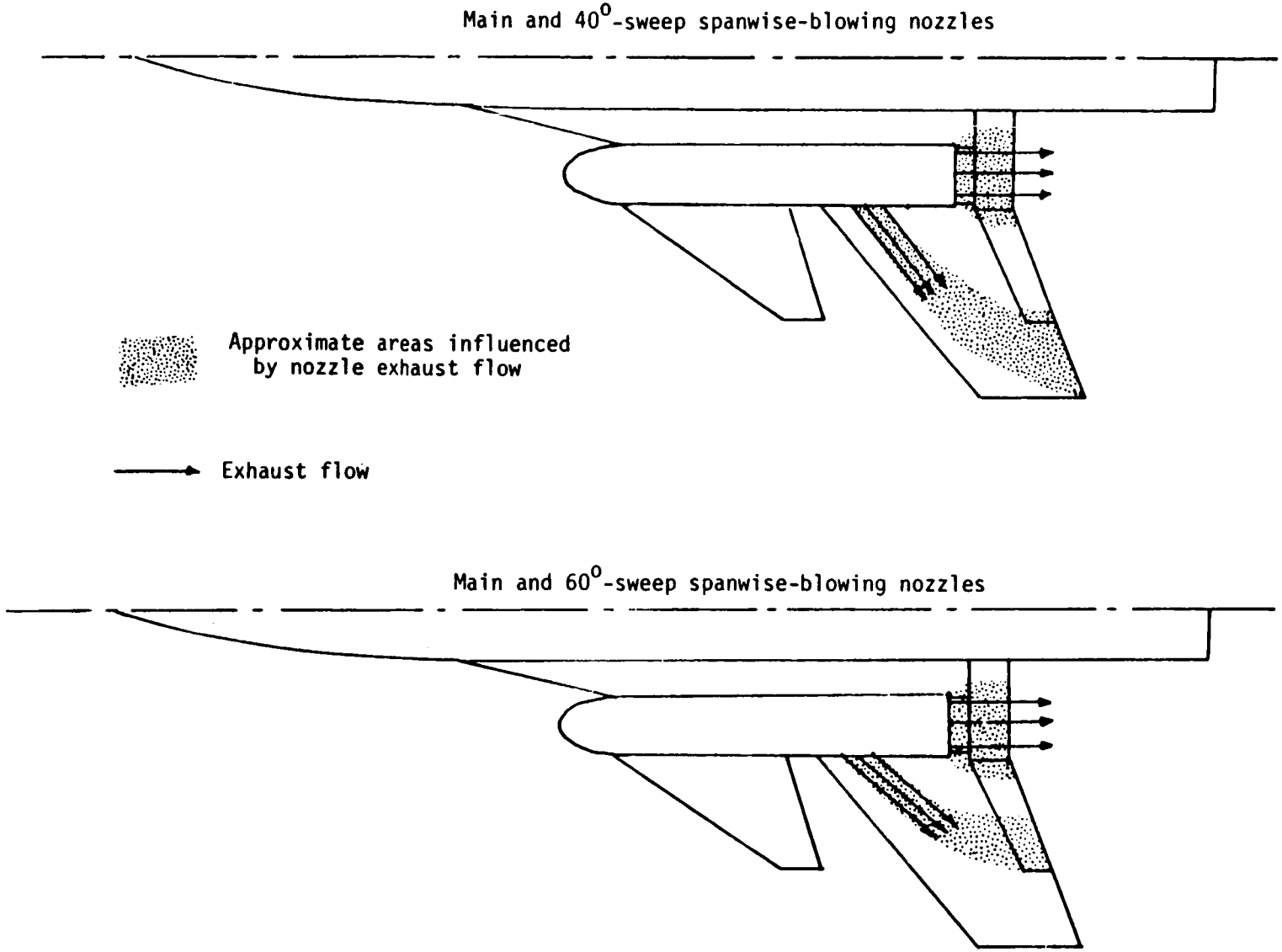

Figure 19. Schematic of spanwise nozzle exhaust flow on VEO-wing configuration.

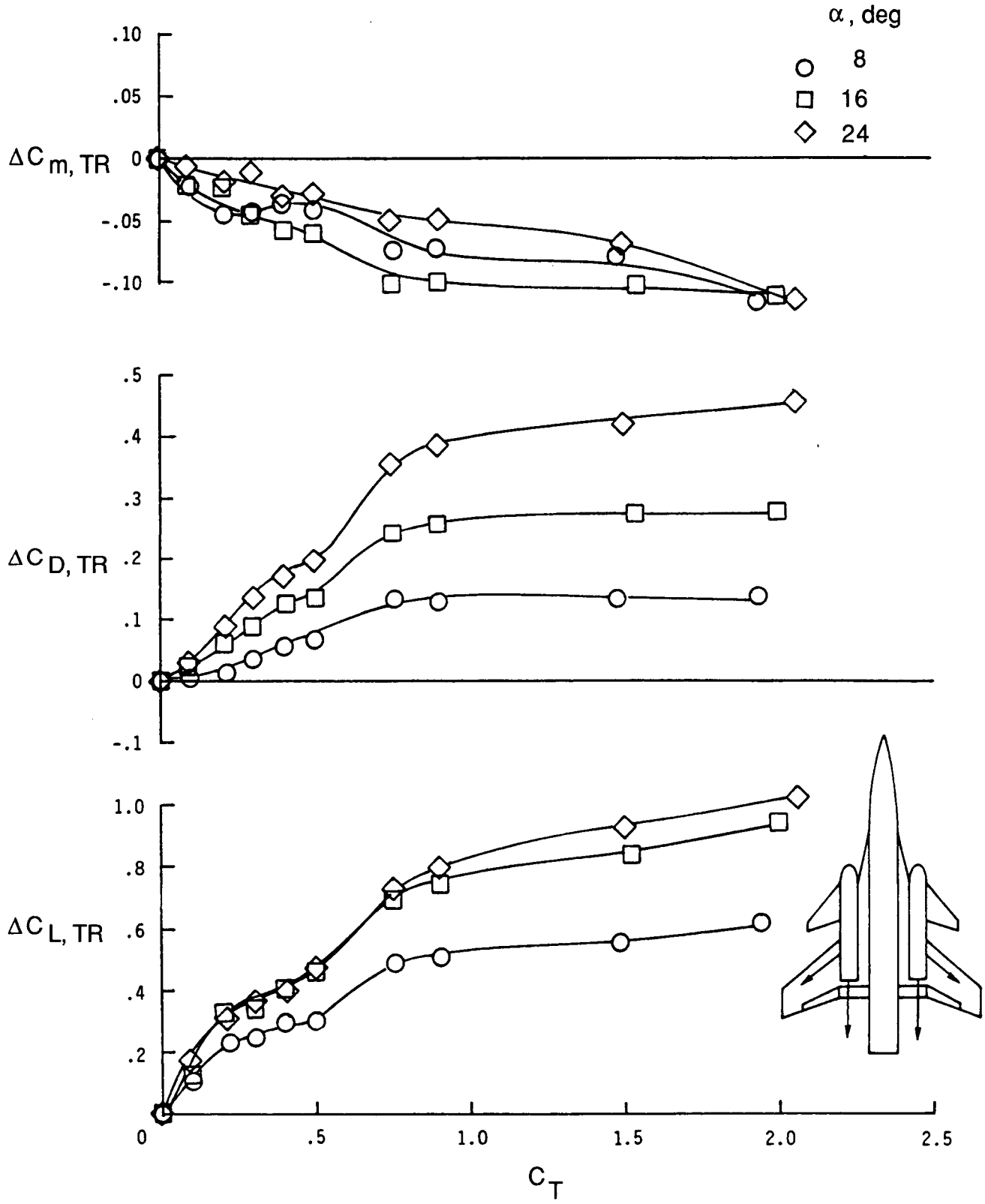

Figure 20. Thrust-induced longitudinal aerodynamic characteristics for VEO-wing configuration. $\delta_f = 30°$; $\Lambda_{SWB} = 40°$; $\delta_N = 30°$.

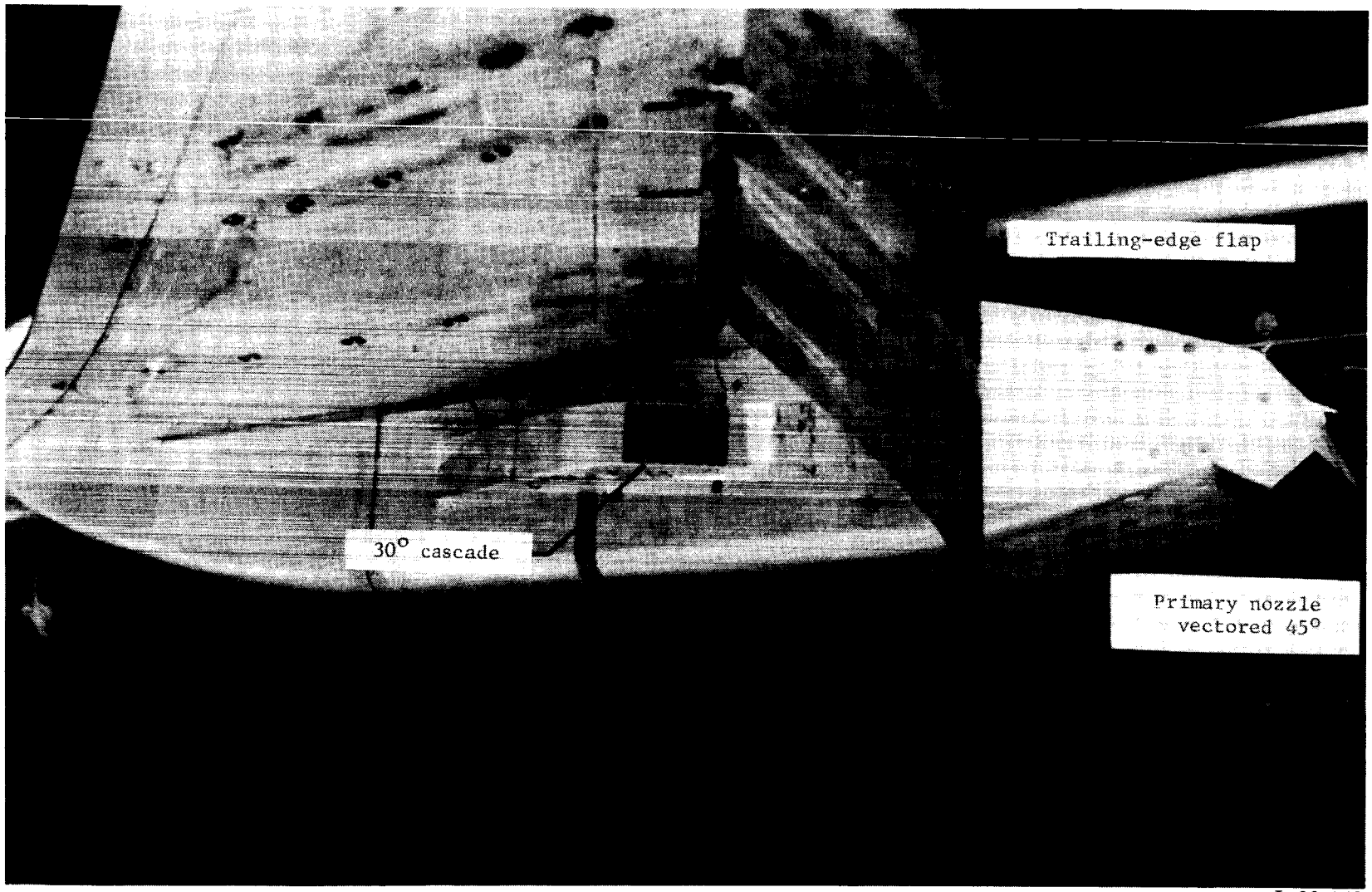

L-83-143

(a) Photograph of SWB nozzle. $\Lambda_{SWB} = 30°$; $\delta_f = 45°/45°$.

Figure 21. Spanwise blowing on trailing-edge flap system on modified generic wing-canard fighter configuration.

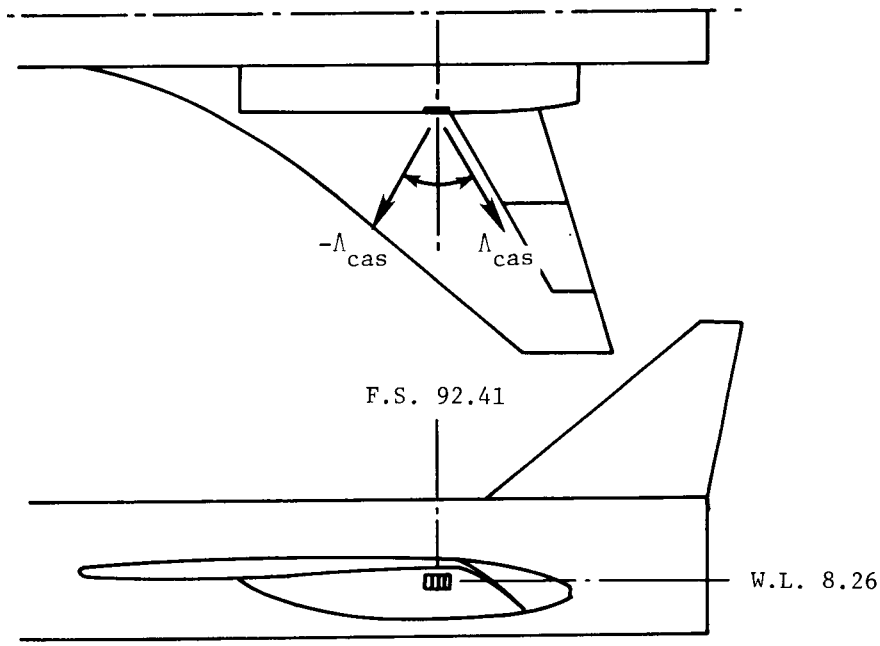

(b) Geometry sketch. Linear dimensions are given in inches.

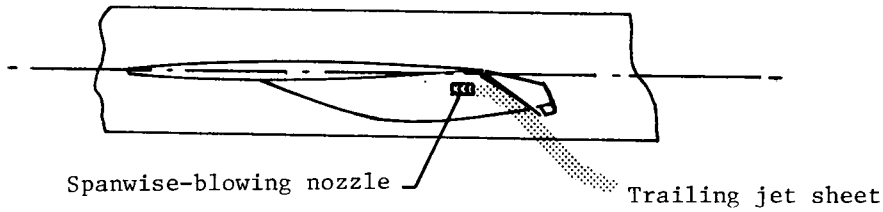

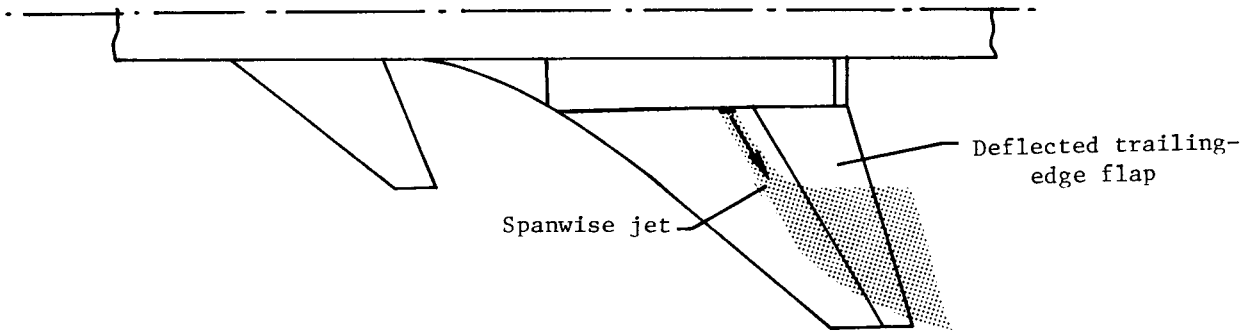

(c) Sketch of SWB flow field.

Figure 21. Concluded.

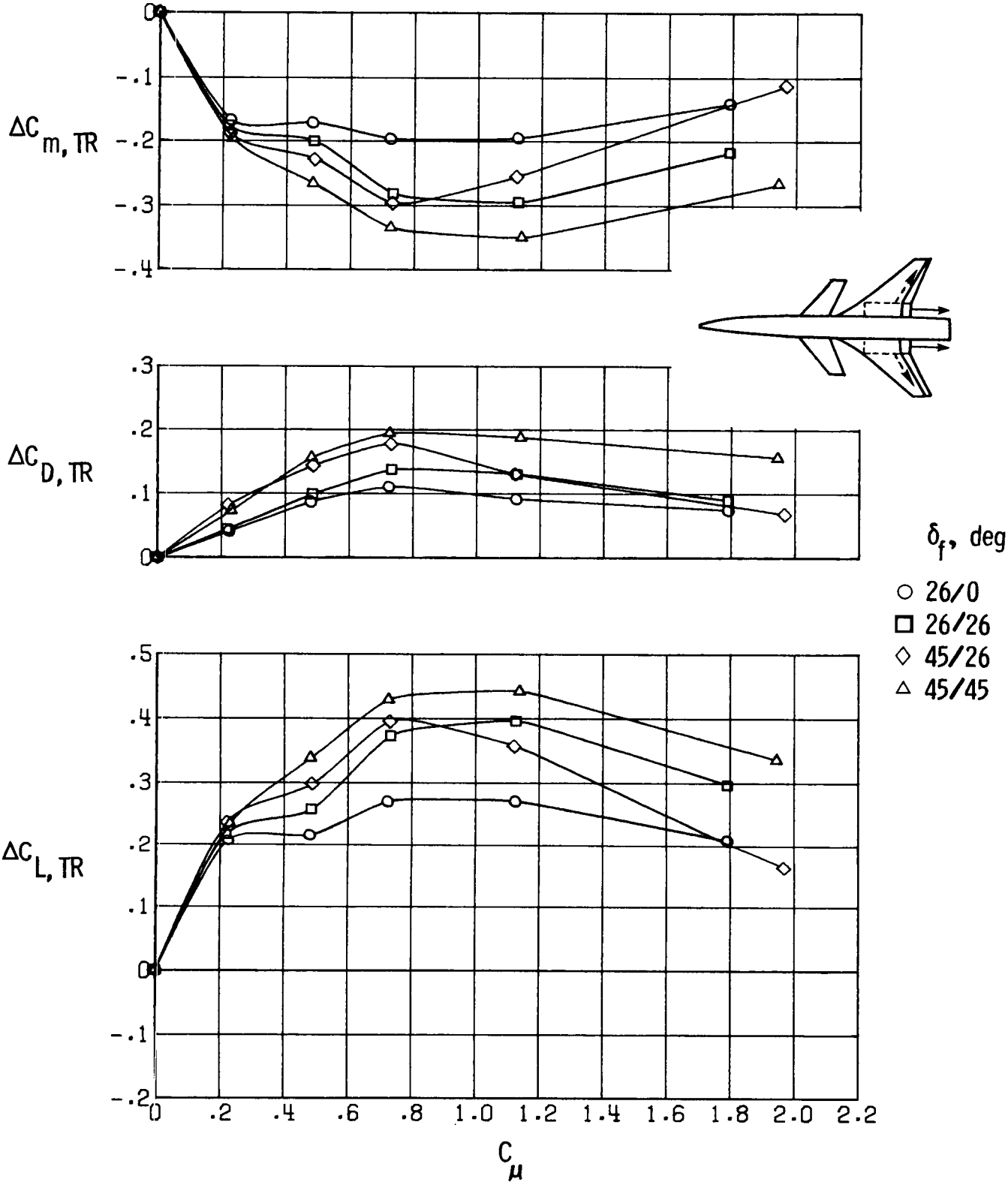

Figure 22. Thrust-induced aerodynamics for generic wing-canard fighter configuration with SWB on trailing-edge flap system. $\delta_N = 45°$; $\Lambda_{SWB} = 30°$.

L-83-146

Figure 23. Oil flow of SWB flow field on modified generic wing-canard fighter configuration. $\Lambda_{SWB} = 30°$.

ORIGINAL PAGE IS
OF POOR QUALITY

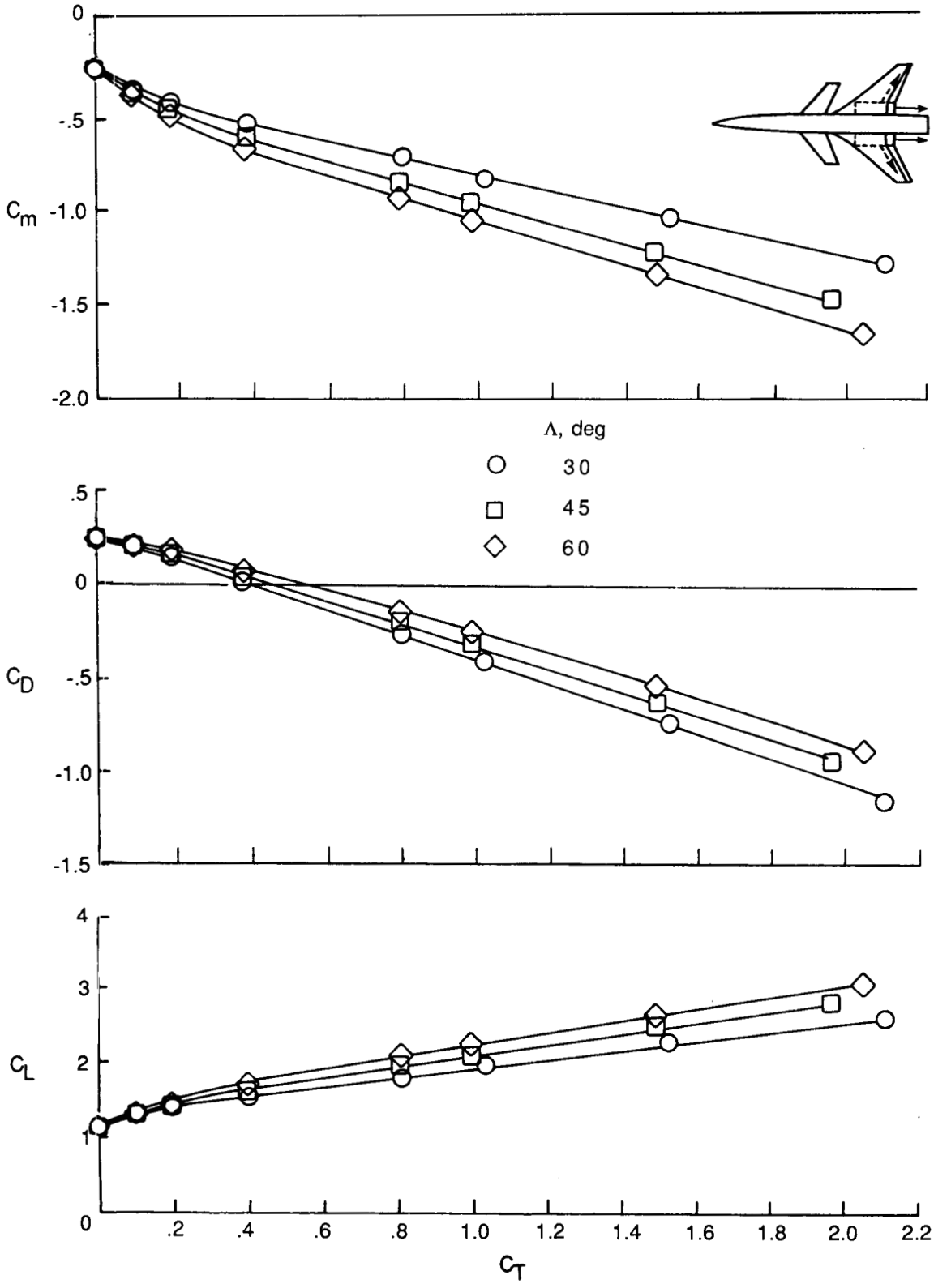

(a) Total aerodynamic coefficients. $\delta_f = 26°/26°$.

Figure 24. Longitudinal aerodynamics of modified generic wing-canard fighter configuration with SWB on trailing-edge flap system. $\alpha = 12°$.

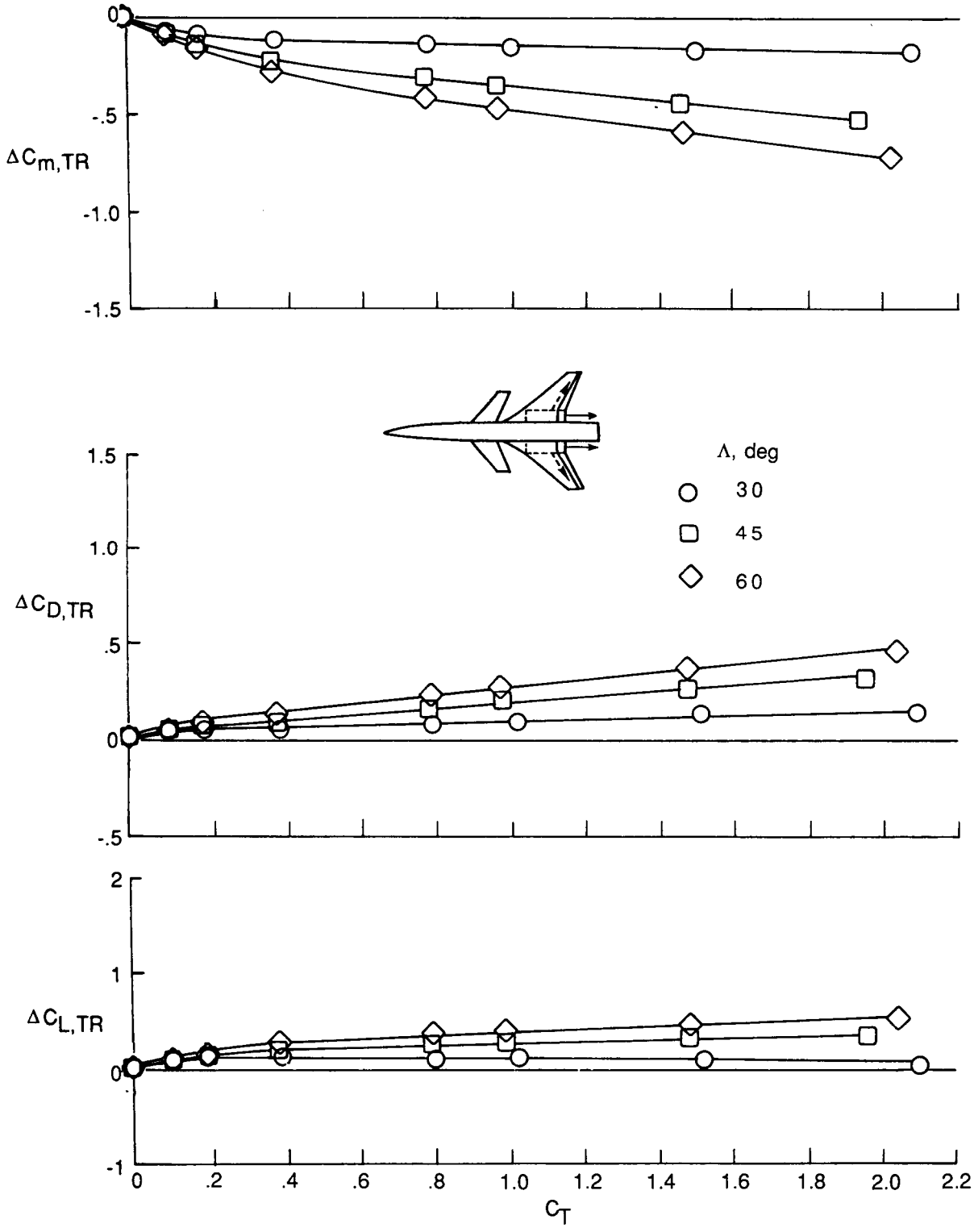

(b) Thrust-induced aerodynamic coefficients. $\delta_f = 26°/26°$.

Figure 24. Continued.

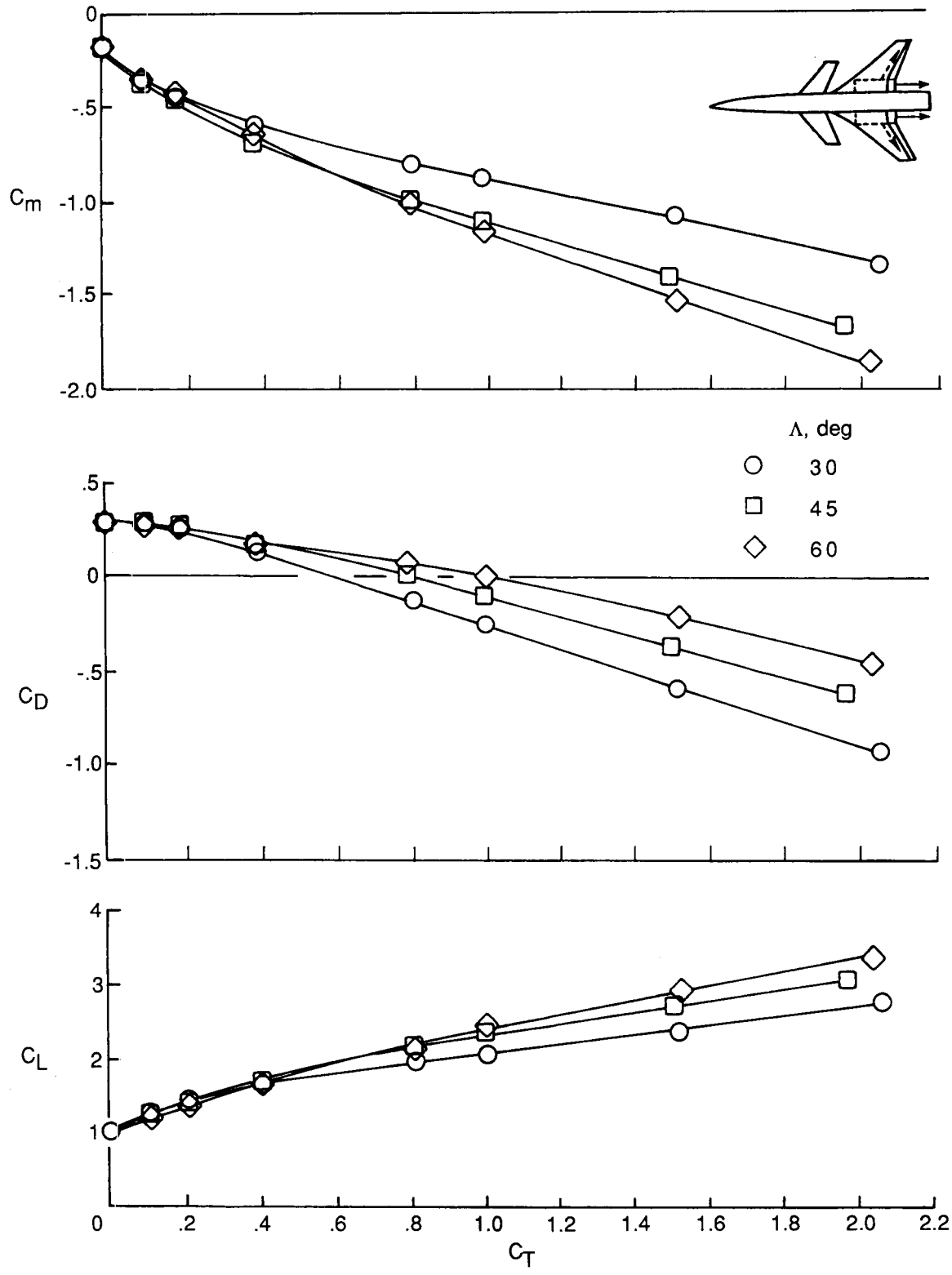

(c) Total aerodynamic coefficients. $\delta_f = 45°/45°$.

Figure 24. Continued.

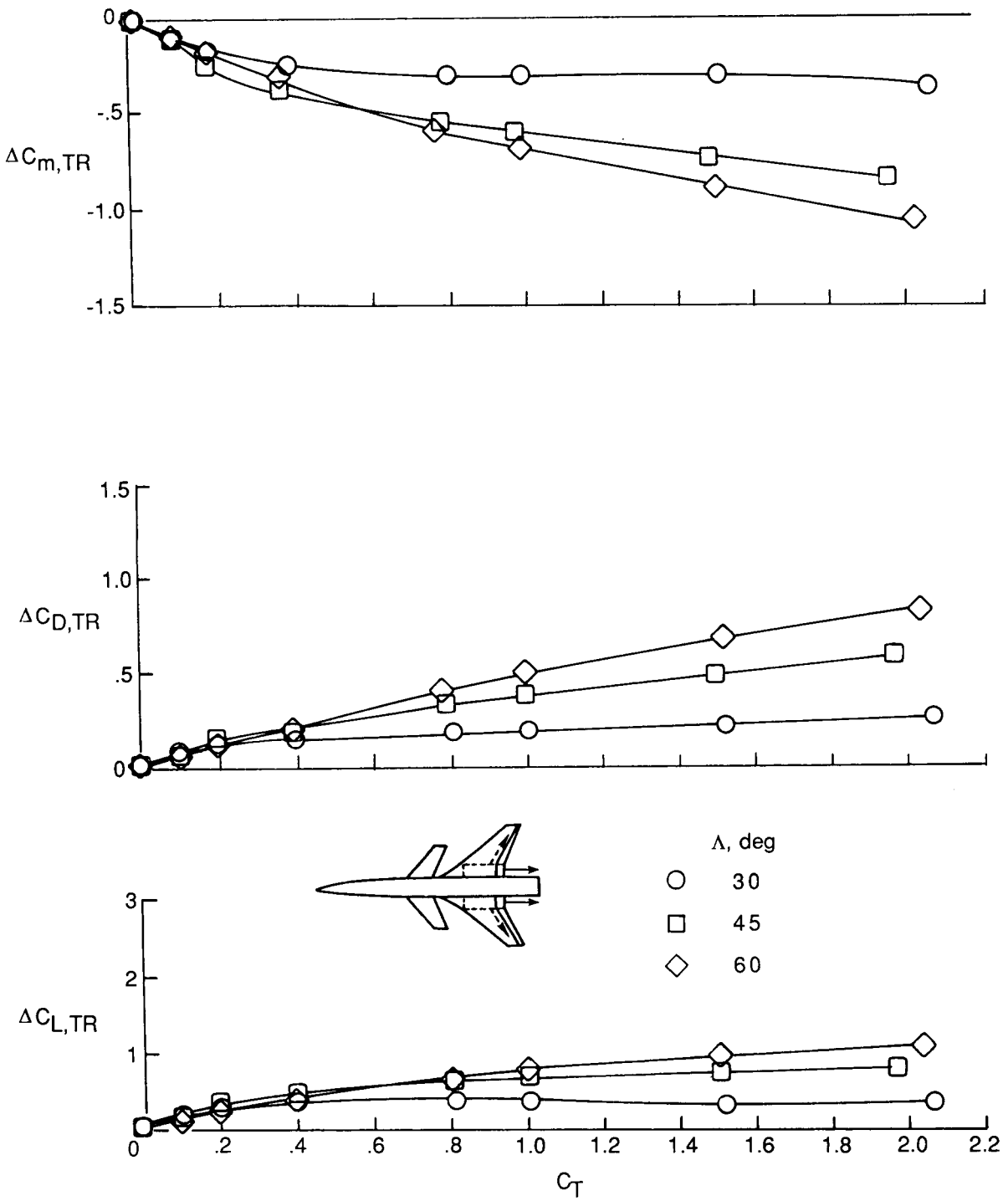

(d) Thrust-induced aerodynamic coefficients. $\delta_f = 45°/45°$.

Figure 24. Concluded.

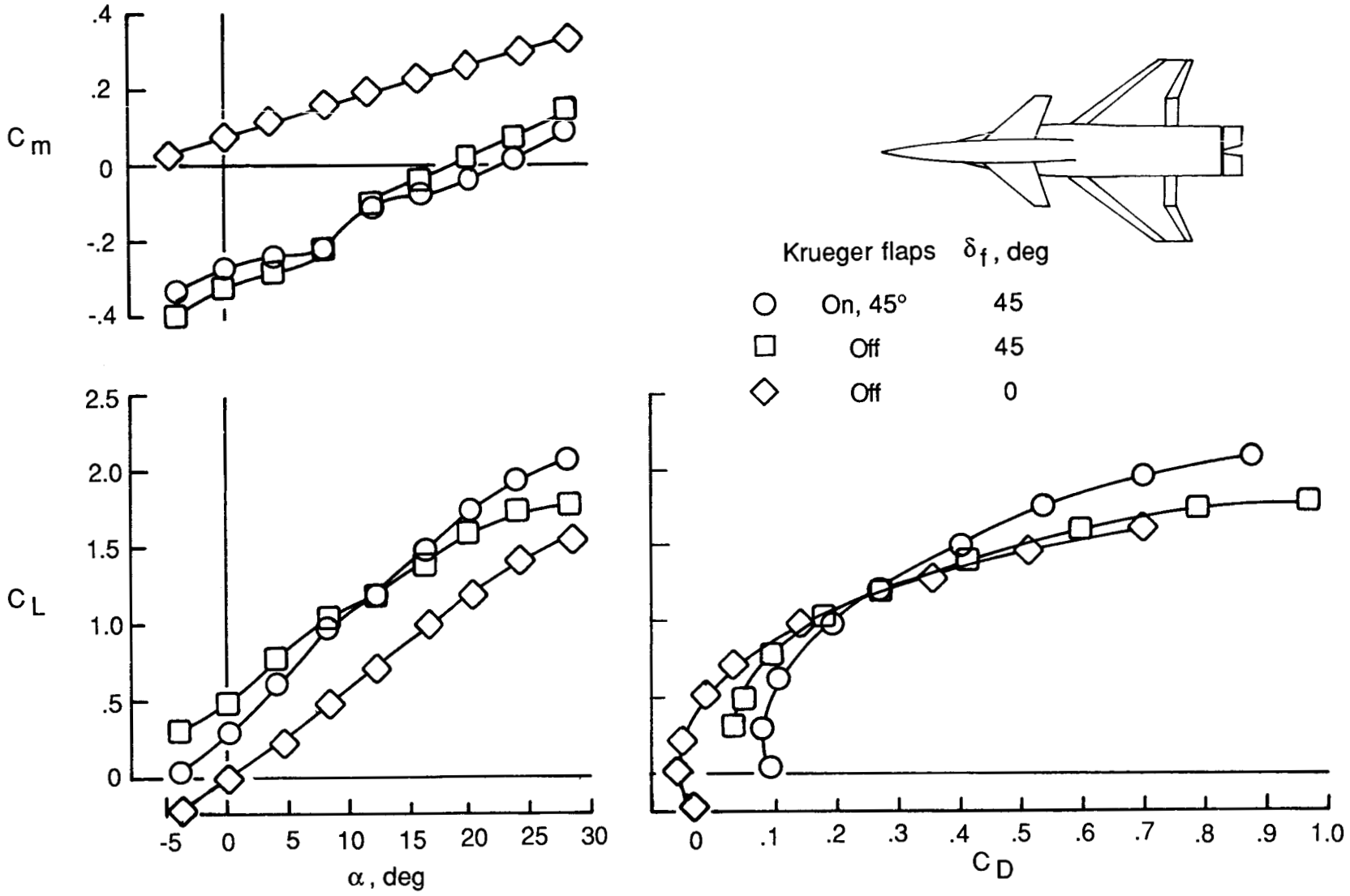

Figure 25. Effect of Krueger leading-edge and slotted trailing-edge flaps on longitudinal aerodynamics of ANC-B wing-canard configuration.

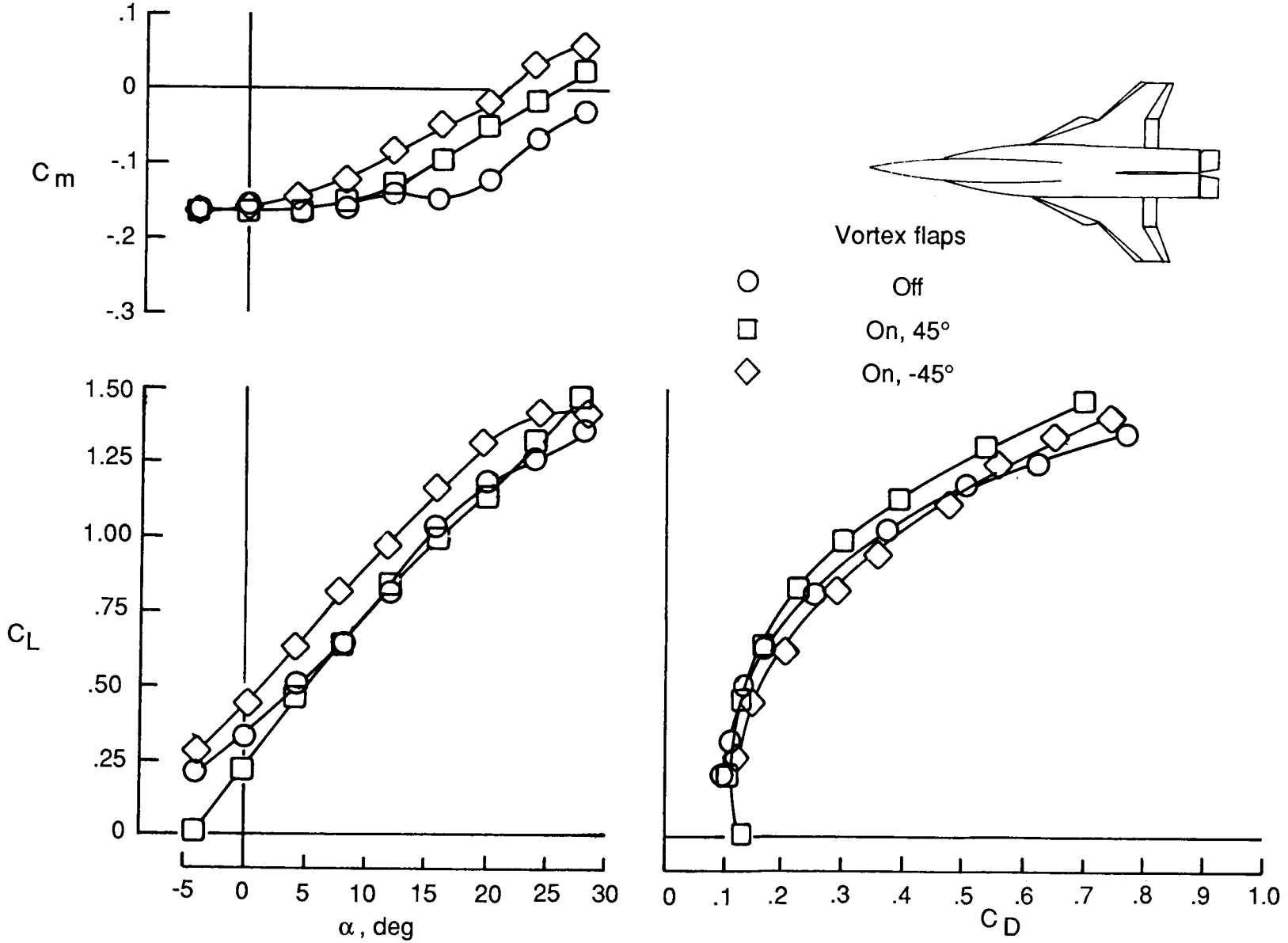

Figure 26. Effect of vortex flaps on aerodynamics of ANC-B wing-alone configuration. $\delta_f = 45°$.

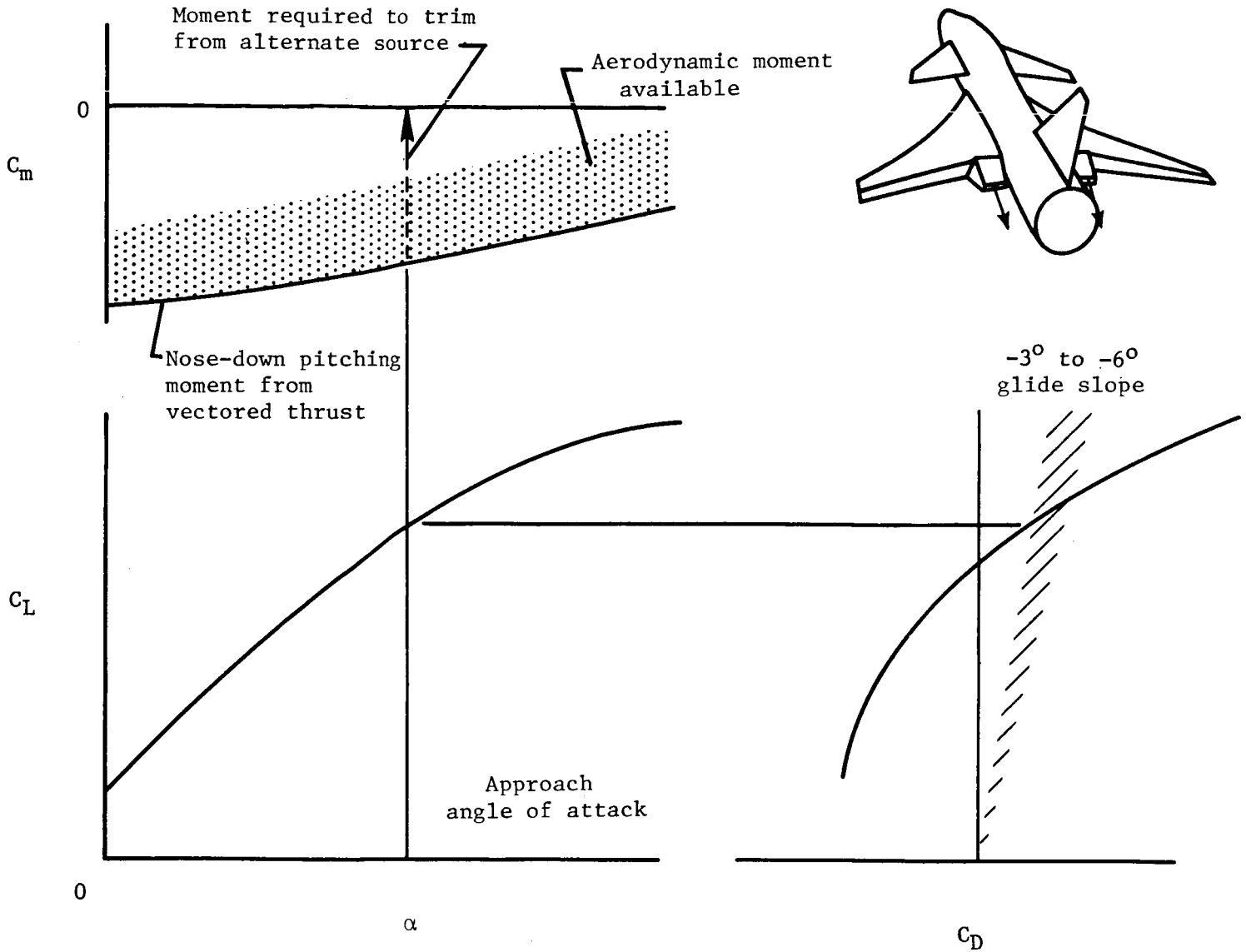

Figure 27. Schematic of approach aerodynamics for STOL fighter configuration with vectored thrust.

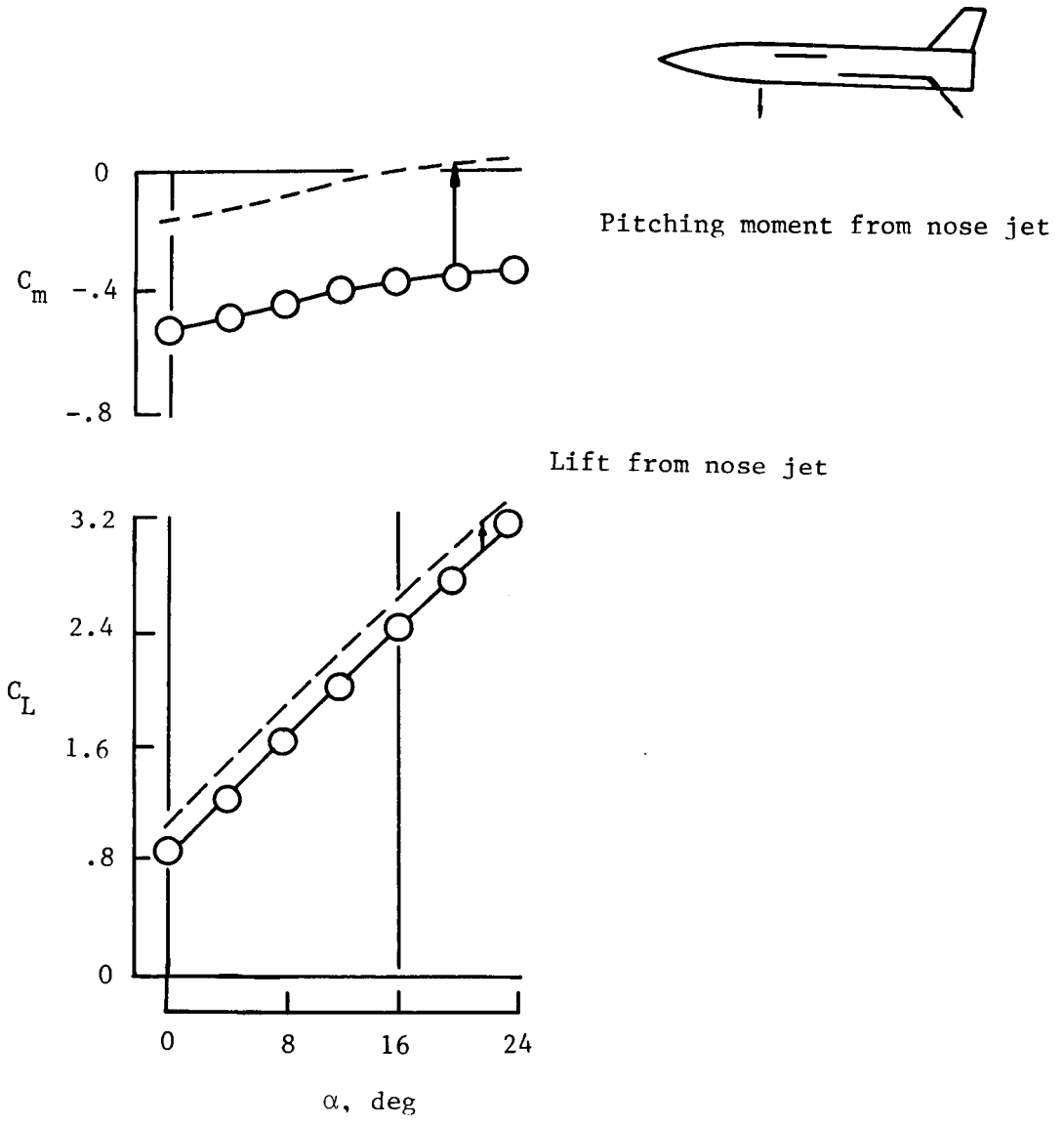

(a) Takeoff. $\delta_f = 20°$; $\delta_N = 20°$; $C_T = 1.0$.

Figure 28. Trim analysis for takeoff and landing for generic wing-canard fighter configuration.

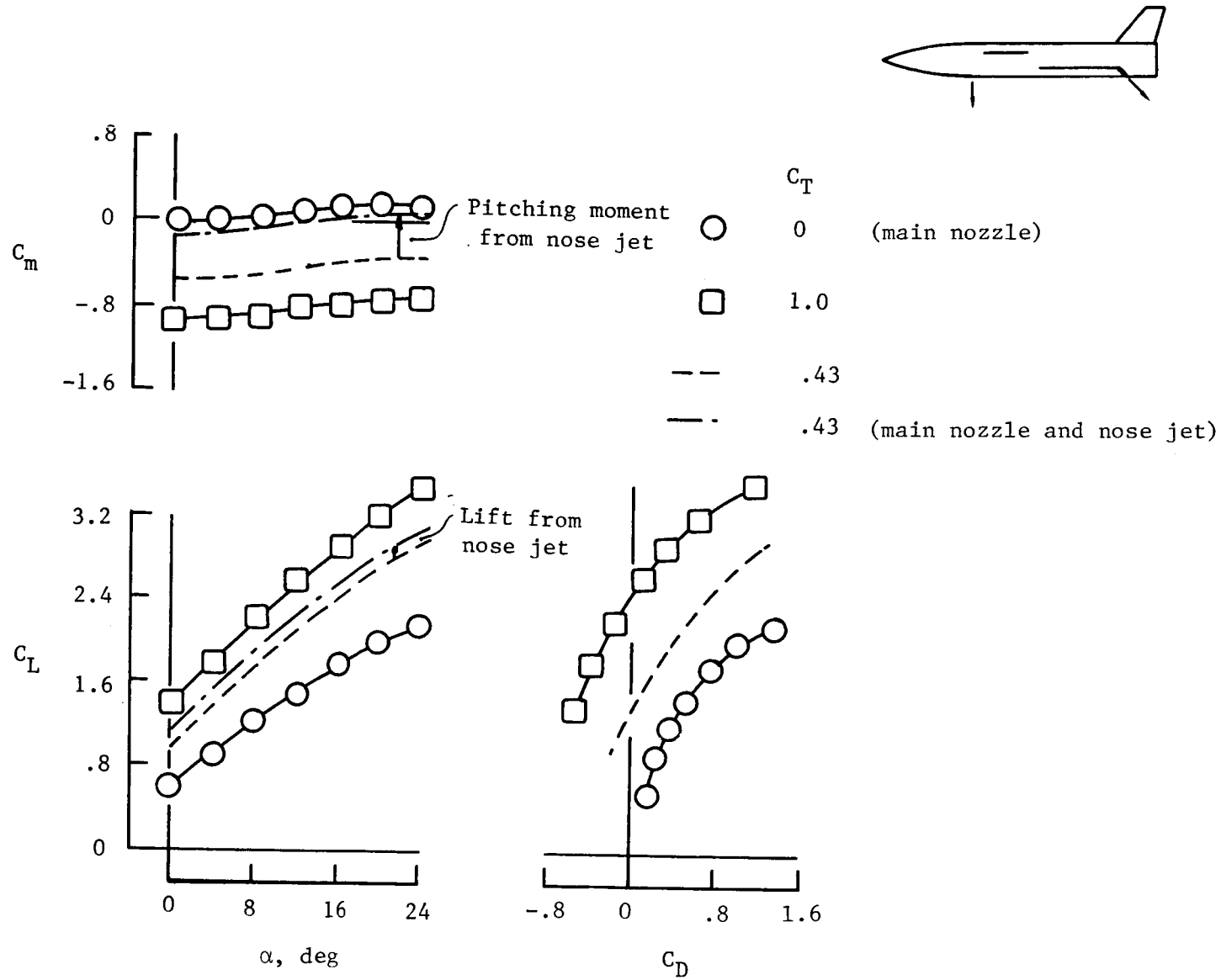

(b) Landing. $\delta_f = 40°$; $\delta_N = 40°$.

Figure 28. Concluded.

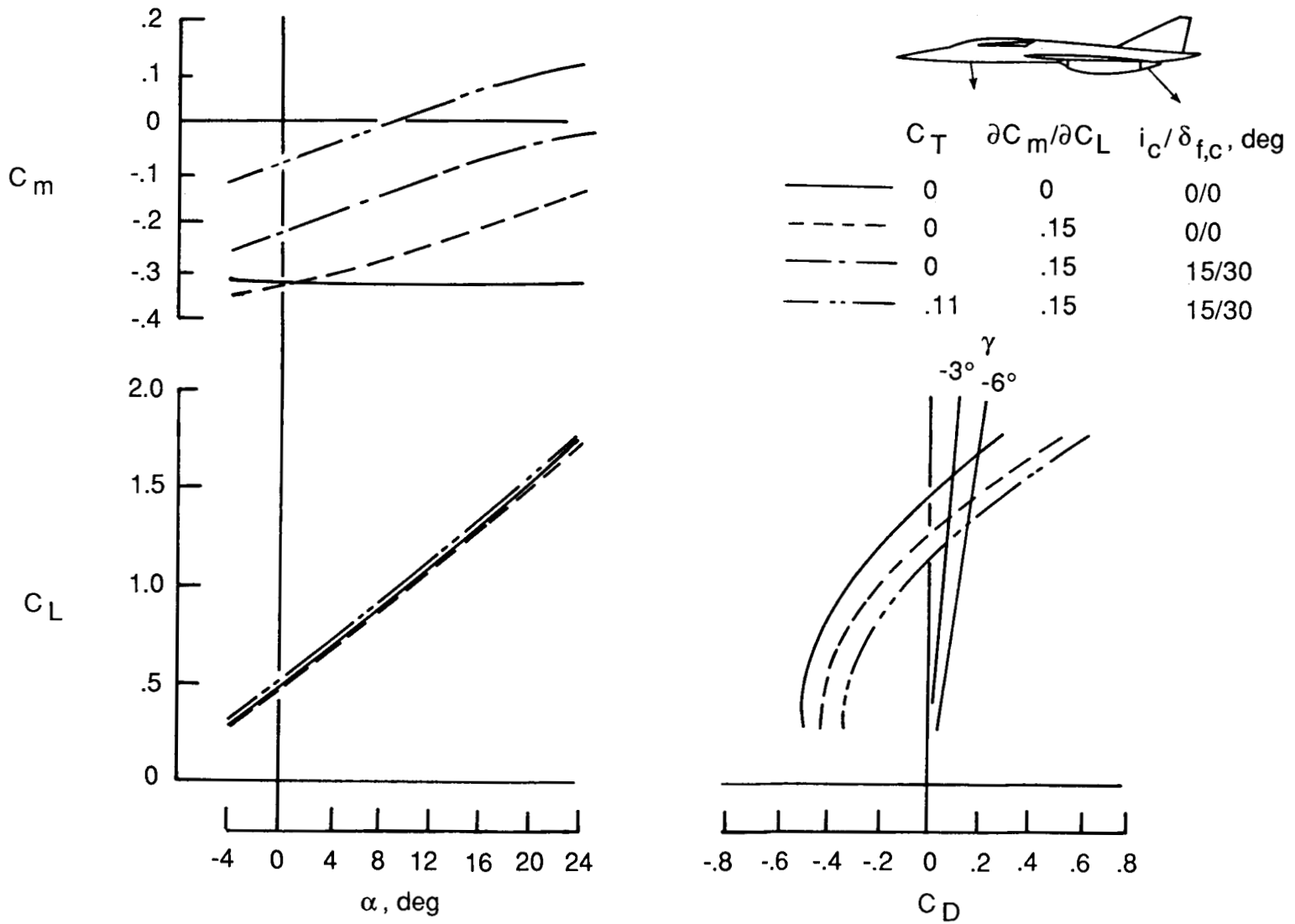

Figure 29. Trim analysis for landing of Mach 2 supercruiser configuration. $C_T = 0.75$; $\delta_N = 43°$.

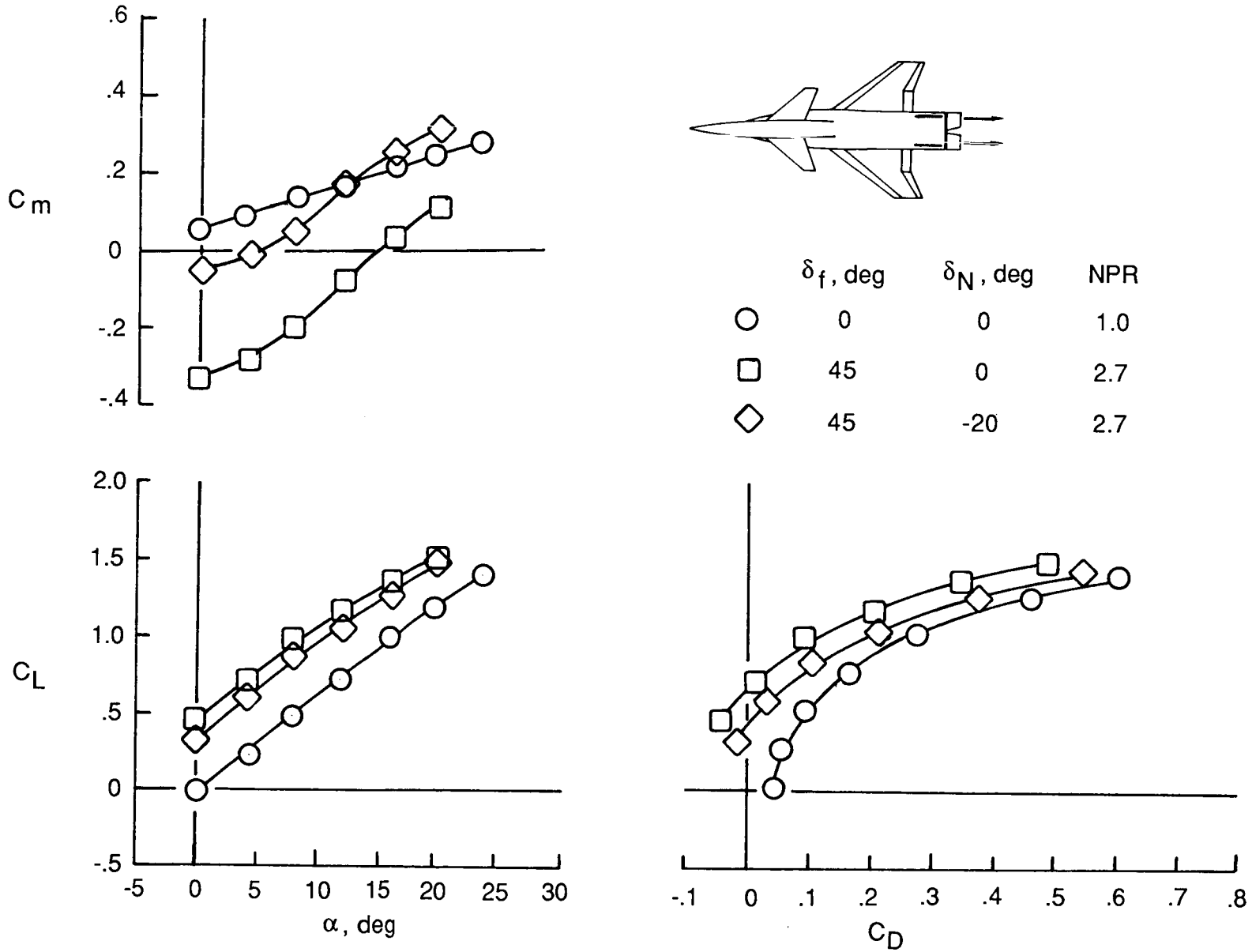

Figure 30. Approach aerodynamics for ANC-B wing-canard configuration.

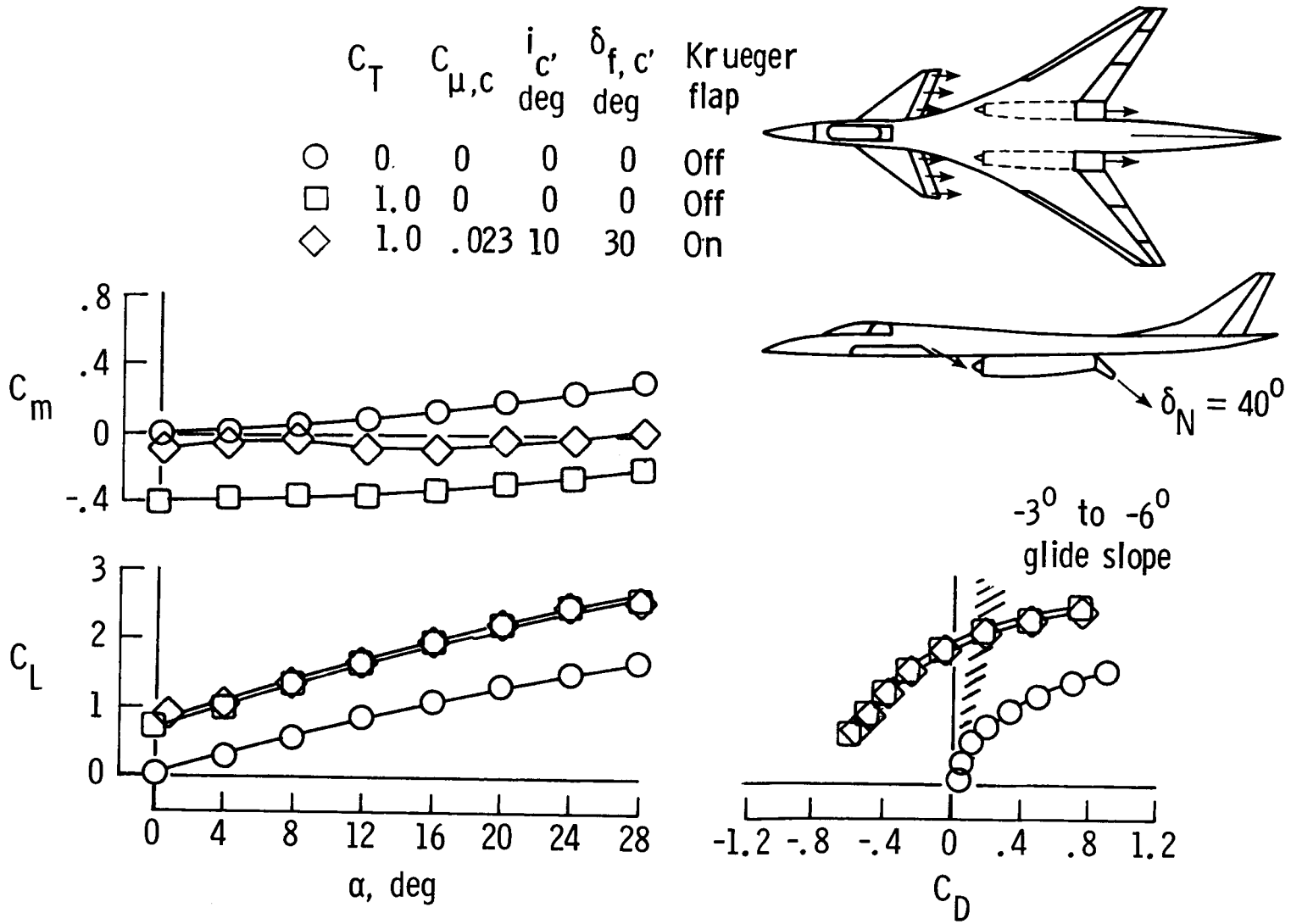

(a) Effect of thrust and high-lift canard.

Figure 31. Approach aerodynamics for ATTAC configuration. $\delta_N = 40°$.

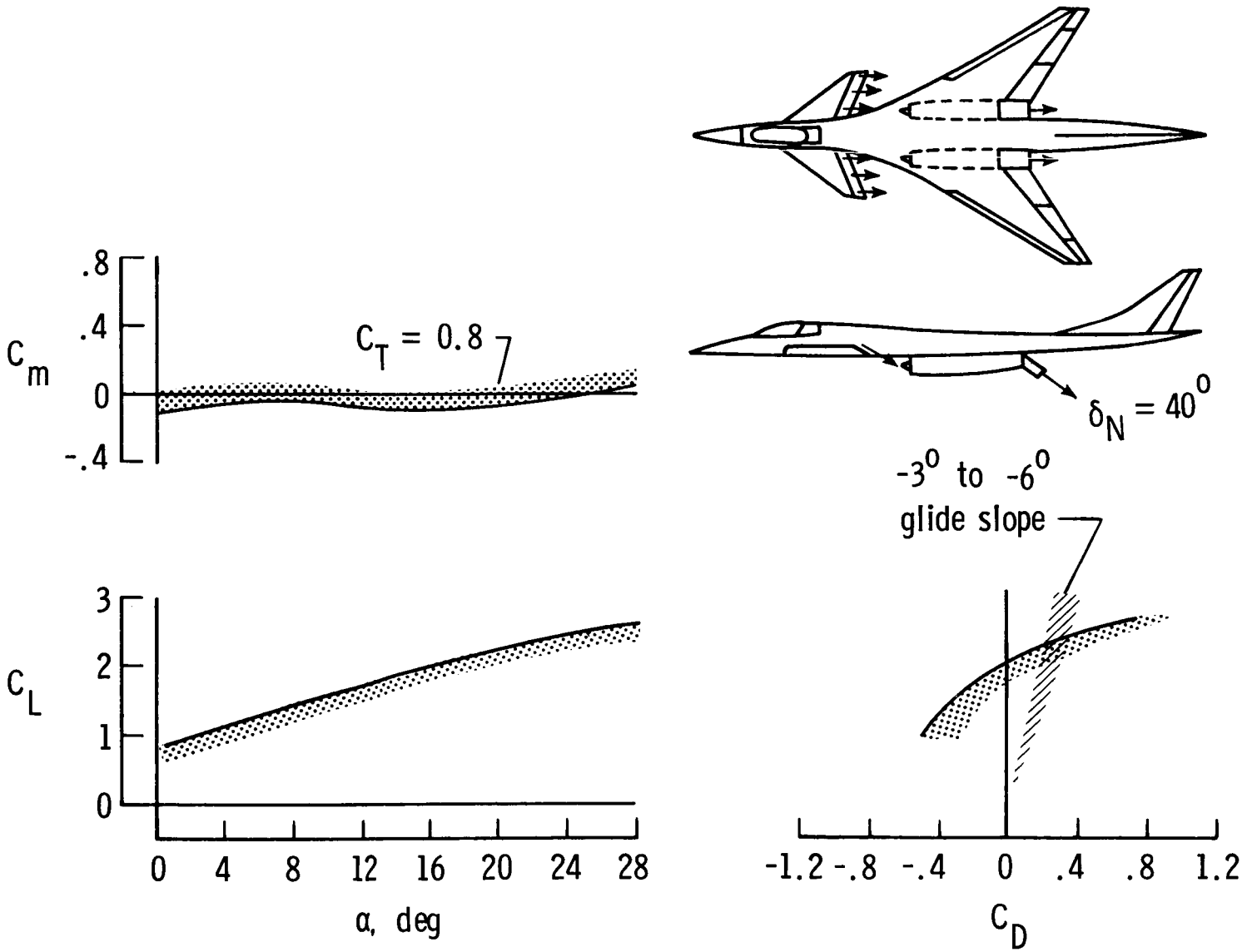

(b) Trimmed approach aerodynamics.

Figure 31. Concluded.

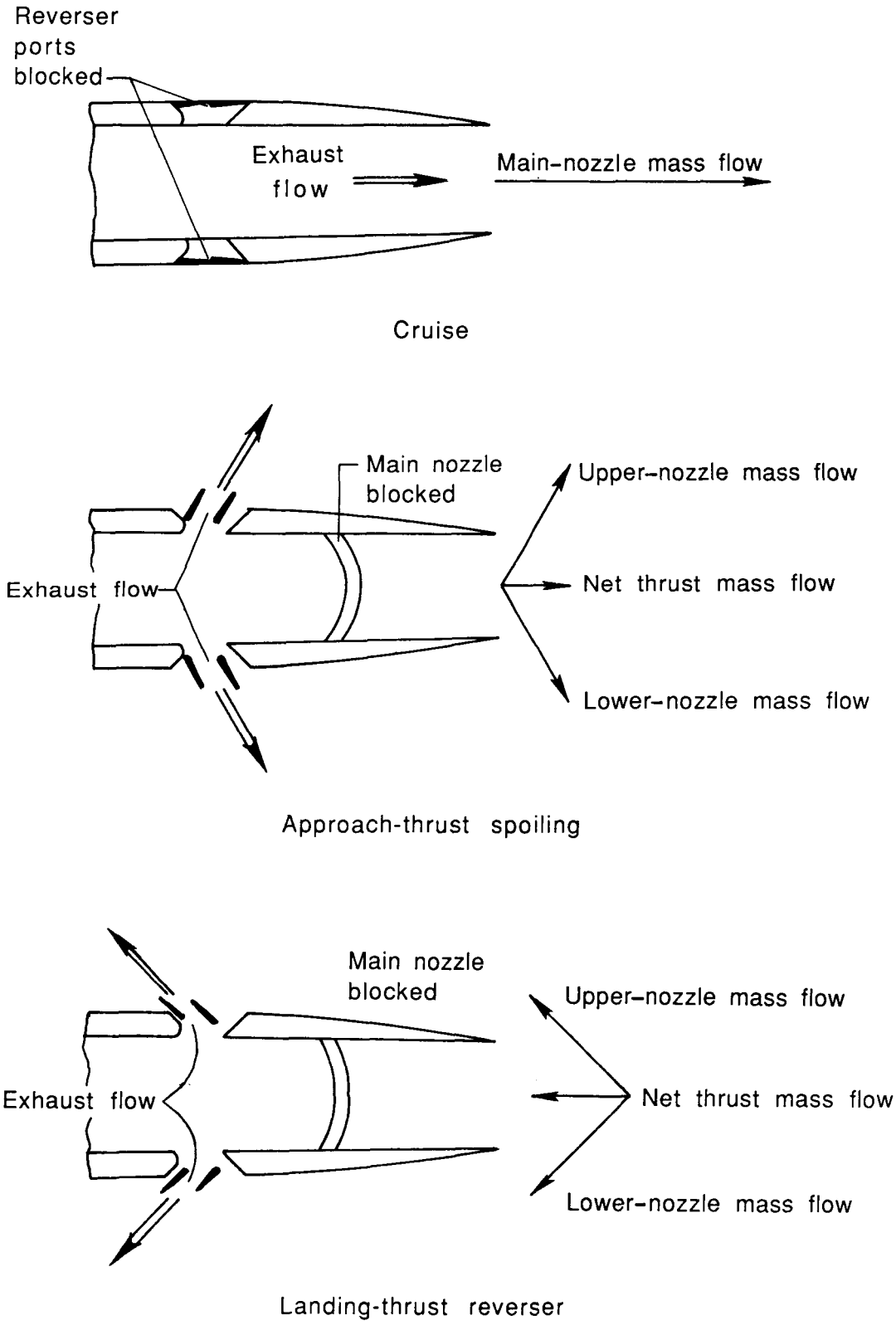

Figure 32. Schematic of rotating-vane type of thrust reverser.

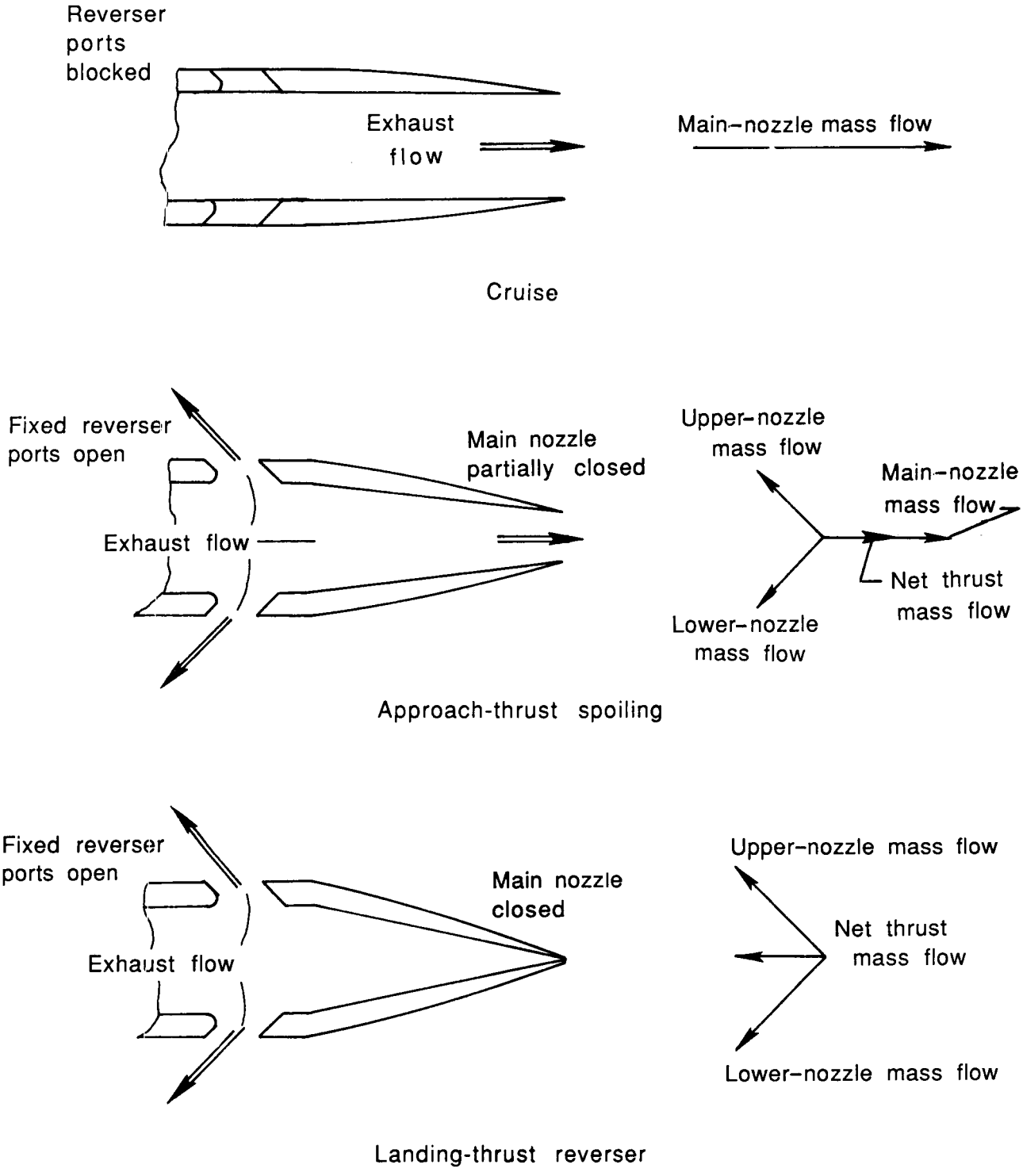

Figure 33. Schematic of multifunction-nozzle type of thrust reverser.

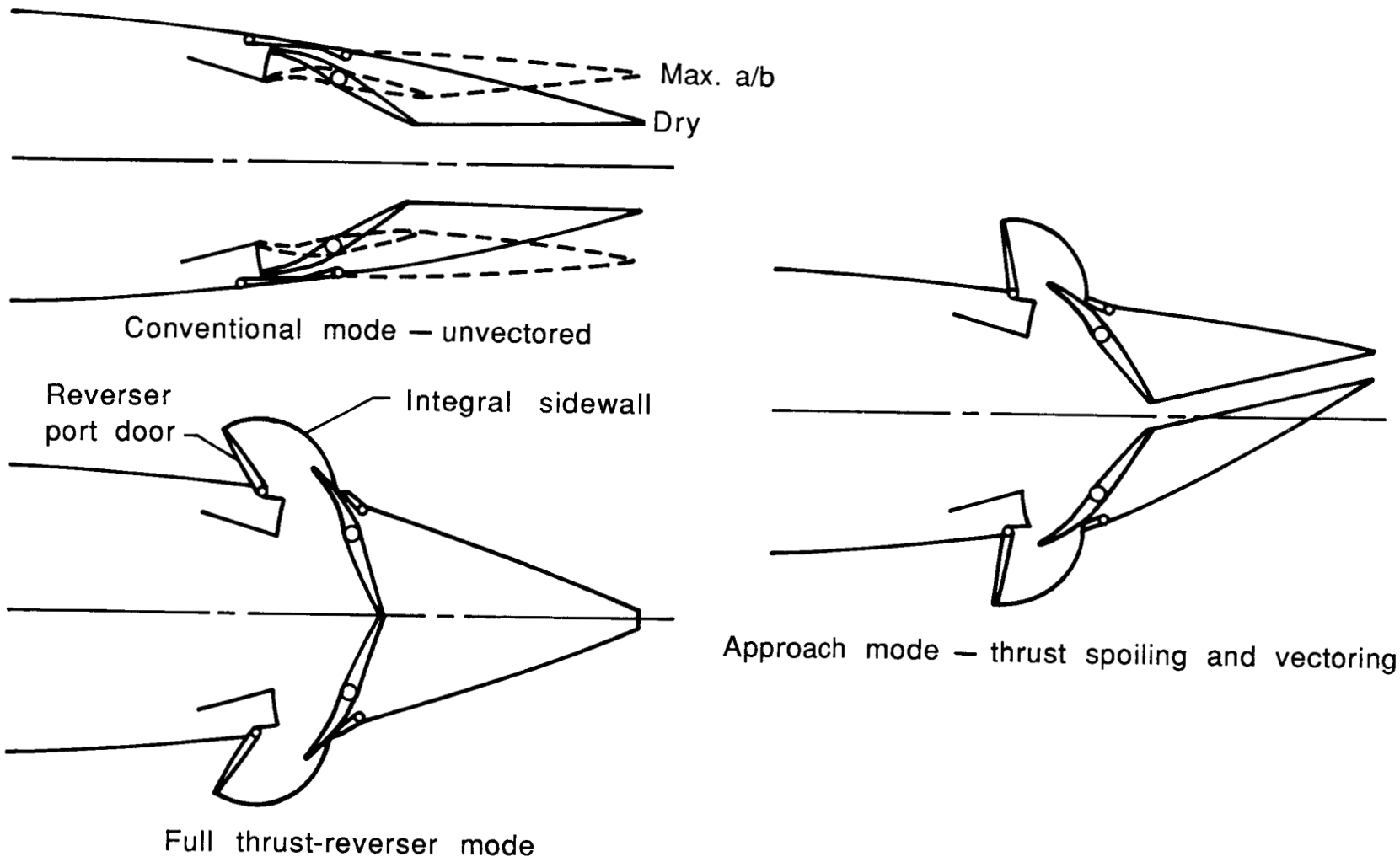

(a) Geometry sketch.

Figure 34. Two-dimensional convergent-divergent multifunction nozzle.

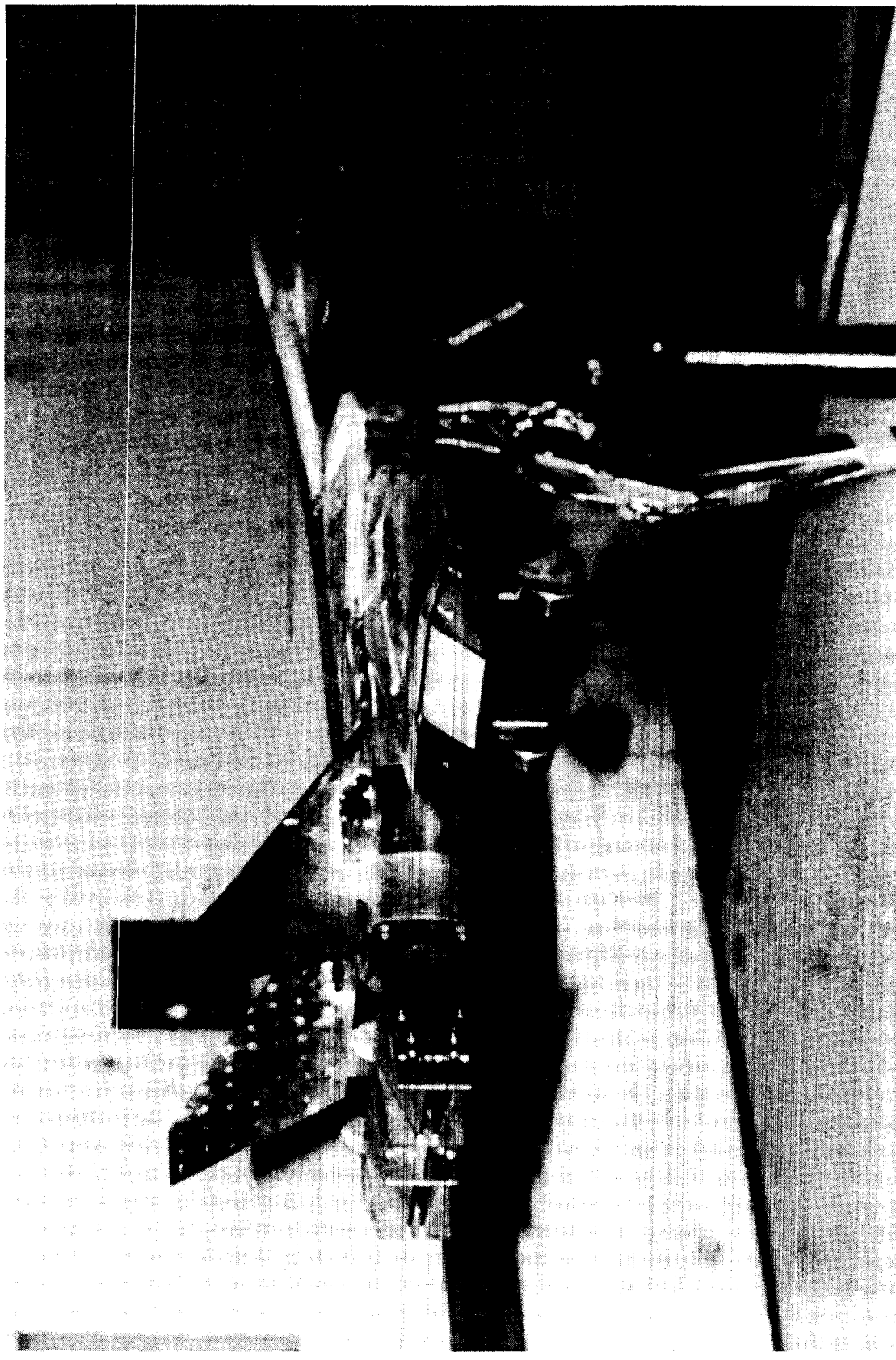

L-88-18

(b) Installation on ANC-B configuration.

Figure 34. Concluded.

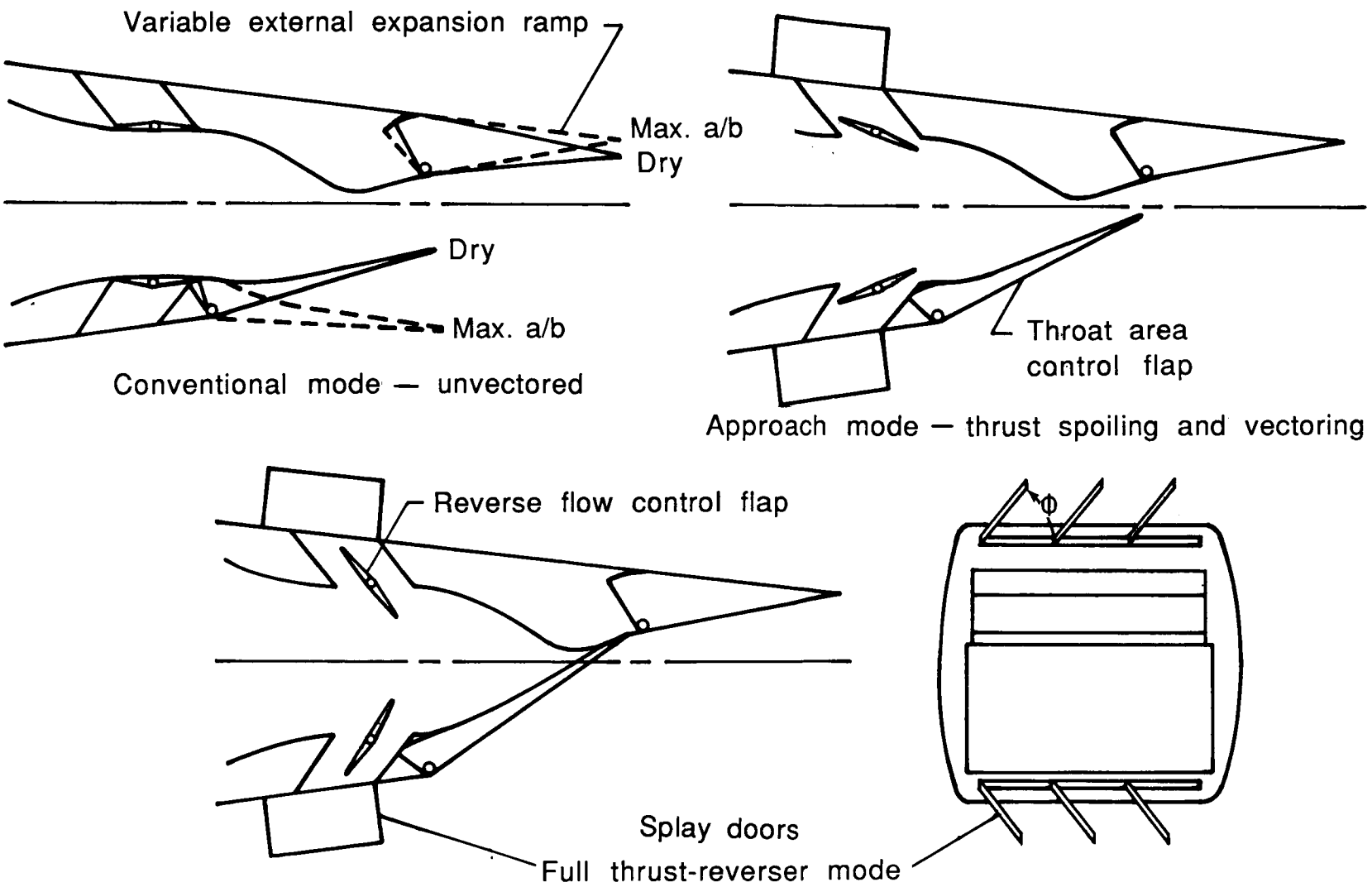

(a) Geometry sketch.

Figure 35. Single-expansion ramp nozzle with splay doors.

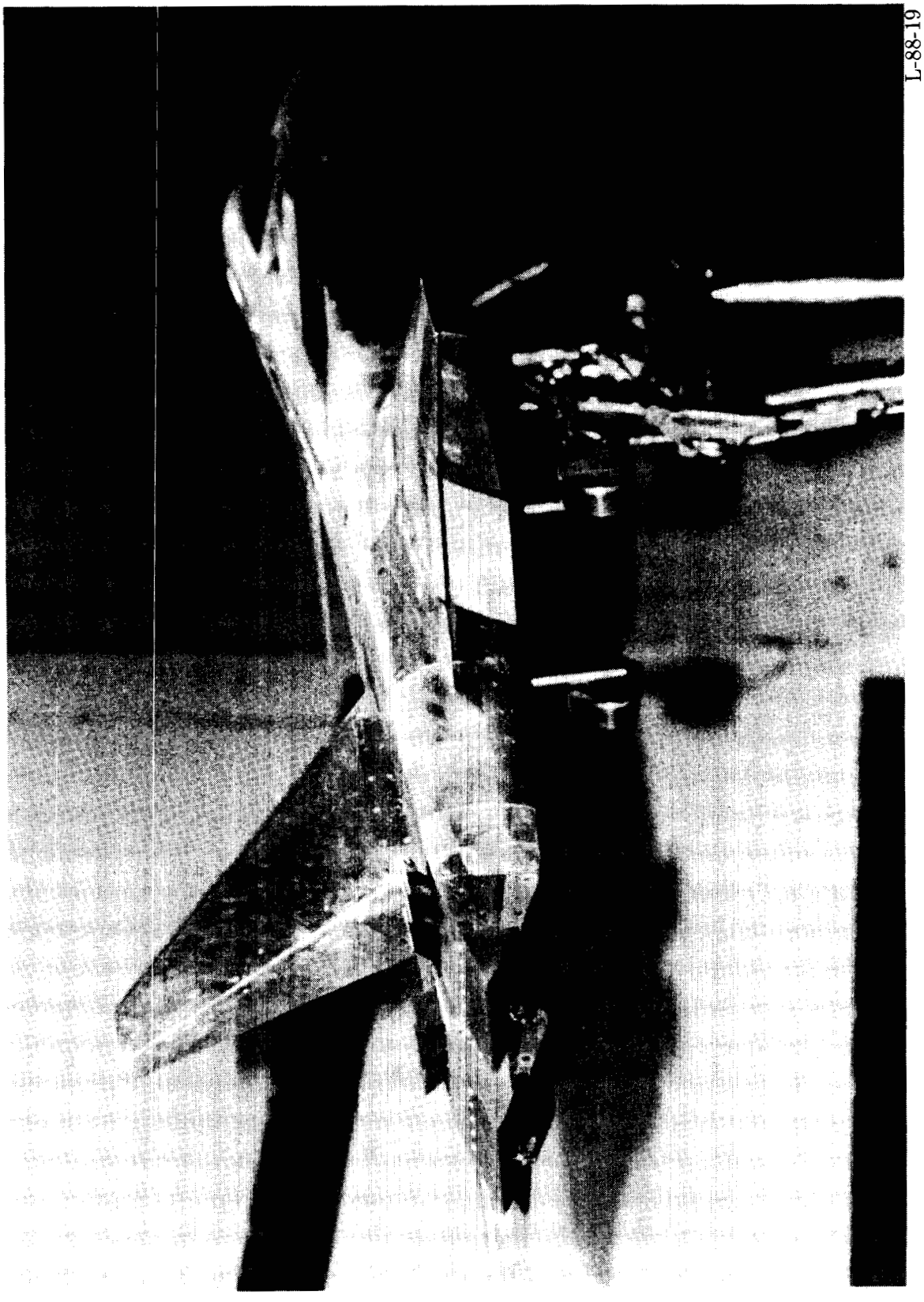

L-88-19

(b) Installation on ANC-B configuration.

Figure 35. Concluded.

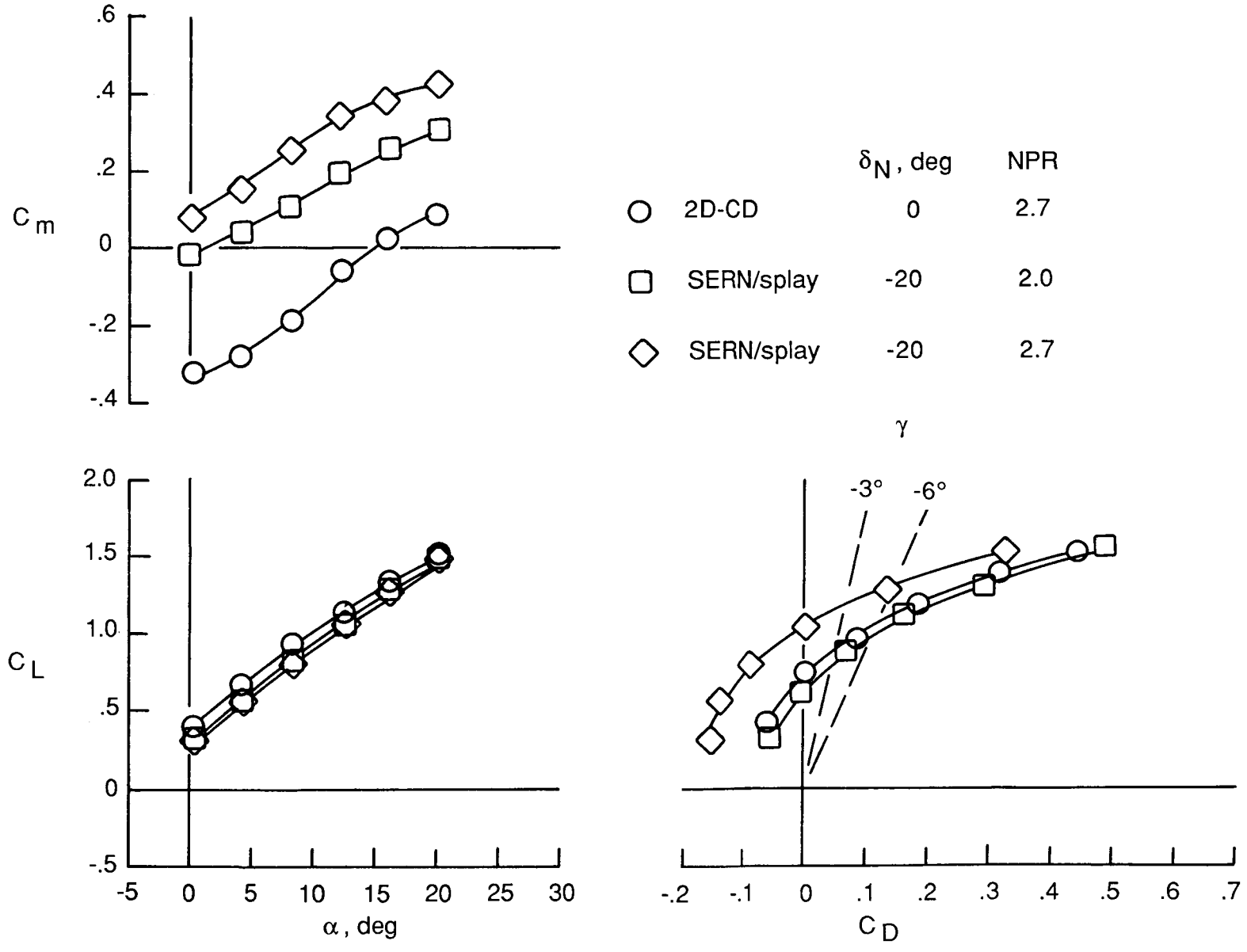

Figure 36. Approach longitudinal aerodynamics of ANC-B configuration with 2D-CD and SERN nozzles.

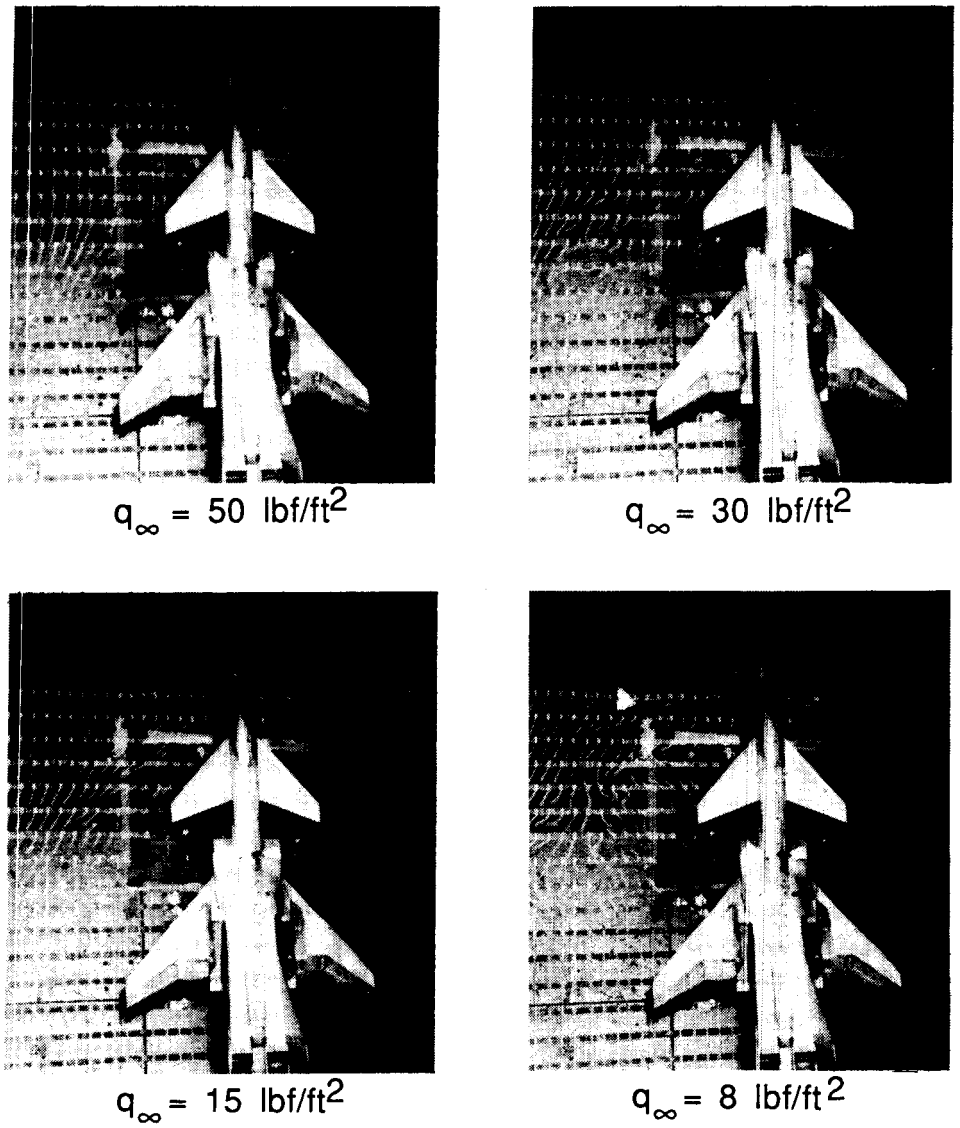

L-85-2633

(a) 2D-CD nozzle.

Figure 37. Flow patterns from thrust-reverser nozzles on ANC-B configuration.

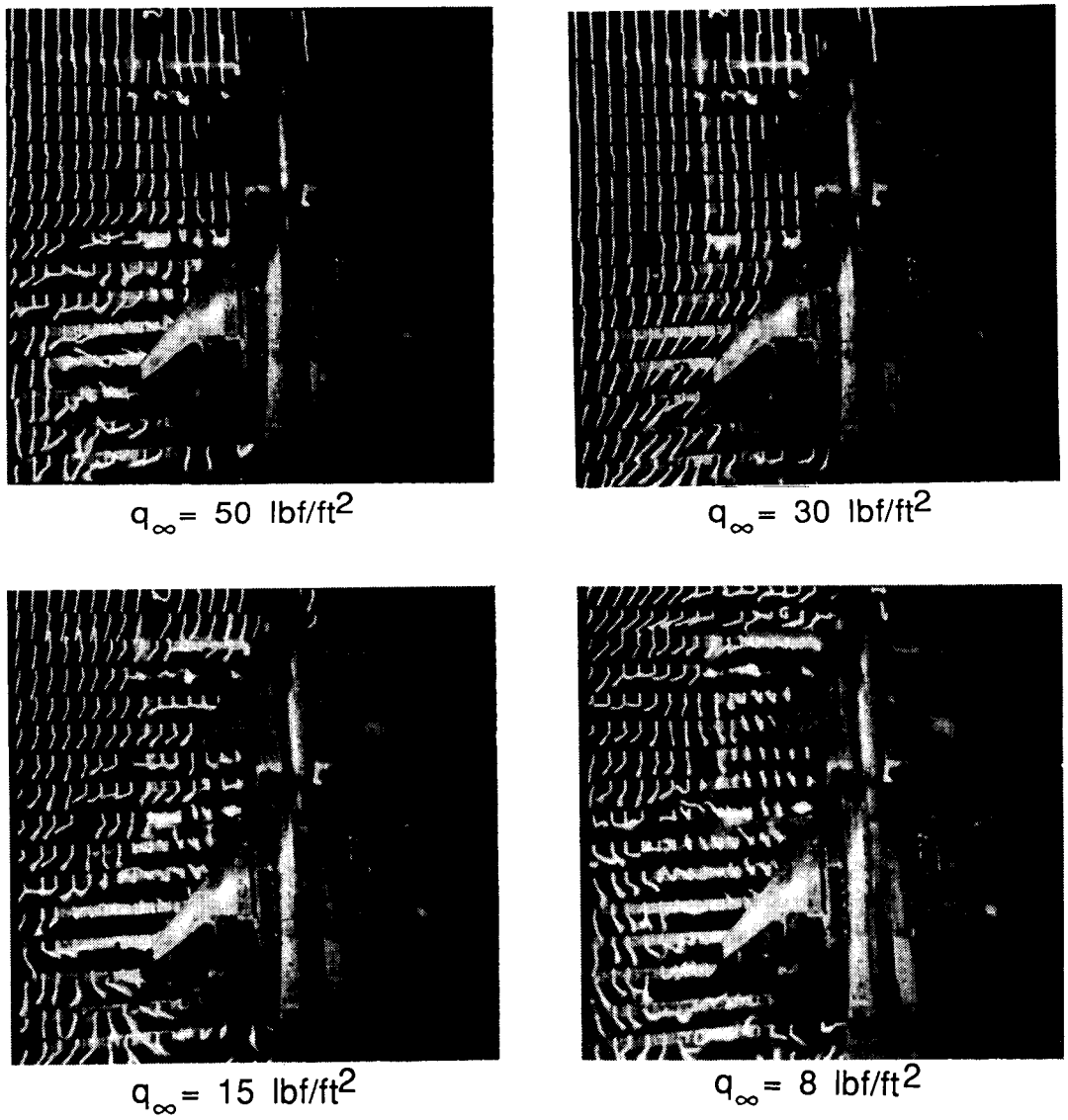

L-85-2634

(b) SERN with splay doors.

Figure 37. Concluded.

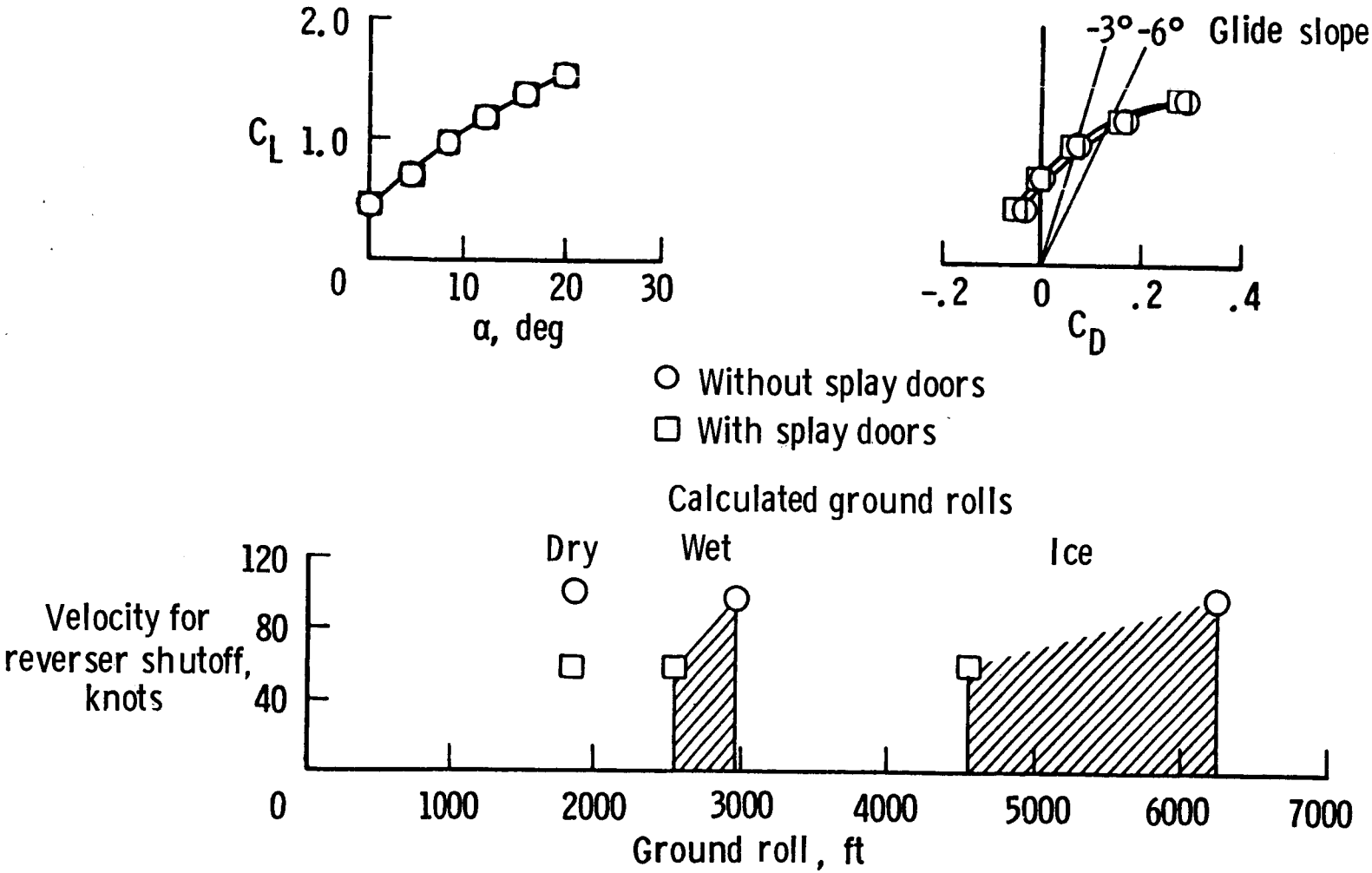

Figure 38. Approach aerodynamics and calculated ground rolls for ANC-B configuration with and without splay doors.

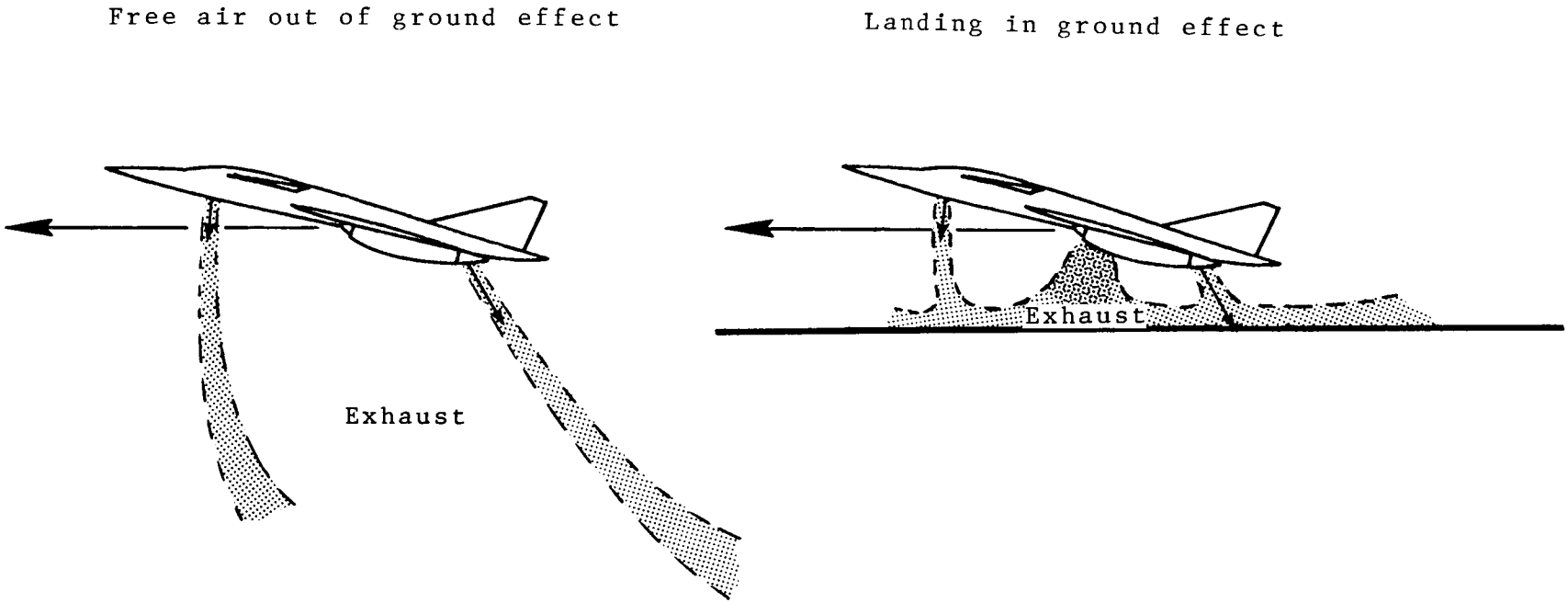

Figure 39. Sketch of effect of ground plane on aircraft flow field.

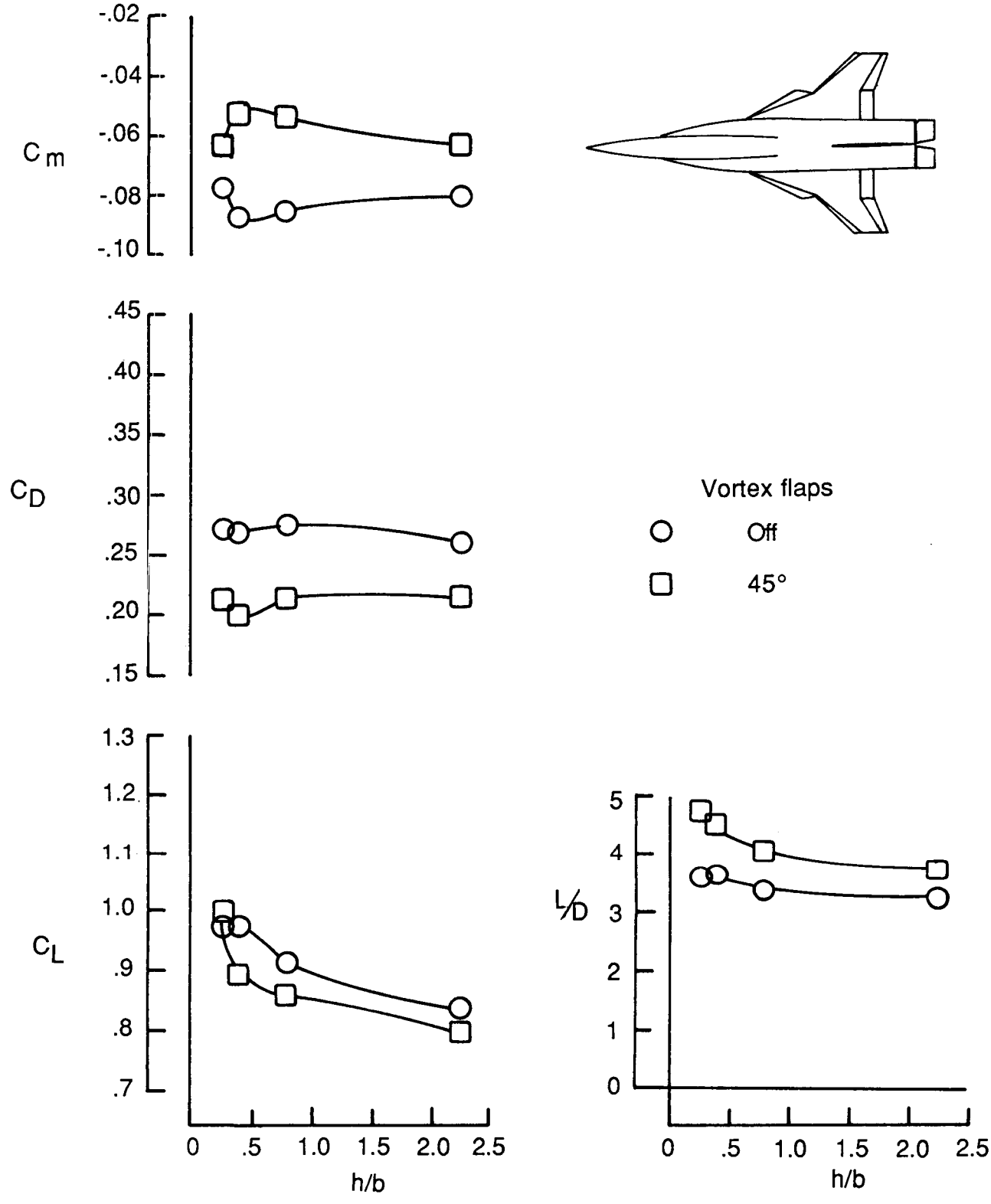

Figure 40. Effect of ground plane on longitudinal aerodynamics of ANC-B wing-alone configuration. $\delta_f = 45°$.

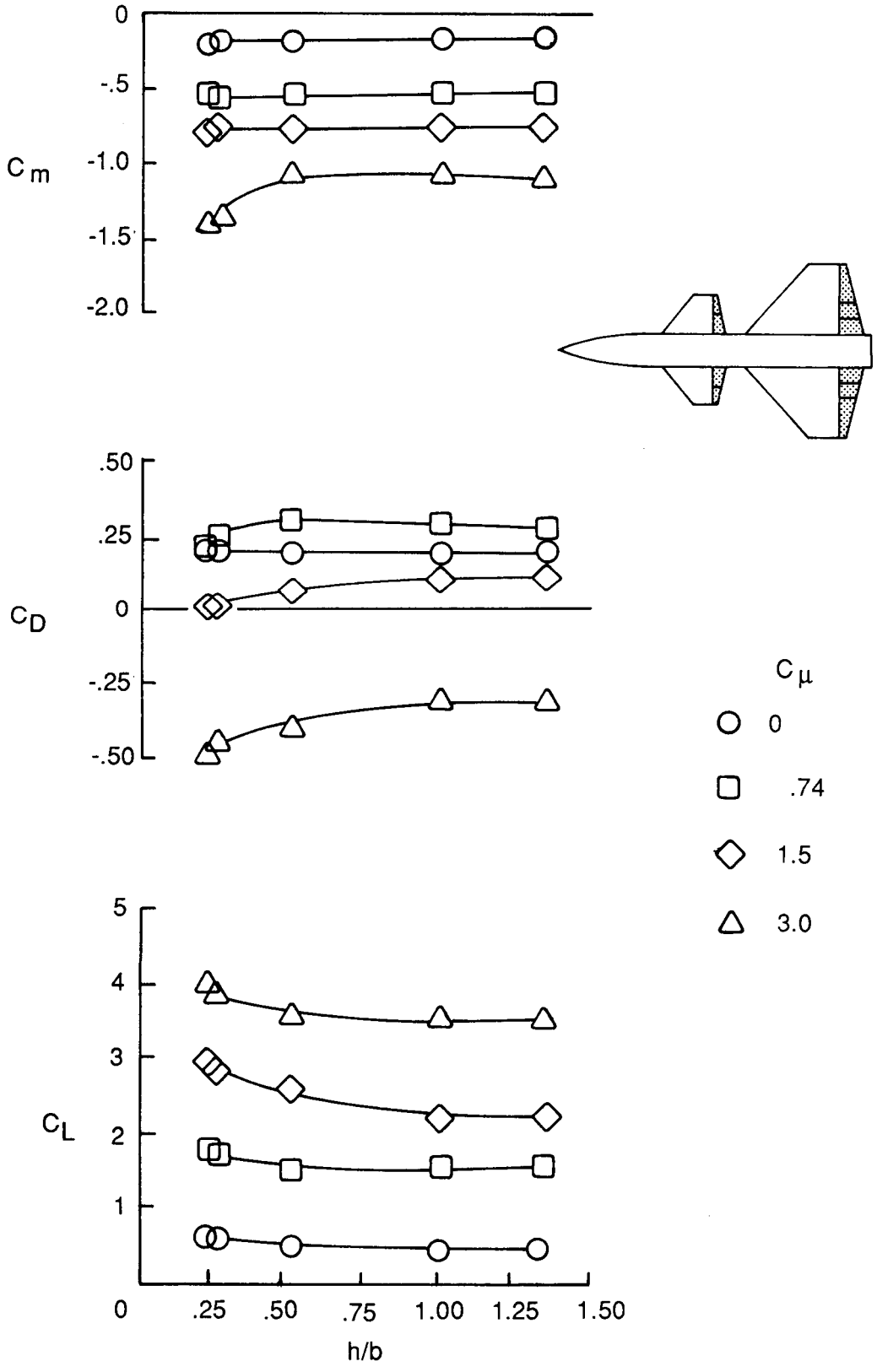

Figure 41. Ground effects on propulsive wing-canard configuration. $\delta_f = 45°$.

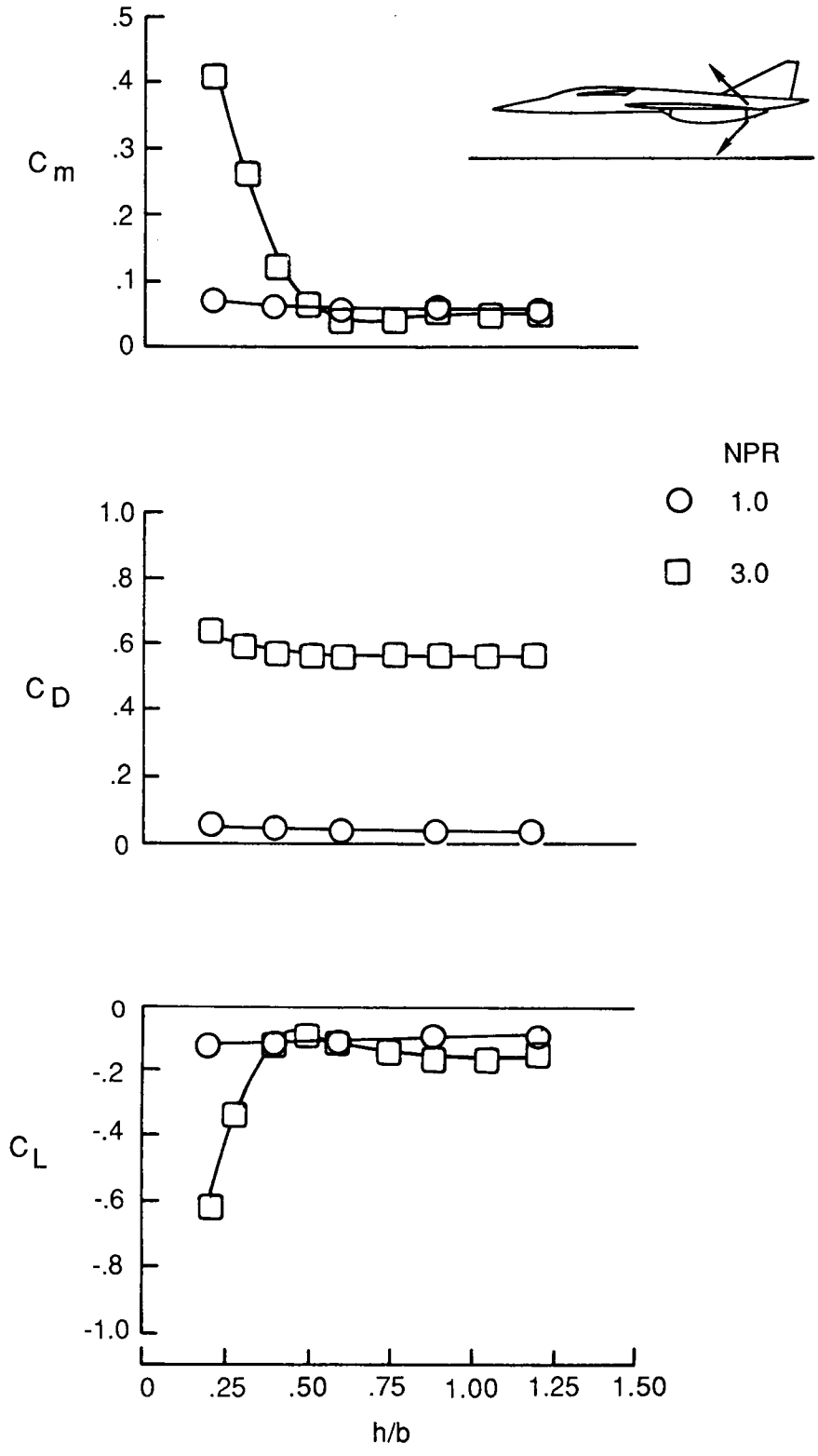

Figure 42. Ground effects on Mach 2 supercruiser configuration with thrust reversers. $A = 4.0$.

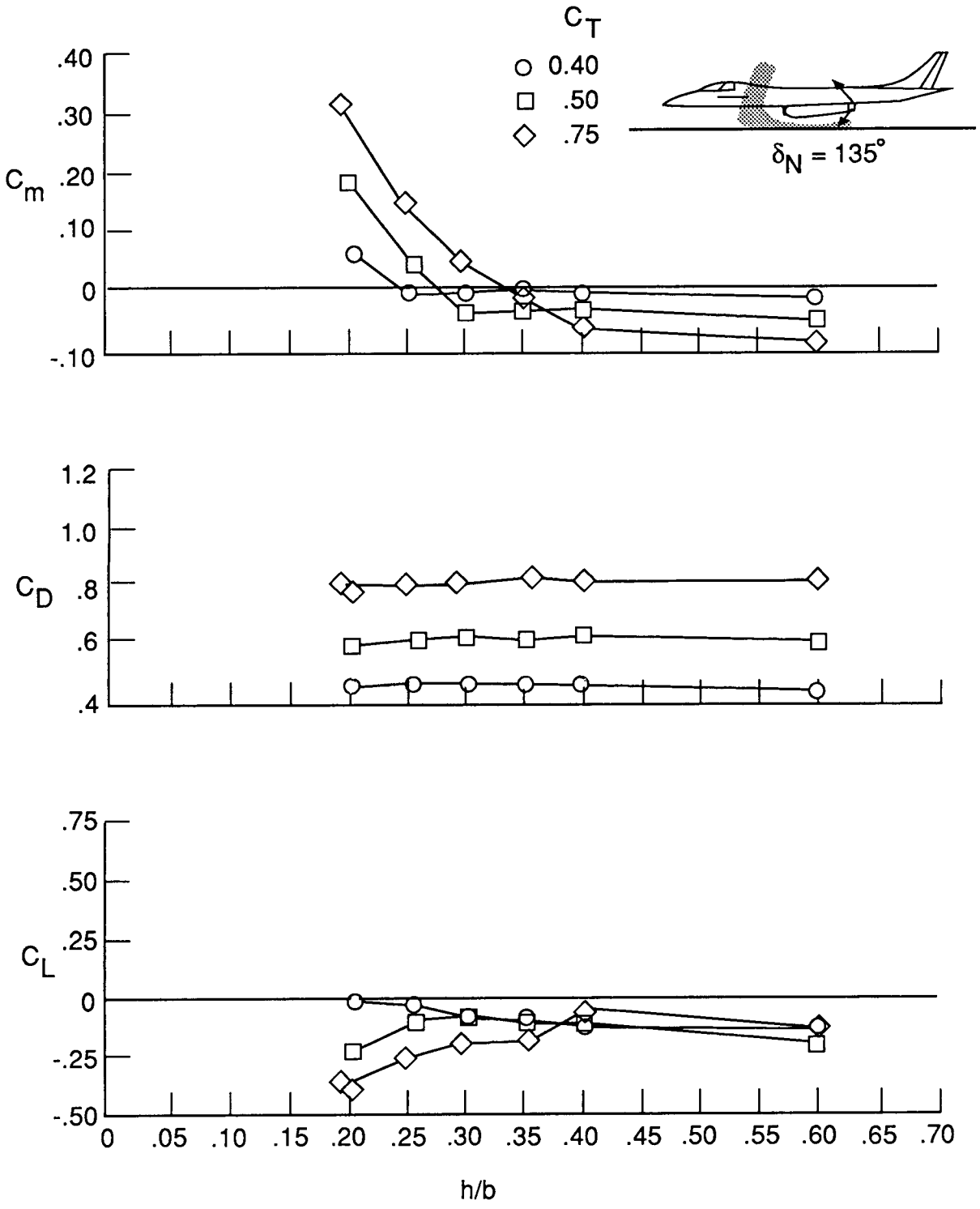

(a) $\alpha = 0°$.

Figure 43. Ground effects on ATTAC configuration with thrust reversers.

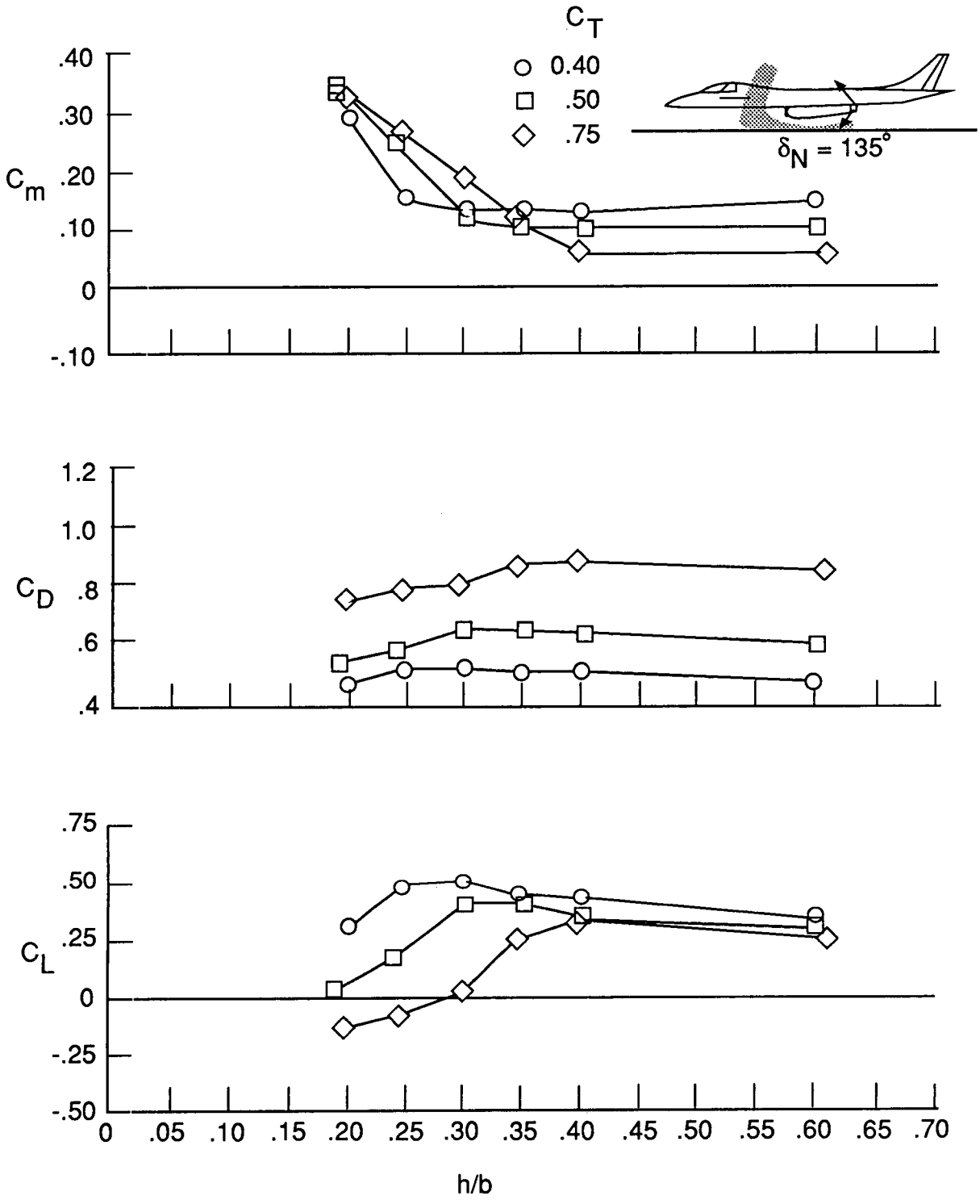

(b) $\alpha = 12°$.

Figure 43. Concluded.

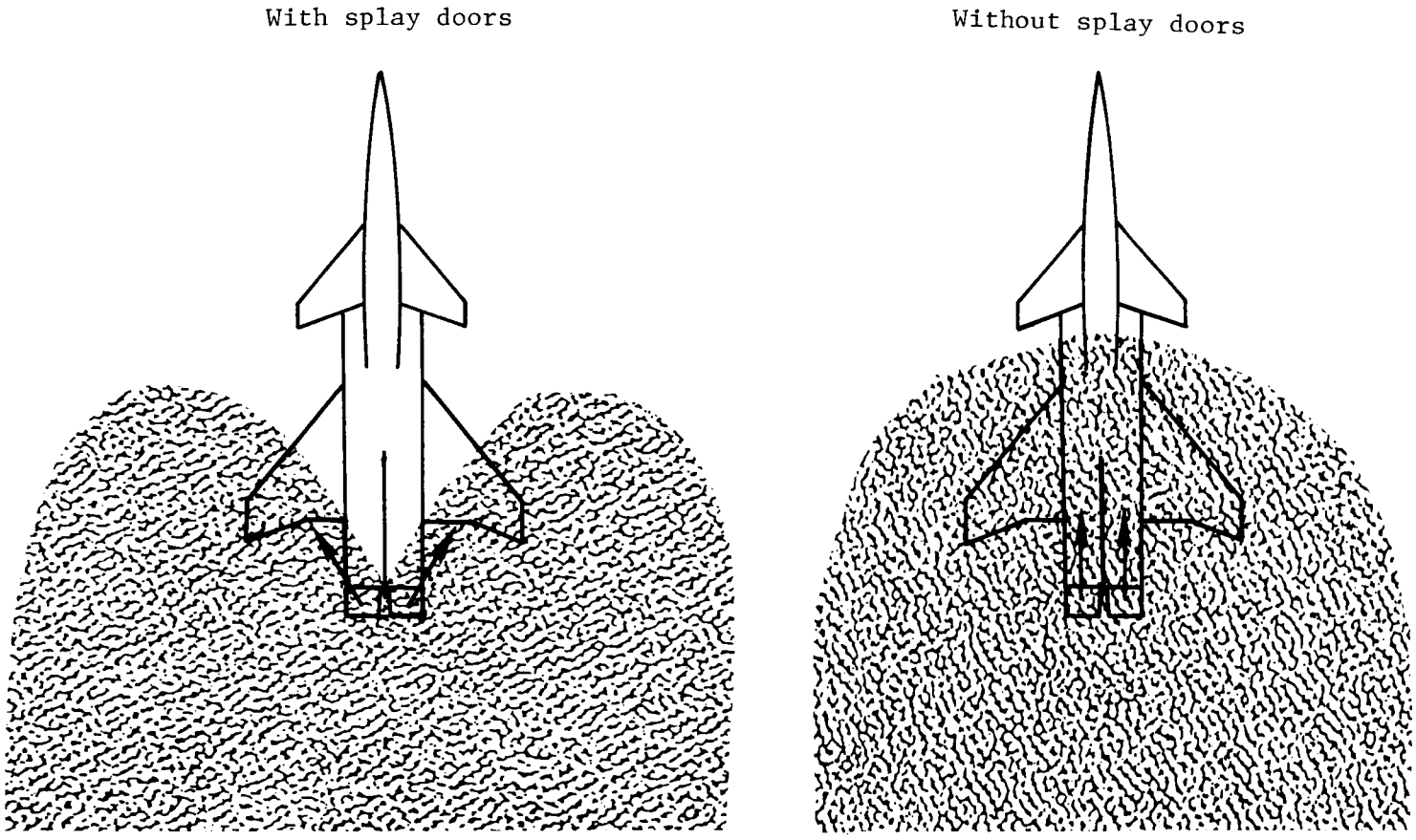

Figure 44. Sketch of reverse-thrust flow field with and without splay doors vectoring flow away from configuration centerline.

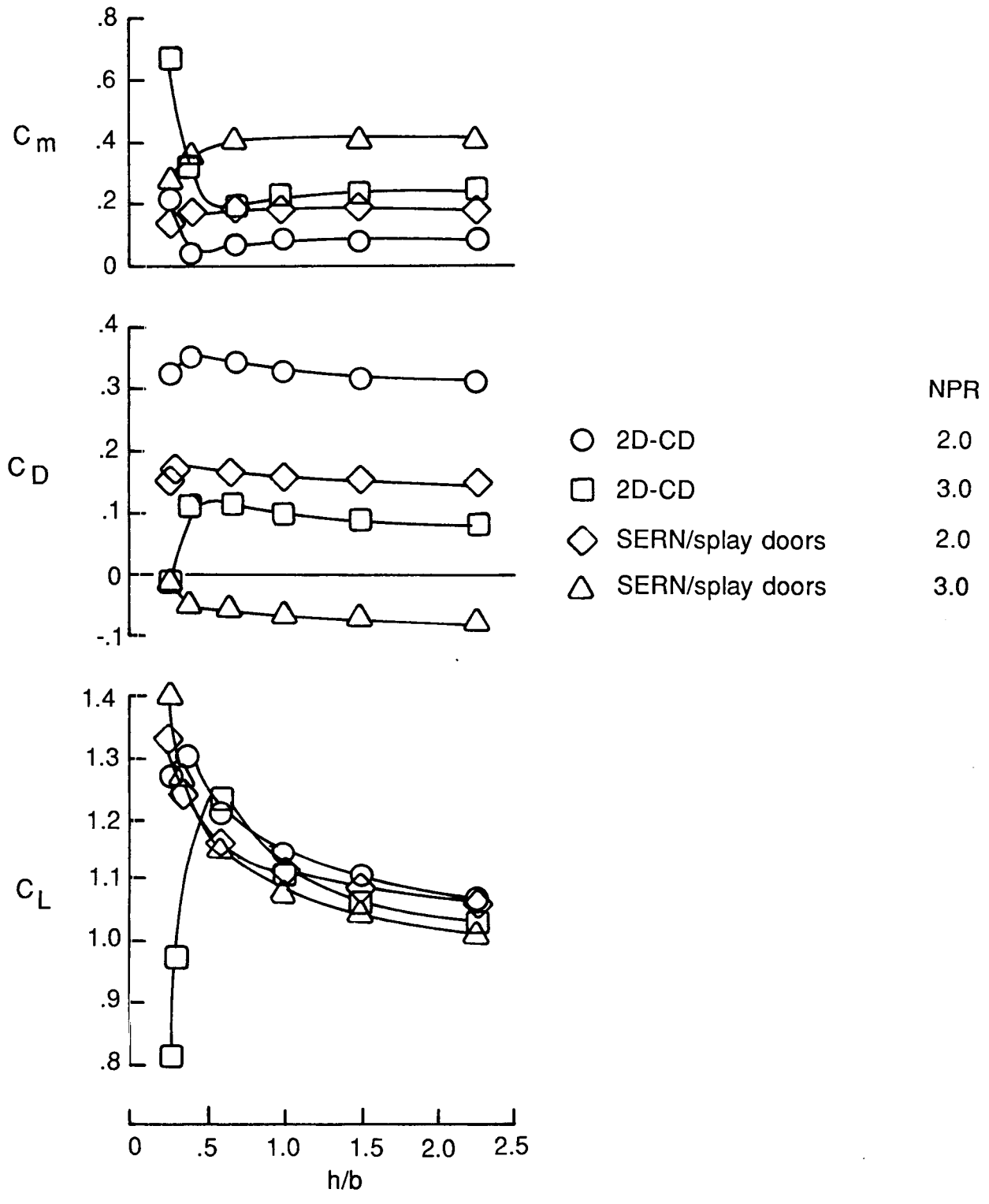

Figure 45. Comparison of ground effects of ANC-B approach configurations with and without splay doors.

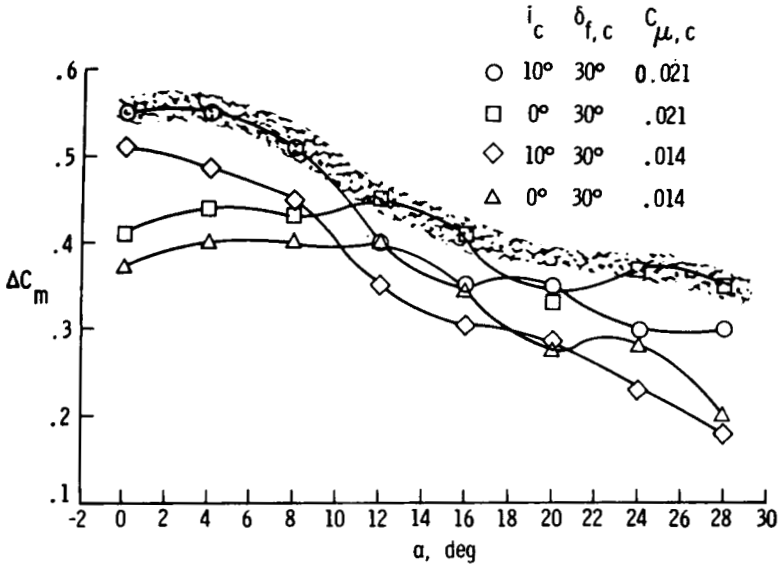

Figure 46. Increments in nose-up pitching moment available for various canard conditions on ATTAC configuration. Shaded area denotes range of maximum C_m.

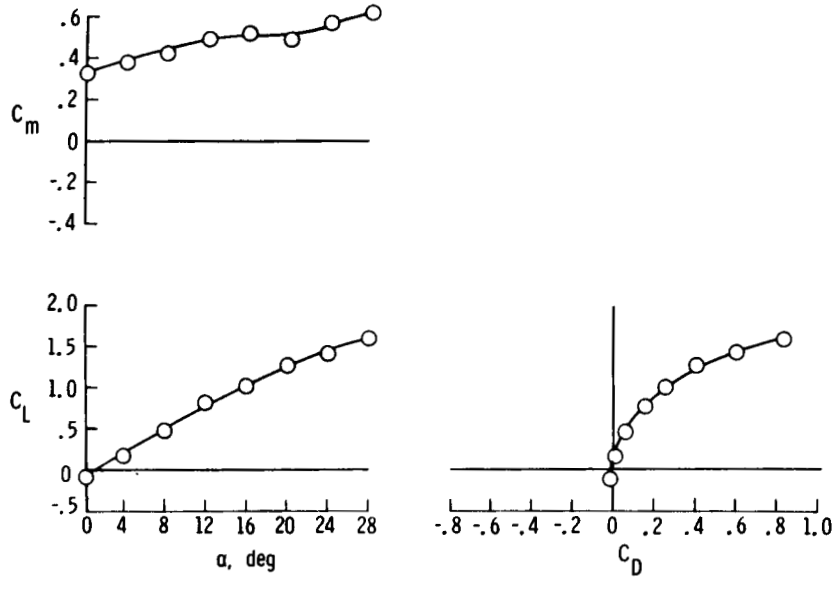

Figure 47. Baseline aerodynamic data for advanced STOL fighter configuration. $\delta_N = 0°$; $C_{\mu,c} = 0.021$; $C_{T,\mathrm{PRI}} = 0$.

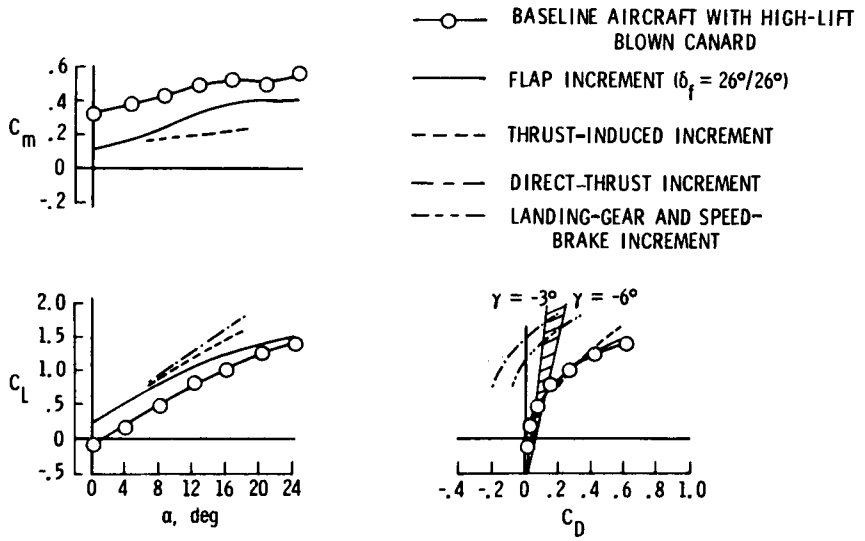

Figure 48. Incremental buildup of aerodynamics for advanced STOL fighter configuration.

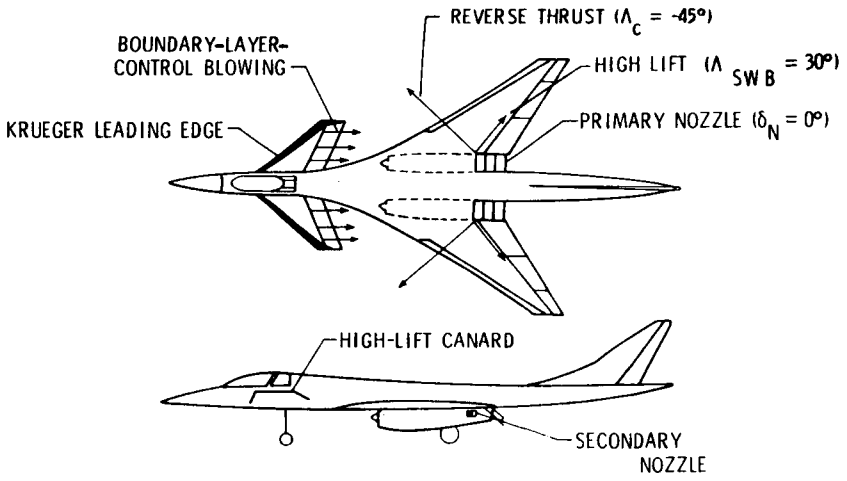

Figure 49. Sketch of advanced STOL fighter configuration.

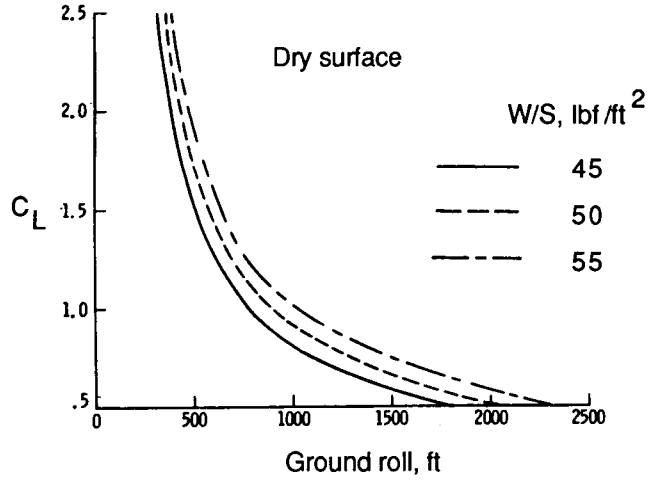

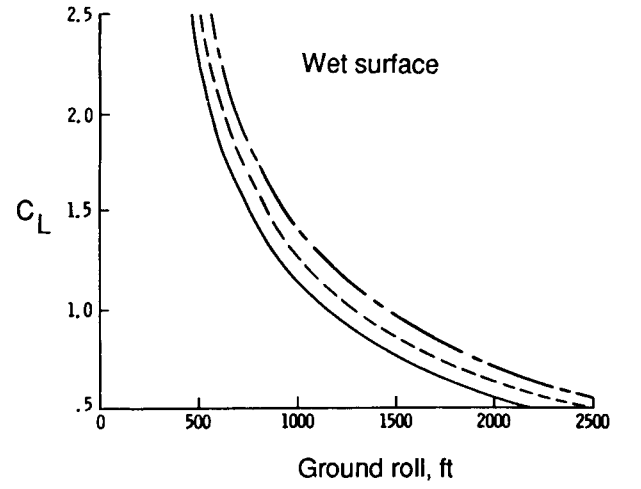

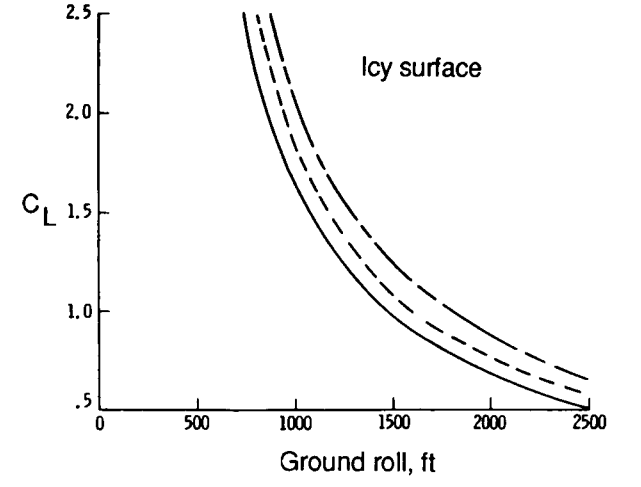

Figure 50. Calculated landing ground roll for an advanced STOL fighter with 50-percent effective thrust reverser.

NASA
National Aeronautics and Space Administration

Report Documentation Page

1. Report No.	2. Government Accession No.	3. Recipient's Catalog No.
NASA TP-2796		

4. Title and Subtitle	5. Report Date
A Review of Technologies Applicable to Low-Speed Flight of High-Performance Aircraft Investigated in the Langley 14- by 22-Foot Subsonic Tunnel	May 1988
	6. Performing Organization Code
7. Author(s)	8. Performing Organization Report No.
John W. Paulson, Jr., P. Frank Quinto, Daniel W. Banks, Guy T. Kemmerly, and Gregory M. Gatlin	L-16364
9. Performing Organization Name and Address	10. Work Unit No.
NASA Langley Research Center Hampton, VA 23665-5225	505-61-71-02
	11. Contract or Grant No.
12. Sponsoring Agency Name and Address	13. Type of Report and Period Covered
National Aeronautics and Space Administration Washington, DC 20546-0001	Technical Paper
	14. Sponsoring Agency Code

15. Supplementary Notes

16. Abstract

An extensive research program has been underway at the NASA Langley Research Center to define and develop the technologies required for low-speed flight of high-performance aircraft. This 10-year program has placed emphasis on both short takeoff and landing (STOL) and short takeoff and vertical landing (STOVL) operations rather than on regular "up and away" flight. A series of NASA in-house as well as joint projects have studied various technologies including high lift, vectored thrust, thrust-induced lift, reversed thrust, an alternate method of providing trim and control, and ground effects. These technologies have been investigated on a number of configurations ranging from industry designs for advanced fighter aircraft to generic wing-canard research models. Test conditions have ranged from hover (or static) through transition to wing-borne flight at angles of attack from $-5°$ to $40°$ at representative thrust coefficients.

17. Key Words (Suggested by Authors(s))

Powered lift
Thrust vectoring/reversing
Trim
STOL aircraft
Ground effects

18. Distribution Statement

Unclassified–Unlimited

Subject Category 02

19. Security Classif.(of this report)	20. Security Classif.(of this page)	21. No. of Pages	22. Price
Unclassified	Unclassified	93	A05

NASA FORM 1626 OCT 86

NASA-Langley, 1988

For sale by the National Technical Information Service, Springfield, Virginia 22161-2171